Nuklearmedizinische Klinik und Poliklinik
der Technischen Universität München
Klinikum rechts der Isar
(Direktor: Univ.-Prof. Dr. M. Schwaiger)

Characterisation of Glucose Metabolism in Pig Hearts During Regional Chronic Ischaemia in Comparison to Normal Hearts

Alexander Praus

Vollständiger Abdruck der von der Fakultät für Medizin der Technischen Universität München zur Erlangung des akademischen Grades eines

Doktors der Medizin

genehmigten Dissertation.

Vorsitzender:	Univ.-Prof. Dr. D. Neumeier
Prüfer der Dissertation:	1. Univ.-Prof. Dr. M. Schwaiger
	2. Univ.-Prof. A. Kastrati
	3. Univ.-Prof. Dr. A. Schömig

Die Dissertation wurde am 24.05.2004 bei der Technischen Universität München eingereicht und durch die Fakultät für Medizin am 02.02.2005 angenommen.

TABLE OF CONTENTS

1 INTRODUCTION

The mortality rate from ischaemic heart disease has decreased in recent years although it is still the disease with the highest mortality rate. This improvement is mainly due to a better understanding of risk factors associated with the development and pathophysiology of coronary artery disease, prevention and improvements in medical and interventional therapy.

Since the discovery that the mammalian heart receives its nutrients through the coronary circulation (Langendorff O., 1895), the tight coupling of coronary flow, myocardial oxygen consumption and contractile performance is one of the fundamental principles of cardiovascular physiology. Cellular responses to a decrease in coronary flow are both immediate and sustained. Immediate are those affecting the transfer of energy from substrates to ATP and entail the activation or deactivation of highly regulated enzymes. Sustained responses involve adaptive changes in gene expression of involved proteins and enzymes. Energy metabolism is linked to both gene expression and enzyme regulation, as well as to contractile function. There is a clear interdependence of metabolism, contractile function and gene expression, through specific signals, sensors and effectors. The most common disturbance challenging this dynamic equilibrium is myocardial ischaemia. This work focuses on sustained responses examining the gene and protein expression of GLUT1, GLUT3, GLUT4 and hexokinase type II in normal and ischaemically injured porcine hearts.

1.1 Myocardial Metabolism

1.1.1 Normal Heart (Stryer L, 1995; Bergmann, 1997)

The myocardium uses a variety of substrates, including fatty acids and glucose, and to a lesser extent lactate, pyruvate, ketones and amino acids (Camici et al., 1989; Neely J.R. and Morgan H.E., 1974). Long-chain fatty acids are the most important substrates (van der Lee et al., 2000). The particular pattern depends on arterial substrate content, myocardial perfusion and oxygenation, the metabolic status of the myocardium and other factors such as hormonal milieu. The heart is an aerobic organ that has high-energy flux, which is necessary for the production of high-energy phosphates essential for contraction as well as for maintenance of normal cellular homeostasis and the electrophysiological properties of the heart.

Normally oxidative metabolism of free fatty acids provides 40 to 60% of the energy used by the heart (Camici et al., 1989; Neely J.R. and Morgan H.E., 1974). Glucose provides an important alternate fuel and accounts for approximately 20 to 40% of the energy needs under fasting conditions. After glucose load more than 60% of the energy needs of the heart can be supplied by aerobic, oxidative metabolism of glucose. Metabolism of fatty acids occurs by ß-oxidation in the mitochondria, although a fraction of extracted fats are incorporated into neutral lipid storage forms such as triglycerides as well as into membrane phospholipids. After carbohydrate load, the utilisation of fatty acids is diminished due to the effect of insulin, which diminishes lipolysis and therefore also free fatty acids in the plasma. Additionally, insulin directly stimulates myocardial glucose utilization.

Glucose transport into the cardiomyocytes is mediated by glucose transporters and is accelerated in the presence of insulin. Inside the cell glucose is phosphorylated to glucose-6-phosphate by hexokinase. The further breakdown to pyruvate is well regulated in the glycolytic pathway. Normally pyruvate is converted to acetyl-coenzyme A (CoA), which is then oxidized aerobically in the Krebs (tricarboxylic acid – TCA) cycle. Oxidation of glucose is inhibited by fatty acids at several regulatory levels. Glucose can also be stored as myocardial glycogen, the preferred pathway with increased intracellular level of glucose-6-phosphate and in presence of insulin.

The Krebs cycle is the final pathway in oxidative metabolism. Substrates are converted by ß-oxidation or glycolysis to acetyl-CoA, which is normally metabolised to CO_2 in the TCA cycle while building up $NADH/H^+$. This yields hydrogen atoms that enter the electron transport chain of the cytochrome system where ADP is phosphorylated to ATP.

1.1.2 Ischaemic Heart

During ischaemia profound alterations in metabolism occur (Camici et al., 1989), (Neely J.R. and Morgan H.E., 1974), (Myears et al., 1987). Without oxygen oxidative phosphorylation of ADP in the cytochrome system is impossible. Accordingly $NADH/H^+$ accumulates and inhibits the TCA cycle. Therefore, pyruvate cannot be oxidized aerobically and thus is metabolised anaerobically with production of lactate.

Early after hypoxia ß-oxidation of free fatty acids decreases since several enzymes involved in this pathway are inhibited by lactate and $NADH/H^+$. Therefore, fatty acids are shunted into phospho- and neutral lipids (Fox et al., 1985), (Rosamond et al., 1987). Long-chain acyl-CoA and acyl-carnitines, which can be arrhythmogenic or may be negative inotropes, can accumulate and worsen the outcome (Stanley et al., 1997b). Also, the expression of

enzymes being part of fatty acid metabolism is decreased (Remondino et al., 2000). Now the predominant source for energy supply is the anaerobic metabolism of glucose to lactate (Myears et al., 1987; Neely J.R. and Morgan H.E., 1974; Camici et al., 1989). However this compensation is short-lived because the accumulating lactate, NADH and hydrogen ions depress the regulatory enzymes of the glycolytic pathway and thus are deleterious (King and Opie, 1998a),(King and Opie, 1998b). All these regulations can compensate for impaired metabolism but cannot meet the high-energy demands of the myocardium. Glycolysis can only supply approximately 10 to 30% of the heart's energy need under this condition, which is only sufficient to maintain cellular viability (Camici et al., 1989). The increased need of glucose is a characteristic feature of the early phase of the response of mammalian tissues to metabolic stress (as ischaemia, hypoxia, osmotic stress, viral infection, etc.). Clinical observations suggest that increased glucose utilization may be an adaptive mechanism in such regions (McNulty et al., 1996). In these conditions cells show an increased rate of glucose uptake (Baldwin et al., 1997) to maintain basal functions necessary for survival. Although they may cease contracting they remain viable. This adaptation dramatically decreases energy demand of myocardial cells, since approximately 60% of oxygen consumption is linked to contractile performance. The energy saving is thought to increase the tolerance of myocardial cells to myocardial ischaemia at the expense of regional dysfunction (Elsasser et al., 1997), (Schwarz et al., 1998). In conclusion, such situations are associated with a reversible left ventricular dysfunction, which is also defined as "hibernating myocardium" (Heusch, 1998). Patients with hibernating myocardium demonstrate recovery after early revascularisation (Heusch, 1998). However, this adaptation is only incomplete because biopsy samples of such regions already show structural degeneration (Elsasser et al., 1997). For the clinical decision the identification of jeopardised but viable myocardium, which may benefit from pharmacological or mechanical intervention is important. There are also studies testing pharmaceutical agents stimulating glucose oxidation in ischaemic hearts (McCormack et al., 1996). Further it has been shown that stimulation of glucose transport with vanadyl sulfate significantly improves ischaemic preservation in a model of hypertrophied rabbit hearts (Takeuchi et al., 1998).

The identification of hibernating regions can be done by PET. Such PET studies of chronically ischaemic hearts, either in animal research or in patients show four patterns of metabolism (FDG uptake) and perfusion (ammonia retention)(Figure 1):

1. In normal myocardium uptake of ammonia and FDG are uniform.
2. In areas of myocardial infarction, a deficit of flow is matched with a deficit in FDG accumulation. This represents scar and is unlikely to recover with revascularisation.

3. Regions with a decrease in flow but with maintained accumulation of FDG (flow – metabolism mismatch) are felt to represent jeopardized but viable myocardium amenable to intervention.
4. Areas with preserved perfusion but reduced glucose metabolism has been identified and appears to be associated with myocardial viability.

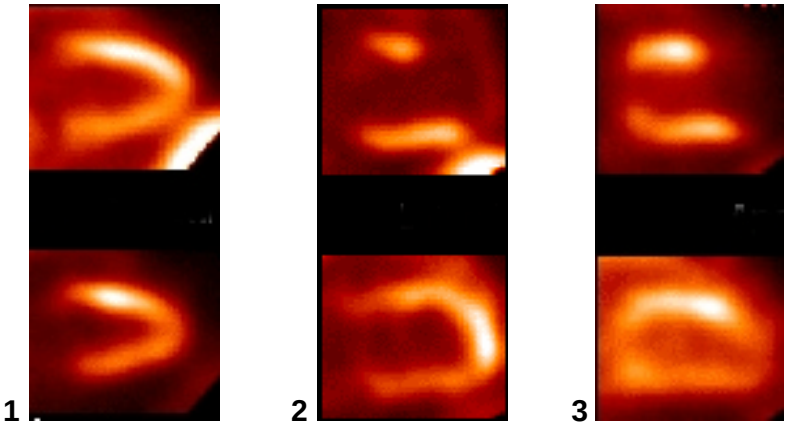

Figure 1 Distribution of myocardial perfusion in a pig heart evaluated with ^{13}N ammonia (upper pictures) and of glucose metabolism evaluated with ^{18}FDG (lower pictures). 1) Normal porcine heart without ischaemia, 2) flow – metabolism mismatch), 3) flow – metabolism match

1.2 Molecular Base of Glucose Metabolism

1.2.1 Glucose Transporters

Glucose and also its analogue FDG enter cells via glucose transporters as they are hydrophilic molecules and cannot penetrate the cell membrane. Therefore, specific carrier proteins are required to facilitate its diffusion along a concentration gradient. These proteins are passive carriers and transport the substrate independently of energy. The overall number of transporters present in the cell reflects the rate of gene transcription, mRNA stability and rates of protein translation and degradation (Charron et al., 1999).

The uptake of glucose is the rate-limiting step in glucose utilization under normal conditions (Depre et al., 1998a). The glucose transporters belong to a family of 13 solute carriers 2A (SLC2A, protein symbol GLUT) with a molecular weight of approximately 35 – 50 kDa and a characteristic morphology (Joost and Thorens, 2001), (Mueckler, 1994), (Lienhard et al., 1992) (Figure 2):

- 12 membrane spanning a-helices
- 7 conserved glycine residues in the helices
- Several basic and acidic residues at the intracellular surface of the proteins

- 2 conserved tryptophan and 2 conserved tyrosine residues. (Joost and Thorens, 2001)

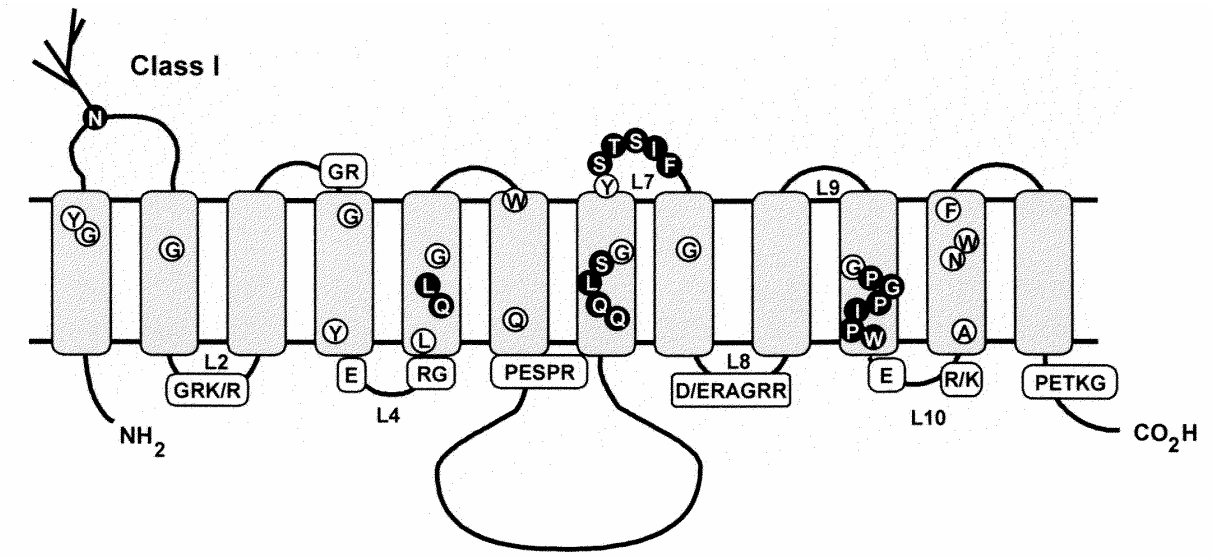

Figure 2 Schematic model of GLUT proteins class I(Joost and Thorens, 2001)

The members of this family are products of distinct genes rather than splice isoforms (Bell et al., 1990). Based on sequence analysis the family can be divided into three subclasses: Class I (GLUT1-4), class II (fructose transporter GLUT5, GLUT7, 9 and 11) and class III (GLUT6, 8, 10, 12 and the myoinositol transporter HMIT1). They exhibit a tissue-specific expression (see Table 1).

Table 1 Family of SLC2A, modified (Joost and Thorens, 2001)

	Expression	*Special characteristic*
GLUT1	Erythrocytes, brain (microvessels), heart, etc.	Expression in almost every tissue; high affinity to glucose
GLUT2	Liver, islets, enterocytes (basolateral), kidney	High-capacity low-affinity transport
GLUT3	Brain (neurons), heart, kidney	Highest efficiency in glucose transport
GLUT4	Heart, skeletal muscle, adipocytes	Insulin regulatible
GLUT5	Intestine, testis, kidney	Fructose transporter
GLUT6	Leukocytes, brain, spleen	
GLUT7	Unknown	
GLUT8	Testis, blastocysts, brain, muscle, adipocytes	Insulin regulatible
GLUT9	Liver, kidney	
GLUT10	Liver, pancreas	
GLUT11	Heart, skeletal muscle	Fructose inhibitable glucose transport
GLUT12	Heart, prostate	
HMIT1	Brain	H^+/myoinositol cotransporter

There exist also four presumed pseudogenes (untranslated mRNA) exhibiting significant similarity with the GLUT family. Three of these are retrotransposons of GLUT3.

The glucose uptake itself happens through an aqueous pore, but not by a continuous pathway across the lipid bilayer. Rather substrate passage must be blocked at one end at any time while the other end is open. So there is always an oscillation between conformations with the outer or inner ending closed, preventing e.g. sodium ions to leak in.

The expression of glucose transporters is determined largely by the activity of GLUT gene transcription. The transcription is under the control of a number of factors that influence the activity of the GLUT promoters directly or indirectly (Charron et al., 1999). GLUT1 e.g. seems to be a stress protein whose expression is increased by a number of factors, including hypoxia.

1.1.1.1 GLUT1

GLUT1 is the prototype of the family of glucose transporters and is responsible for the basal glucose requirement of many tissues. It appears to be the most ubiquitously distributed

isoform and was the first membrane transporter to be purified from human erythrocytes in 1977 (Kasahara and Hinkle, 1977) and also to be cloned (Mueckler et al., 1985). The protein consists of 492 amino acids and appears to be a highly conserved isoform: The human GLUT1 exhibits 97-98% sequence identity with the analogous rat, mouse, rabbit and pig proteins (Mueckler, 1994).

In insulin-sensitive tissues, as e.g. heart, it has a cooperative action with GLUT4 (see 1.1.1.3). GLUT1 is mainly present in the plasma membrane where it presumably guarantees the low level of glucose required for basal cellular activity (Marette et al., 1992). However, GLUT1 itself is also present in intracellular membrane storage pools and translocates in response to certain stimuli (Wheeler et al., 1994), (Young et al., 1997), (Fischer et al., 1997). But compared to GLUT4 it shows a minor recruitment by insulin, which is shown in fat cells (Klip et al., 1994) and also in heart (Wheeler et al., 1994), (Russell, III et al., 1998), (Egert et al., 1999b).

Another fast way of increasing glucose uptake is activation of GLUT1 sites pre-existing in the plasma membrane, which was described in cell cultures after inhibition of oxidative phosphorylation (Shetty et al., 1993). The possible mechanism of this kind of regulation is phosphorylation of the transport protein (see 1.1.1.3). However, such an effect has not been described in heart so far.

Insulin seems to play a major role for the upregulation of GLUT1 expression (Laybutt et al., 1997). High glucose levels lead to the opposite effect, a lower expression of GLUT1 caused by pre- and post-transcriptional mechanisms (Walker et al., 1988), (Walker et al., 1989), (Tordjman et al., 1990), (Wertheimer et al., 1991), (Klip et al., 1994). Thus, glucose deprivation causes rapid and sustained increases in hexose transport, GLUT1 mRNA and protein expression. There have been several studies examining the effect of a number of agents on GLUT1 expression in cell cultures. GLUT1 expression has been shown to be increased by: cAMP (Hiraki et al., 1989), thyroid hormone (Haber et al., 1993), insulin (Walker et al., 1989), (Tordjman et al., 1989), insulin-like growth factor-I (Maher et al., 1989), tumour necrosis factor a (which stabilizes the GLUT mRNA (Stephens et al., 1992)), and finally hypoxia (Loike et al., 1992). A decreased expression has been observed by growth hormone (Iitaka and Katayama, 2000), (Smith et al., 1997).

In heart tissue it likely is regulated by the hypoxia-inducible factor-1a, an important transcriptional factor in heart and other tissues (Ryan et al., 1998). In neonatal cardiocytes, GLUT1 transcription is also subject for regulation by alpha-adrenergic stimulation that

appears to be mediated by activation of MAP kinases (Montessuit and Thorburn, 1999). It is assumed to prevent cardiac apoptosis during hypoxia (Malhotra and Brosius, III, 1999).

The effect of myocardial ischaemia on the expression of GLUT1 has only been shown in a few studies. The only pig study done by Feldhaus showed increased GLUT1 mRNA expression after 40 min of ischaemia with and without reperfusion but a decreased mRNA expression in the hibernation group. However, each group only contained one animal. So further studies are necessary examining the regulation of expression of GLUT1 under ischaemic conditions. Rat studies showed an increased GLUT1 mRNA and protein 24 hours after LAD ligation but baseline values again after eight weeks (Remondino et al., 2000), (Rosenblatt-Velin et al., 2001). Two days of hypobaric hypoxia lead to an increased GLUT1 mRNA but not protein level. After 14 days the protein level is also increased (Sivitz et al., 1992). Brosius also demonstrated increased GLUT1 mRNA and protein levels in ischaemic canine hearts but without regional variations.

1.1.1.2 GLUT3

GLUT3 is the most prominent glucose transporter isoform expressed in parenchymal cells of the adult brain (Kayano et al., 1988), (Nagamatsu et al., 1992). The most distinctive characteristic of this isoform is its low Michaelis-Menten constant and it therefore operates more efficiently at lower glucose concentrations (Gould et al., 1991). Unlike rat and mouse where its expression is reported to be restricted predominantly to nervous tissue and placenta only (Gould et al., 1992), (Nagamatsu et al., 1992), (Krishnan and Haddad, 1995), (Zhou and Bondy, 1993), in human and other species mRNA and protein could be detected in several tissues, including heart. The first description of its protein expression in the human heart was published in 1992 (Shepherd et al., 1992) which was confirmed by Grover-McKay in 1999 (Grover-McKay et al., 1999). But so far there is very few literature about GLUT3 mRNA in myocardium other than human or even in ischaemic heart. Studies on ischaemia in brain displayed a region-specific increase of GLUT3 mRNA (Devaskar et al., 1999).

Translocation of GLUT3 protein is also described but only in platelet plug formation. In platelets, GLUT3 is stored in alpha-granules that fuse with the cell membrane after stimulation with thrombin (Heijnen et al., 1997).

1.1.1.3 GLUT4

GLUT4 has a 65% sequence identity with GLUT1 (Mueckler et al., 1997) and is exclusively expressed in insulin-sensitive tissue (adipocytes, skeletal muscle cells and

cardimyocytes)(Birnbaum, 1989), (Charron et al., 1989), (Fukumoto et al., 1989), (Kaestner et al., 1989), (James et al., 1989). It is expressed at highest levels in brown fat, followed by heart, red muscle, white muscle and white fat (James et al., 1989).

Under normal conditions GLUT4 is largely sequestered in intracellular organelles (over 90%) in contrast to GLUT1 (Marette et al., 1992),(Slot et al., 1991), (Lienhard et al., 1992). Various conditions may cause rapid translocation of GLUT4 from its intracellular storage vesicles to the cell membrane. Translocation as an acute answer of cardiac myocytes is induced by the presence of insulin (Sun et al., 1994), (Fischer et al., 1997), (Russell, III et al., 1998), hypoxia (Wheeler, 1988) and ischaemia (Sun et al., 1994; Young et al., 1997). In an adipocyte cell line it has been shown that the presence of insulin can increase glucose uptake 15-fold in only a few minutes (Lienhard et al., 1992).

The intracellular signal transduction induced by insulin is still not fully known (Figure 3).

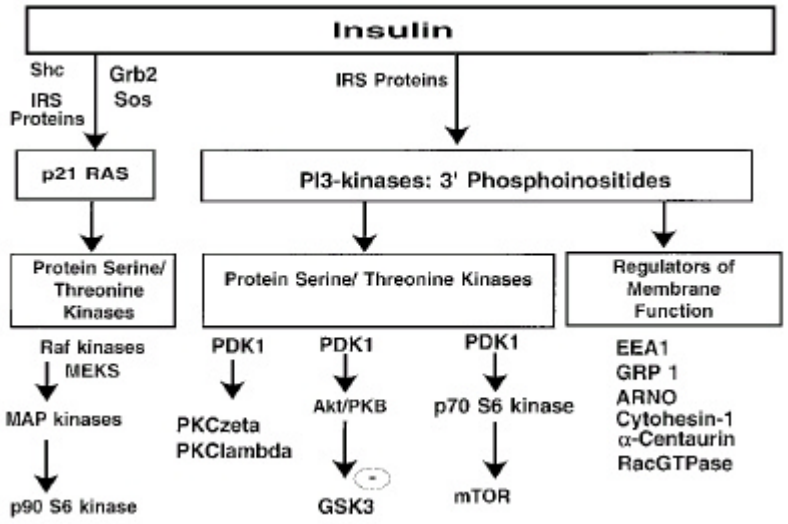

Figure 3 Signalling elements regulated by insulin binding to its receptor (Czech and Corvera, 1999) (modified). ***PKC: Protein kinase C, MAP: Mitogen-activated protein, MEK: MAP kinase kinase.***

In contrast to the insulin pathway, much less is known about the signal transduction in ischaemia. Inhibitors of PI3K such as wortmannin block insulin-stimulated glucose transport but not the stimulation of translocation during myocardial ischaemia (Egert et al., 1997). Therefore, these stimuli do not appear to exert their effects on the translocation through PI3K. Catecholamines stimulate glucose uptake and GLUT4 translocation during exercise and myocardial ischaemia by the a-adrenergic pathway (Egert et al., 1999a). In isolated perfused rat hearts both a- and ß-adrenergic stimulation lead to increased GLUT translocation (Egert et al., 1999a). A further potential mechanism could be the adenosine monophosphate-activated protein kinase (AMPK), which has been described as a metabolic

fuel gauge or energetic stress kinase that activates energy-generating fuel substrate pathways and turns off energy-consuming biosynthetic pathways (Hardie and Carling, 1997). AMPK is activated during myocardial ischaemia (Kudo et al., 1995) and the signal is further amplified by activation of the AMPK kinase that phosphorylates and activates the AMPK.

Membrane transporters can also be activated by phosphorylation of their amino acids residues by protein kinases. GLUT4 undergoes phosphorylation of its COOH terminal end in response to catecholamine stimulation in adipocytes (James et al., 1989), (Lawrence, Jr. et al., 1990), although this phosphorylation does not appear to influence translocation of the transporter. Phosphorylation due to insulin has not been described (Lawrence, Jr. et al., 1990).

Long-term regulation, however, happens via protein expression. The GLUT4 gene has an upstream 2,4 kb promoter element that appears to be critical for GLUT4 transcription (Olson et al., 1993). The GLUT4 promoter sequence contains a myocyte enhancer factor 2-binding domain, which belongs to a family of transcriptional factors that play an important role in myogenesis. It is necessary but not sufficient to support GLUT4 transcription (Thai et al., 1998). However, the factors leading to the selective expression of GLUT4 in insulin-sensitive tissues remain uncertain. The decrease in GLUT4 expression in experimental diabetes is related to decreased GLUT4 gene transcription (Gerrits et al., 1993). This also plays a role in patients with left ventricular hypertrophy, who have an increased GLUT1/GLUT4 ratio (Paternostro et al., 1999) mainly due to a decreased insulin-stimulated glucose uptake. Other studies show that fat cells insulin is a potent and essential stimulator of GLUT4 gene transcription. In contrast, in skeletal muscle neither glycemia nor insulinemia alone can determine the GLUT4 mRNA levels (Klip et al., 1994). When combining both factors changing the expression of GLUT4, as ischaemia and diabetes in pigs, a decrease of protein has been shown (Stanley et al., 1997a). The abundance of GLUT4 protein in adipose tissue correlates with the cellular levels of GLUT4 mRNA. No such correlation is found in skeletal muscle, indicating that studies of mRNA levels cannot completely explain the regulation of the glucose transport system in this tissue (Klip et al., 1994).

But what happens in chronic ischaemia? The number of studies studying this condition is limited. The only study performed in pigs showed in the hibernation group (consisting of one animal) that GLUT4 mRNA expression was slightly decreased (Feldhaus and Liedtke, 1998). Rosenblatt-Velin showed in rats that GLUT4 mRNA and protein is slightly decreased after 24 hours of LAD ligation but returned to baseline values after 8 weeks. After 20 weeks a difference occurred between rats with and without heart failure. Failing hearts had a reduced

expression of GLUT4 mRNA and protein whereas this could not be shown in non-failing hearts (Rosenblatt-Velin et al., 2001). Similar results have been shown by Remondino (Remondino et al., 2000). After two days of hypobaric hypoxia Sivitz showed a decreased GLUT4 mRNA and protein content in the right ventricle while there was no change in the left ventricle. After two weeks expression (mRNA and protein) in both regions did not differ from control anymore (Sivitz et al., 1992). This altogether demonstrates that previous results do not show a homogeneous pattern of change of GLUT4 expression mainly due to variations in experimental induction of ischaemia or evaluation of expression at different time points.

However, not only the transport of glucose into the cell during ischaemia is of interest, also the expression of hexokinase the enzyme catalysing the first reaction in the cell might be influenced by ischaemia.

1.2.2 Hexokinase Type II

After glucose has entered the cell via one of the glucose transporters it is phosphorylated to glucose-6-phosphate by the enzyme hexokinase (ATP:D-hexose 6-phosphotransferase, EC 2.7.1.1.), the very first step of intracellular glucose metabolism. When insulin is present and increases glucose uptake the hexokinase reaction becomes rate limiting (Depre et al., 1998a). This further plays a role in metabolic trapping of ^{18}F-Deoxyglucose (see 2.2.2.2.2). In mammalians hexokinase is tissue-specific expressed with four isoenzymes encoded by distinct genes. Hexokinases I – III have a molecular weight of approximately 100 kDa, a high affinity to glucose and are inhibited allosterically by glucose-6-phosphate. The (human and mouse) type II (HKII) protein consists of 917 amino acids. Hexokinase type IV, also known as glucokinase, which is specific for liver and pancreas has a molecular weight of 50 kDa, a low affinity to glucose and is not inhibited by glucose-6-phosphate (Deeb et al., 1993). These proteins are homologous and are organized in two homologous domains (with the exception of hexokinase type IV, which has only one). The organization of type I – III is believed to be the result of a duplication and tandem fusion event involving the gene encoding for the ancestral hexokinase, which did not happen with type IV (Palma et al., 1996).

Like GLUT, a tissue-specific distribution of the different types of hexokinase was found. Type I is also called brain hexokinase (Smith, 2000). Type II is the predominant isoform in adult cardiac tissue (Tsirka et al., 2001). It is insulin-sensitive and involved in the increased glucose uptake and utilization by adipose and muscle tissue in response to insulin. Regulation by insulin is described on the level of gene transcription (Sochor et al., 1990), (Osawa et al., 1996), (Katzen, 1967), (Levine, 1981) as well as on the level of enzyme activity in rat skeletal muscle (Postic et al., 1993). Wortmannin, an inhibitor of the PI3K

prevents the induction of HKII mRNA indicating that PI3K not only plays a role in GLUT4 translocation (see 1.1.1.3) but also in the signalling pathway of regulation of HKII expression by insulin (Osawa et al., 1996). Furthermore, defects in its synthesis may be implicated in the etiology of NIDDM (Deeb et al., 1993).

The regional expression of hexokinase in myocardial tissue has been examined by De Tata. There it was shown in pig hearts that there are different HK activities in left and right ventricle (De Tata et al., 1986). Under conditions of repetitive short-term ischaemia an increased activity has been shown (McFalls et al., 2002). Three weeks of normobaric hypoxia in rat hearts resulted also in an increased activity of hexokinase (Daneshrad et al., 2000). All these studies only measured the activity of the enzyme, which could also be elevated due to activation of the enzyme and therefore does not reflect changes in expression. Thus, the effect of ischaemia on the expression of HKII mRNA and protein is still to be elucidated.

1.3 Aim of the Study

Metabolic imaging studies have indicated that myocardial glucose metabolism can be heterogeneous in the normal heart(Gropler et al., 1990; Schwaiger and Hicks, 1990). Therefore, it is not clear either if the distribution of different GLUT isoforms is homogeneous throughout different parts of a normal heart. Thus, the first purpose of this study was to evaluate the regional homogeneity of the expression (mRNA and protein) of the glucose transporters GLUT1, 3, 4 and hexokinase type II in the normal swine heart.

Furthermore, in literature it is not clear so far, which and to which extent regulatory mechanisms are prevailing for increased glucose utilization in chronic ischaemia lasting for several days. For GLUT1 and GLUT4 several studies mainly working with rat hearts are published already. But there are only few dealing with pig tissue (Feldhaus and Liedtke, 1998), (McFalls et al., 2002), (Stanley et al., 1997a), (Stanley et al., 1994) – only the first two worked with non-diabetic pigs and the size of the groups consisted of only one animal. Since the definite description of GLUT3 protein in the human heart in 1999 (Grover-McKay et al., 1999) there is no literature dealing with this isoform in the ischaemic heart and also no literature about GLUT3 mRNA in the heart at all. Studies examining expression of HKII are few, too, and only showed changes in activity of the enzyme in rodents so far. Consequently the effect of chronic regional ischaemia on the expression of these proteins is still not well characterised. So the second aim was to examine the regulation of expression of the four mentioned proteins and their mRNA during regional ischaemia.

To fulfil these aims two groups of pig hearts were investigated. The first group comprised four six month old normal pigs without intervention (controls). They served to examine the “normal” distribution of gene and protein expression. The second group contained four pigs (four months of age) with a 7-day ischaemia.

To produce this chronic regional ischaemia a modified stent graft was implanted in the proximal LAD. This stent had an initial 75% stenosis that was proceeding to complete occlusion within the seven days. With PET hibernating regions were determined as regions of hypoperfusion and increased glucose metabolism. Samples were taken from these regions, as well as from remote regions (remote left ventricle, right ventricle and both atria). From normal hearts the samples were taken from several left ventricular regions, the right ventricle and both atria to obtain tissue for RNA and membrane preparation. RT-PCR and immunoblotting was performed on these preparation samples to evaluate the regional mRNA and protein expression.

2 MATERIAL AND METHODS

2.1 Material

2.1.1 Instruments

BioPhotometer	Eppendorf, Hamburg
GelCam + Instant Pack Film, Professional Coaterless B&W, ISO 3000/36°	Polaroid, St. Albans, UK
Glas-Glas Homogeniser	Braun-Melsungen, Melsungen
LightCycler	Roche, Mannheim
Mighty Small™ II Gel Electrophoresis Unit	Hoefer Scientific Instruments, San Francisco, USA
OmniGene Thermal Cycler	Hybaid GmbH, Heidelberg
PET Scanner ECAT Exact	Siemens, München
Phosphorimager 445 SI, Storage Phosphorscreen GP, ImageEraser	Molecular Dynamics, Krefeld
Power Supply Model 1000/500 and Model 200/2.0)	BIO-RAD Laboratories GmbH, Munich
Power supply Multidrive XL	Amersham Pharmacia Biotech, Freiburg
Protean II xi cell	BIO-RAD Laboratories GmbH, Munich
Sonicator UP 200S	Dr. Hielscher GmbH, Stahnsdorf
T25 Ultra-Turrax	IKA-Labortechnik, Staufen
Thermomixer comfort	Eppendorf, Hamburg
Trans-Blot Cell System	BIO-RAD Laboratories GmbH, Munich
Transilluminator	Biometra, Göttingen
Ultracentrifuge L8-70M, Rotor TI 70.1	Beckmann Instruments GmbH, Munich
Uvikon Spectrophotometer 931	Kontron Instruments, Neufahrn

2.1.2 Material

		Order number
Aluminium Cooling Block with Capillary Adapters	Roche, Mannheim	
Jostent – Coronary Stent Graft	8F Judkins Right	
LightCycler Glass Capillaries	Roche, Mannheim	1909339
Multiple Gel Caster SE 200 Series	Hoefer Scientific Instruments, San Francisco, USA	
Nitrocellulose membrane	Schleicher & Schuell, Dassel	439396
Uvette (Cuvette) 220 – 1600 nm	Eppendorf, Hamburg	0030 106.300
Whatman paper	Schleicher & Schuell, Dassel	10426994

2.1.3 Chemicals

		Order number
1st Strand cDNA Synthesis Kit for RT-PCR (AMV) (30 reactions)	Roche, Mannheim	1483188
Acrylamide 30% (w/v): Bisacrylamide 0,8% (w/v) (ProtoGel)	Biozym, Hessisch Oldendorf	900200
Acrylamide:Bisacrylamide 40% (w/v) (29:1) (AccuGel)	Biozym, Hessisch Oldendorf	900150
AmpliTaq Gold	PE Applied Biosystems	N808-0241
Antifoam A	Sigma, Deisenhofen	A-5758
APS (Ammonium persulfate)	Sigma, Deisenhofen	A9164
BCA Protein Assay Protein Standard Stock Solution (2 mg/ml),	Pierce, Rockford, USA	UP 36859A,
Reagent A & B	Uptima	UP 95424A, UP 95425A
Bromophenol blue	Merck,Darmstadt	Art. 8122
Calcium chloride	Merck,Darmstadt	1.02382.0500
Chloroform	Sigma, Deisenhofen	C2432
Collagenase Type CLS II	Biochrom KG	C2-22
DATP	Amersham Pharmacia Biotech, Freiburg	27-2050-01
DCTP	Amersham Pharmacia Biotech, Freiburg	27-2060-01
DEPC (Diethyl pyrocarbonate)	Sigma, Deisenhofen	D5758
DGTP	Amersham Pharmacia Biotech, Freiburg	27-2070-01
DTTP	Amersham Pharmacia Biotech, Freiburg	27-2080-01
EDTA (Ethylenediamine-N,N,N',N'-tetraacetic acid)	Sigma, Deisenhofen	E0396
EDTA, pH 8,0	Life Technologies	15575-020
EGTA (Ethylene glycol-bis(2-aminoethyl)-tetraacetic acid)	Sigma, Deisenhofen	E3889
Ethanol, molecular biology grade	Calbiochem, Bad Soden	331542
Ethidium Bromide		
Glycerol	Sigma, Deisenhofen	G5516
Glycine	Sigma, Deisenhofen	G-8898
Hepes	Sigma, Deisenhofen	H3375
Hybridisation Probes	TibMolbiol	
Igepal Ca-630	ICN, Eschwege	198596
Isopropanol	Merck,Darmstadt	1.08544.0250
LightCycler – DNA Master Hybridisation Probes (480 reactions)	Roche, Mannheim	2158825
LightCycler – DNA Master SYBR Green I (96 reactions)	Roche, Mannheim	2015099
LightCycler – FastStart DNA Master Hybridisation Probes (480 reactions)	Roche, Mannheim	2239272
ß-Mercaptoethanol	Sigma, Deisenhofen	M7154
Methanol	Merck,Darmstadt	106018
Molecular Weight Marker VIII	Roche, Mannheim	1336045
NaOH 0.1 N	Merck,Darmstadt	109141.1000
PBS Dulbecco w/o Ca^{2+}/Mg^{2+} (ingredients see 2.1.5)	Biochrom KG, Berlin	L 1825
Plasmid pCR 2.1 GLUT1	GenExpress, Berlin	
Plasmid pCR 2.1 GLUT3		
Plasmid pCR 2.1 GLUT4		
Plasmid pCR 2.1 Cyclophilin		
Ponceau S	Sigma, Deisenhofen	P-3504
Potassium chloride	Merck,Darmstadt	4936.1000
Primer	TibMolbiol	
Rainbow coloured molecular weight marker	Amersham Pharmacia Biotech, Freiburg	RPN 800
RNase-free water	Eppendorf, Hamburg	0032 006.205
SDS (Sodium dodecylsulfate)	Biorad, München	161-0302
Skim milk powder	ICN, Eschwege	902887
	Altromin, Lage	-

Sodium azide	Sigma, Deisenhofen	S2002
Sodium chloride	Merck,Darmstadt	1.06404.1000
Sulfosalicylic acid	Sigma, Deisenhofen	S-2130
TaqStart Antibody	Clontech	5400-1
TBE 10 x, see 2.1.5	GibcoBRL	15581-036
Temed	Sigma, Deisenhofen	T7024
TRI Reagent	Sigma, Deisenhofen	T9424
Trichloroacetic acid	Merck,Darmstadt	1.00807.0250
Triton X-100 (Polyoxyethylene(10) isooctylphenyl ether)	Plusone / Pharmacia Biotech	17-1315-01
Trizma Base	Sigma, Deisenhofen	T1503
Tween 20	Sigma, Deisenhofen	P-1379
Xylene Cyanole	Sigma, Deisenhofen	X4126

2.1.4 PET-Tracers

Tracer	**Half-Life (min)**	**Physiological Process**
^{13}N-Ammonia	10,0	Perfusion
^{18}F-Deoxyglucose (FDG)	110	Glucose utilisation

2.1.5 Buffers And Gels

Blocking buffer	25	g	Skim milk powder	5,0	%
	2	ml	Tween 20	0,4	%
	1	ml	1,0 M $CaCl_2$	2,0	mM
	25	ml	1,0 M Tris pH 8.0	50,0	mM
	100	µl	Antifoam	0,02	%
	ad 500	ml	TBS		
Blotting buffer	8,4	g	Trisma Base	20	mM
	40,3	g	Glycine	153	mM
	0,7	l	Methanol	20	%
	ad 3,5	l	H_2O bidest		
Homogenisation buffer, pH 7,5	1191,5	mg	Hepes	20	mM
	73,0	mg	EDTA	1	mM
	95,0	mg	EGTA	1	mM
	81,3	mg	Sodium azide (NaN_3)	5	mM
	2516,4	mg	Potassium chloride (KCl)	135	mM
	ad 250	ml	H_2O bidest		
PBS, pH 7,3	8000	ml	NaCl	136,8	mM
	200	ml	KCl	2,7	mM
	1150	ml	Na_2HPO_4	8,0	mM
	200	ml	KH_2PO_4	1,5	mM
Polyacrylamide Gel (for cDNA)	12,9	ml	Acrylamide:Bisacrylamide (30:0.8)	5,7	%
	7,0	ml	10 x TBE	1	x
	49,4	ml	H_2O		
	0,7	ml	10 % APS	0,1	%
	70	µl	Temed	0,01	%
Ponceau S master solution	10	g	Ponceau S	2	%
	150	g	TCA	30	%
	150	g	Sulfosalicylic acid	30	%
	ad 500	ml	H_2O bidest		
Running buffer	6,0	g	Trizma Base	25	mM
	28,8	g	Glycine	190	mM
	20,0	ml	10% SDS	0,1	%
	ad 2000	ml	H_2O bidest		
Sample buffer	6,25	ml	2 M Tris, pH 6,8	125	mM
	40,00	ml	10% SDS	4	%
	20,00	ml	100% Glycerol	20	%
	ad 100	ml	H_2O bidest		
			+ bromphenol blue		
Separating gel 10%	21,57	ml	H_2O bidest	40	%
	11,25	ml	40% Acrylamide:Bisacryl-amide (29:1)	10	%
	11,25	ml	1,5 M Tris, pH 8,8	375	mM
	450	µl	10% SDS	0,1	%
	45	µl	Temed (>99%)	0,1	%
	450	µl	10% APS	0,1	%
	⇨ **1 Gel**				

Stacking gel 4%	9,45	ml	H_2O bidest	40		%
	1,50	ml	Acrylamide:Bisacrylamide (29:1)	4		%
			0,5 M Tris pH 6,8			
	3,75	ml	10% SDS	125		mM
	150	µl	Temed (>99%)	0,1		%
	15	µl	10% APS	0,1		%
	150	µl		0,1		%
	⇨ **1 Gel**					

Storage buffer	476,6	ml	Hepes	20		mM
	14,6	ml	EDTA	1		mM
	19,0	ml	EGTA	1		mM
	16,3	ml	Sodium azide (NaN_3)	5		mM
	250	µl	Triton X-100	0,5		%
TBS, pH 7,5	40	ml	1,0 M Tris, pH 7,5	20,0		mM
	100	ml	3,0 M NaCl	150,0		mM
	2	ml	Igepal CA	0,1		%
	ad 2	l	H_2O bidest			
Blocking buffer	25	g	Skim milk powder	5,0		%
	2	ml	Tween 20	0,4		%
	1	ml	1,0 M $CaCl_2$	2,0		mM
	25	ml	1,0 M Tris pH 8.0	50,0		mM
	100	µl	Antifoam	0,02		%
	ad 500	ml	TBS			
Blotting buffer	8,4	g	Trisma Base	20		mM
	40,3	g	Glycine	153		mM
	0,7	l	Methanol	20		%
	ad 3,5	l	H_2O bidest			
Homogenisation	1191,5	mg	Hepes	20		mM
buffer, pH 7,5	73,0	mg	EDTA		1	mM
	95,0	mg	EGTA	1		mM
	81,3	mg	Sodium azide (NaN_3)	5		mM
	2516,4	mg	Potassium chloride (KCl)	135		mM
	ad 250	ml	H_2O bidest			
PBS, pH 7,3	8000	ml	NaCl	136,8		mM
	200	ml	KCl	2,7		mM
	1150	ml	Na_2HPO_4	8,0		mM
	200	ml	KH_2PO_4	1,5		mM
Polyacrylamide Gel	12,9	ml	Acrylamide:Bisacrylamide (30:0.8)	5,7		%
(for cDNA)	7,0	ml	10 x TBE	1		x
	49,4	ml	H_2O			
	0,7	ml	10 % APS	0,1		%
	70	µl	Temed	0,01		%
Ponceau S master	10	g	Ponceau S	2		%
solution	150	g	TCA	30		%
	150	g	Sulfosalicylic acid	30		%
	ad 500	ml	H_2O bidest			
Running buffer	6,0	g	Trizma Base	25		mM
	28,8	g	Glycine	190		mM
	20,0	ml	10% SDS	0,1		%
	ad 2000	ml	H_2O bidest			
Sample buffer	6,25	ml	2 M Tris, pH 6,8	125		mM
	40,00	ml	10% SDS	4		%
	20,00	ml	100% Glycerol	20		%
	ad 100	ml	H_2O bidest + bromphenol blue			
Sample buffer (5x)			EDTA pH 8,0	70		mM
			Xylene Cyanole		0,25	%
			100% Glycerol		36,00	%
			Bromphenol blue	0,25		%
			H_2O RNase-free			
Separating gel 10%	21,57	ml	H_2O bidest	40		%
	11,25	ml	40% Acrylamide:Bisacryl-amide (29:1)	10		%
	11,25	ml	1,5 M Tris, pH 8,8	375		mM
	450	µl	10% SDS	0,1		%
	45	µl	Temed (>99%)	0,1		%
	450	µl	10% APS	0,1		%
	⇨ **1 Gel**					

Stacking gel 4%	9,45	ml	H_2O bidest	40		%
	1,50	ml	Acrylamide:Bisacrylamide (29:1)	4		%
			0,5 M Tris pH 6,8			
	3,75	ml	10% SDS	125		mM
	150	µl	Temed (>99%)	0,1		%
	15	µl	10% APS	0,1		%
	150	µl		0,1		%
	⇨ **1 Gel**					

Storage buffer	476,6	ml	Hepes	20	mM
	14,6	ml	EDTA	1	mM
	19,0	ml	EGTA	1	mM
	16,3	ml	Sodium azide (NaN_3)	5	mM
	250	µl	Triton X-100	0,5	%
TBE 10 x			Tris	1,0	M
pH 8,4 ± 0.1			Boric Acid	0,9	M
			EDTA	0,01	M
TBS, pH 7,5	40	ml	1,0 M Tris, pH 7,5	20,0	mM
	100	ml	3,0 M NaCl	150,0	mM
	2	ml	Igepal CA	0,1	%
	ad 2	l	H_2O bidest		

2.1.6 Antibodies and Peptides

Product	Dilution	Company
^{125}I-Goat-Anti-Rabbit IgG, 5-20 µCi/µg antibody (100 µCi/ml solution)		Amersham Pharmacia Biotech, Freiburg
Anti-GLUT1 (against human, mouse und rat): Polyclonal antibody directed against the Terminal carboxyl group (Thorens et al., 1990b; Thorens et al., 1990a)	1:800	Diagnostik International, Karlsdorf
Anti-GLUT3 (against human, AA-Sequence SIEPAKETTTNV) (Younes et al., 1997b), (Younes et al., 1997a)	1:2000	Chemicon International
Anti-GLUT3 (against mouse and rat)(Gould et al., 1992), (Nagamatsu et al., 1992), (Brant et al., 1992b), (Brant et al., 1992a), (Mueckler, 1994), (Baldwin, 1993)	1:800	Alpha Diagnostic, USA
Anti-GLUT3 (against mouse): Affinity purified antibody(Gould et al., 1992), (Nagamatsu et al., 1992), (Mueckler, 1994)	1:15000	Diagnostik International, Karlsdorf
Anti-GLUT4 (against rat): Antiserum directed against the terminal carboxyl group (Kahn et al., 1989)	1:800	Maureen Charron, Albert Einstein College of Medicine, New York, USA
Anti-HK-II (against human; host: goat): Affinity purified IgG(Katzen and Schimke, 1965), (Palma et al., 1996), (Arora et al., 1990), (Deeb et al., 1993), (Stoffel et al., 1992)	1:500	Linaris, Wertheim-Bettingen
Anti-HK-II (against rat, C terminal Sequence IREAGQR)(Tsai and Wilson, 1997; Tsai and Wilson, 1996)	1:800	Chemicon
Peptide GLUT3 human, AA--Sequence: SIEPAKETTTNV		Biotrend, Köln
Peptide GLUT3 mouse		Alpha Diagnostic, USA

2.1.7 Primers

		Sequence	Amplicon Length	Gene Bank Accession Nr.
GLUT1	**3´-Primer** **5´-Primer**	ATA CTg gAA gCA CAT gCC C TCC ACA AgC ATC TTC gAg AA	393 bp	X17058
GLUT3	**3´-Primer** **5´-Primer**	TTg gAg gAT CTC CTT AgC ATT CTC CCg ATT gAT TAT Tgg CCT CT	314 bp	AF054836
GLUT4	**3´-Primer** **5´-Primer**	TTC TTC CTT CCC AgC CAC TgA CTT CCA ACA gAT Agg CTC CgA A	319 bp	AF 141956
CYCL	**3´-Primer** **5´-Primer**	TCT Tgg CAg TgC AAA TgA AA CCC ACC gTC TTC TTC gAC	344 bp	C94597 AY008846*

* Overlapping sequences

2.1.8 Hybridisation Probes

GLUT1	**FL-Label** **LC-Label**	5´-gCC ggA gCC gAT ggT ggC ATA C X 5´-LC Red640-CAg gCT gCT gCA CCC CCg CCT T p
GLUT3	**FL-Label** **LC-Label**	5´-ATT CCA gCT gTC CTg CAg TgT gCC X 5´-LC Red640-CCC TTC CCT TTT gCC CTg AAA gTC C p
GLUT4	**FL-Label** **LC-Label**	5´-ACC ACC CTC Tgg gCT CTC TCC gT X 5´-LC Red640-CCA TCT TCT CTg Tgg gTg gCA TgT p
CYCL	**FL-Label** **LC-Label**	5´-CAg ggT ggT gAC TTC ACA CgC CAT X 5´-LC Red640-Tgg CAC Tgg Tgg CAA gTC CAT CTA T p

2.2 Methods

2.2.1 Acquisition and Preparation of the Hearts

2.2.1.1 Non-ischaemic Hearts

The non-ischaemic pig hearts were obtained from Munich's slaughterhouse. The domestic pigs there are six months old with a weight of about 100 kg. They are killed by a bolt shot against the forehead followed by an incision into the carotid artery. Subsequently they are hung up, the body is split in half and the thoracic and abdominal entrails are taken out. The heart was quickly removed after a few minutes and then immediately rinsed with ice-cold PBS solution to remove excess blood. Myocardial cross-sections were cut from apex to base producing slices of about 1.5 cm thickness. The slices were numbered starting at the apex with 1. The anterior wall was marked with a cannula and then was flashfrozen in liquid nitrogen (-196°C). The whole procedure was conducted in RNase-free material and solutions.

2.2.1.2 Ischaemic Hearts

2.2.1.2.1 Model of Chronic Ischaemia

We used hearts with an ischaemica-model applied by the department of cardiology, Großhadern, Ludwig-Maximilian-University Munich to induce a chronic one-week ischaemia in domestic pigs. It is based on a stent with a preformed stenosis, which is implanted in the LAD causing an initial stenosis degree of about 75 %. Although the pigs are treated with anticoagulant therapy and thrombocyte aggregation is inhibited for the whole period, the stenosis increases. The reason for this is not known exactly, but it is most likely that platelet aggregation occurs in spite of its inhibition. Intima proliferation in the bordering parts of the vessel may play a minor role. After one week cardiac echography, coronar angiography and PET studies are performed prior to scarification of the animal.

2.2.1.2.2 Animals

Female domestic pigs with an age of four months and a weight of 37.25 ± 1.5 kg were ordered from the Staatsversuchsgut Grub. Three days before intervention the pigs received a daily dose of 300 mg Clopidogrel and 100 mg Acetylsalicylic acid per os.

2.2.1.2.3 Anaesthesia

Anaesthesia and stent implantation took place in the Department of Experimental Oncology and Therapy Research. The pigs were sedated with an intramuscular injection of 1 mg Atropin, 2 mg/kg Azaperon and 10 mg/kg Ketamine. Then an i.v.-line was put into the ear vein through which the animals received 6 mg/kg Methylbarbiturate. After intubation they were ventilated with 1.5 % Isoflurane and 66% Nitrous oxide. In addition 4 ml/hour Propofol was administered intravenously. Afterwards, 500 mg acetylsalicylic acid and the antibiotic Benzylpenicillin were injected. Before the catheterisation and afterwards, if required, they were given Fentanyl for analgesia (starting bolus 0.05 mg). If required, Dopamine (50 mg in 500 ml normal saline) was also administered to obtain a stable heart rate.
During the operation oxygen saturation was measured as well as ECG. Arterial blood was taken for CBC, electrolytes and measurement of glucose, insulin and free fatty acids. Plasma and serum were obtained by centrifugation at 4°C.

2.2.1.2.4 Stent Implantation

Stent Preparation

The stent graft that was used contained a membrane avoiding leakage blood flow bypassing the stenosis. The stent was placed on a 1,7 mm cannula which served as the inner standard diameter. A 5/0 prolene suture was tied twice over the midportion, producing an initial stenosis of 75 % after fixing the stent in the left anterior descending artery. The stent was mounted on the balloon (3.0, 20 mm in length) of a delivery PTCA catheter and fixed by blocking the balloon slightly with 0.5 to 1.0 bar. Figure 4 shows the stent before and after inflating the balloon.

Figure 4 Stent graft with the double-tied suture (blue) before and after inflating the balloon

Catheterisation and Implantation

A central arterial line was placed in the carotid artery of the pig. 20 000 IE Heparin were administered and a coronary angiography performed to judge the pig's coronary status. After that the stent is placed just distal the first diagonal branch (D1) and fixed by inflating the balloon with approximately 16 to 20 bar. The result was documented by means of

angiography (see Figure 5). Figure 6 shows the position of the stent after excision of the heart.

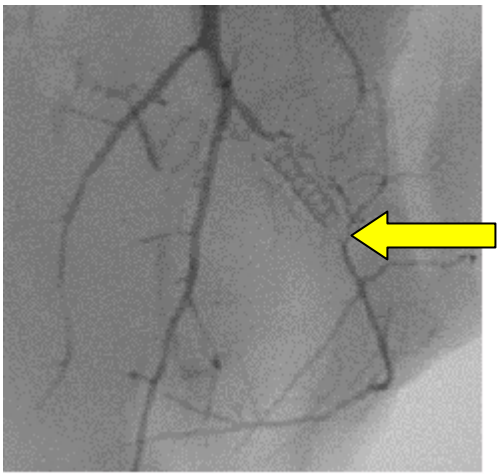

Figure 5 Angiography showing the placed stent (arrow)

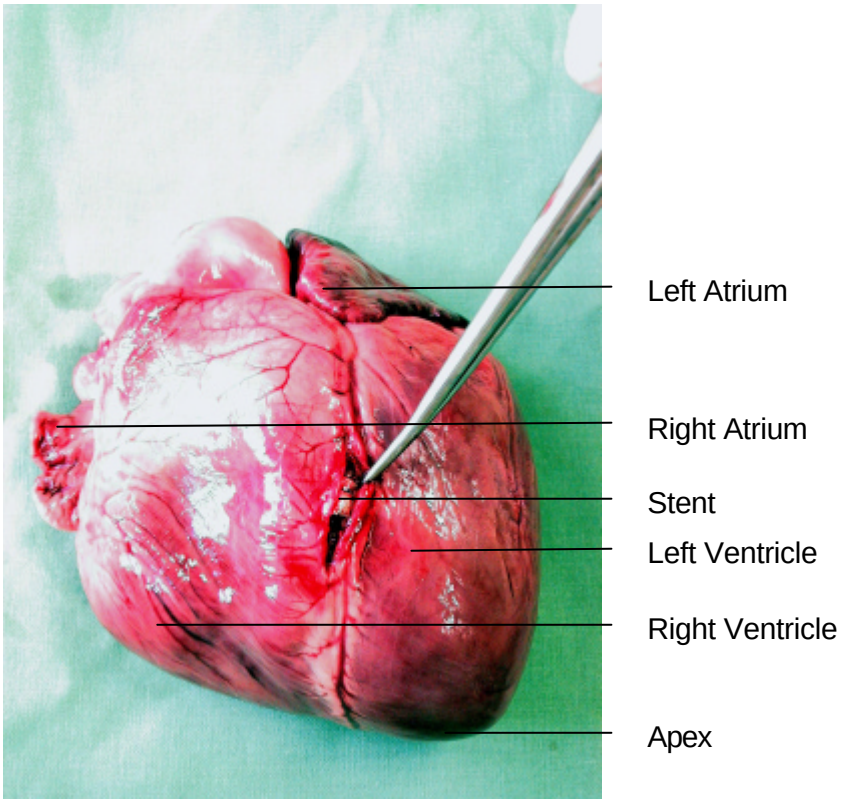

Figure 6 Excised heart showing the stent in the open LAD

A subcutaneous dose of 5000 IE of heparin continued the anticoagulant therapy. After stent implantation the pigs were given daily doses of 75 mg Clopidogrel and 100 mg acetylsalicylic acid orally and 5000 IE Nadroparin subcutaneously. On days 1, 2, 4 and 6 after intervention they were given benzylpenicillin and on demand 100 mg Carprofen.

2.2.1.2.5 Studies After One Week, Scarification

The pigs werer fasted for 12 – 16 hours prior to scarification. Only the medication was given as before. As described in 2.2.1.2.3, narcosis was performed. Prior to PET, a heart echo examination was done to visualize the hypokinesia of the anterior wall. Coronar angiography was undertaken to show the extent of the stenosis und probable collaterals.

Subsequently after the PET the animal was sacrificed by an overdose of Methylbarbiturate and an injection of potassium chloride. A thoracotomy was done and the heart removed immediately. Sampling procedure was identical to the non-ischaemic hearts from the slaughterhouse (see 2.2.1.1).

2.2.2 Positron Emission Tomography (PET)

PET was used to determine the myocardial blood flow (MBF) (with $^{13}NH_3$) and the myocardial rate of glucose utilisation (MRGU) (with ^{18}FDG). With the help of PET regions with increased FDG uptake and decreased MBF (mismatch) were revealed as well as regions with both decreased MRGU and decreased MBF (match). So they could be taken for tissue homogenisation for immunoblot and PCR (see 2.2.3.1.1).

2.2.2.1 Principle

PET studies are imaging studies showing function and metabolism in contrast to radiologic imaging studies showing morphology. The nature of the emitted radiation enables the construction of camera systems with high resolution to detect the resulting photons. Positron-emitting radionuclides are inherently unstable. When the high-energy positron is emitted from a nucleus, it rapidly loses energy and interacts with an electron to yield two photons emitted at an angle of approximately 180°, each with an energy of 511 keV, which can be detected by coincidence counting (detection of two photons by opposing detectors within a given time window of 5 to 20 ns) (Volkow et al., 1988) (Figure 7).

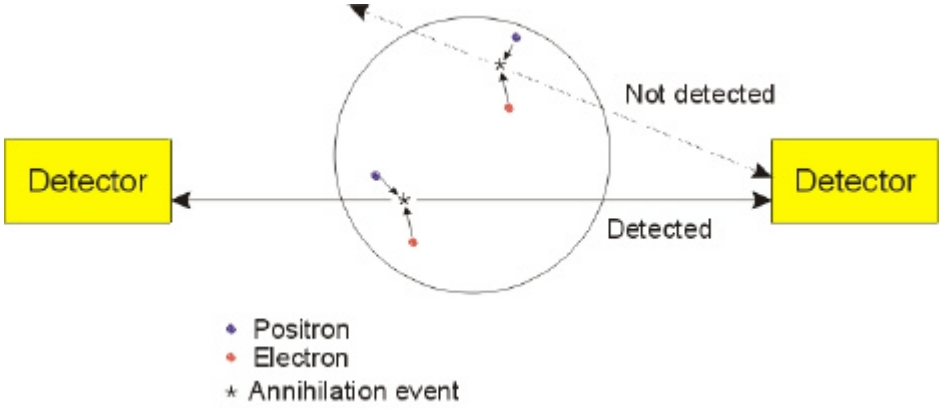

Figure 7 Schematic diagram of positron emission and annihilation photon detection

The data are reconstructed in three projections: short axis, horizontal long axis and vertical long axis (Figure 8).

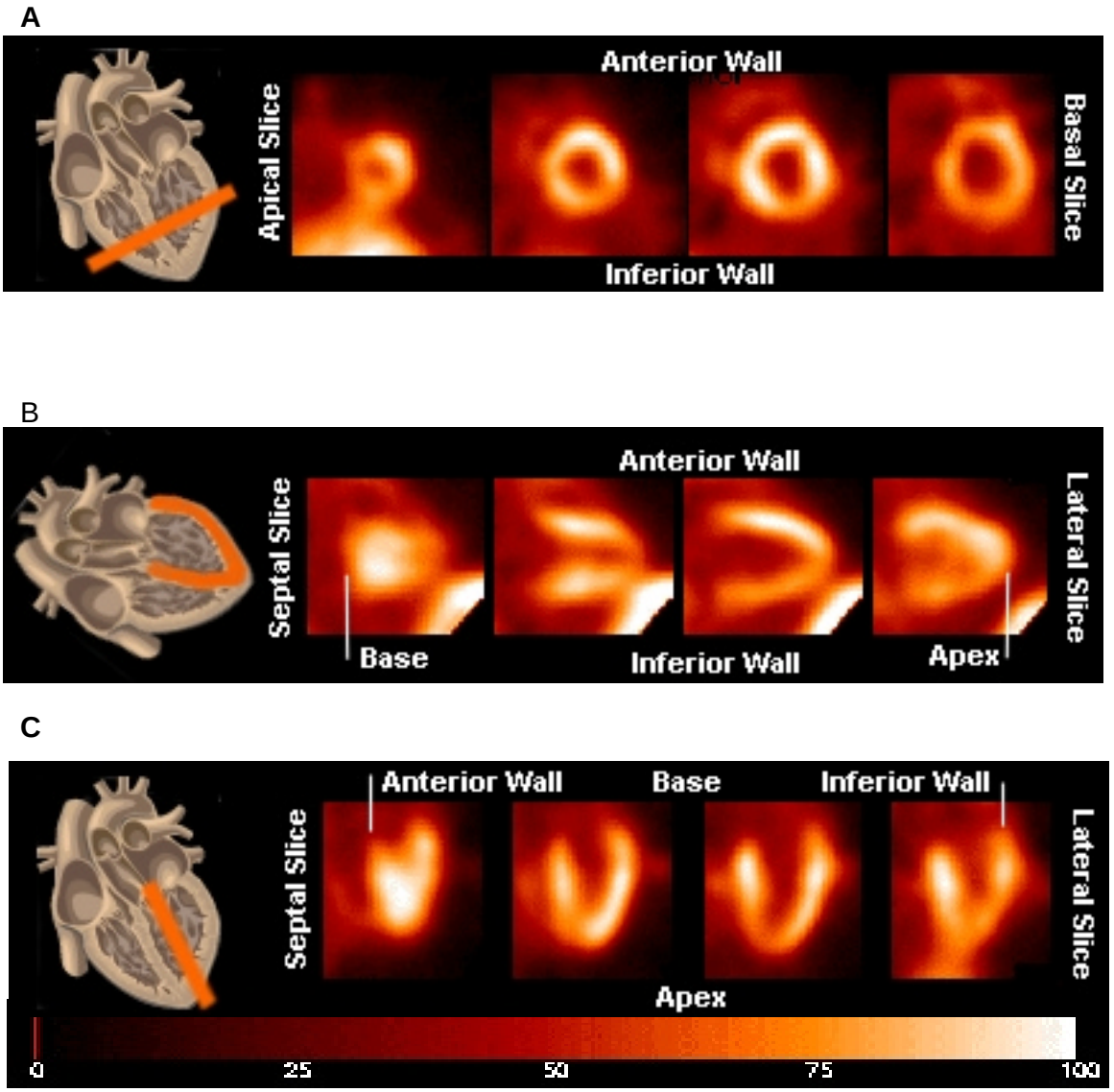

Figure 8 Short axis (A), vertical long axis (B) and horizontal long axis (C) reconstruction of a pig heart after the intravenous administration of ^{13}N ammonia

Radionuclides used for labelling other molecules in this study were ^{13}N (e.g. for ^{13}N-ammonia) and ^{18}F (e.g. for ^{18}F-deoxyglucose – FDG) (see 2.1.4). With these tracers it is possible to observe glucose utilisation (with FDG) and perfusion (with ^{13}N-ammonia) in cardiac PET quantitatively.

2.2.2.2 Tracers (Bergmann, 1997)

2.2.2.2.1 ^{13}N-Ammonia

^{13}N-labelled ammonia is used for measurement of myocardial perfusion. It is the cornerstone for diagnosis of perfusion defects and has a relatively prolonged retention by the heart of 80 to 400 minutes after i.v. injection while the blood-pool clearance is rapid. The trapping by the myocardium depends on conversion of ammonia to glutamine via the glutamine synthetase pathway (Bergmann et al., 1980).

2.2.2.2.2 ^{18}F-Deoxyglucose (FDG)

Metabolic dysfunction can be detected with this glucose analogon. This may provide early and/or more specific identification of derangements in the relationship between myocardial perfusion and metabolism. As described in 1.1.1 and 1.1.2 glucose becomes the predominant source for energy production in ischaemic conditions. Thus, observation of glucose metabolism with a positron emitting glucose analogon can detect an increased uptake of this analogon in hibernating regions and displays viable myocardium.

After entering a cell it is phosphorylated by the hexokinase(Phelps et al., 1983; Ratib et al., 1982). Further breakdown of FDG-6-phosphate is inhibited in contrast to Glucose-6-phosphate. Metabolism back to FDG is improbable because the required enzyme glucose-6-phosphatase is not highly expressed in. FDG-6-phosphate is trapped in the cell since this molecule is too polar to pass the sarcolemma

The intracellular concentration of FDG is proportional to glucose utilisation of the tissue (Gallagher et al., 1978). Under fasting conditions FDG uptake is markedly suppressed by fatty acids. This enhances the identification of ischaemic myocardium showing an increased FDG uptake (Tamaki et al., 1992). There are marked regional inhomogeneities of uptake in the heart, despite normal perfusion which seriously compromises interpretations made under fasting conditions (Gropler et al., 1990).

2.2.2.3 Method

To determine the MBF, 20 mCi ^{13}N-Ammonia were injected via a peripheral iv-line (bolus over 30 s) and the distribution of this tracer in the heart was measured dynamically for 10 minutes in time-frames of 12 x 10 s, 6 x 30 s and 1 x 300 s. Also, gated studies were performed then without further tracer application.

After measuring the actual blood glucose level 10 mCi FDG were injected in a bolus. Now in time-frames of 12 x 10 s, 6 x 30 s, 3 x 300 s and 2 x 600s the regional uptake of FDG was measured. As with ammonia gated studies were also performed for 20 minutes.

The acquired data was processed with dedicated software (Munich Heart). The defect sizes (expressed as percent of LV surface) were calculated for each tracer uptake using a threshold of 50%. Quantitative analysis of dynamic N13-ammonia images will be performed by kinetic modeling of Michigan, yielding regional assessment of myocardial blood flow (MBF = ml/g of myocardium/min). Values of MBF will be considered in the area of reduced N13-ammonia uptake (LAD territory) and remote area (Left circumflex artery territory). Quantitative dynamic FDG images will be processed by Patlak graphic analysis and regional values of the myocardial rate of glucose uptake MRGU) will be obtained (µmol/g of myocardium) in the same hypoperfused LAD and remote regions. The ECG synchronized images will be automatically processed using the Munich-Heart software to obtain values of global left ventricular function parameters: ejection fraction (LVEF %), end-diastolic (EDV) and end-systolic volumes (ESV).

2.2.3 Proteins

2.2.3.1 Membrane Preparation

2.2.3.1.1 Examined Regions

In order to create a sort of map of the distribution of the examined proteins in non-ischaemic and ischaemic hearts, representative samples had to be taken from different regions. In non-ischaemic hearts the left ventricle was divided into several regions in order to get an even more detailed view. In ischaemic hearts the left ventricle was divided into match, mismatch and remote region. Further, they were additionally divided into subendocardial and subepicardial as differences between these two parts have been reported (Brosius, III et al.,

1997a). Considering this, the following regions in non-ischaemic and ischaemic hearts were defined:

Non-ischaemic Hearts	Ischaemic Hearts
1. LV, anterior wall, subendocardial	1. LV, remote region, subendocardial
2. LV, anterior wall, subepicardial	2. LV, remote region, subepicardial
3. LV, lateral wall, subendocardial	3. LV, mismatch region, subendocardial
4. LV, lateral wall, subepicardial	4. LV, mismatch region, subepicardial
5. LV, inferior wall, subendocardial	5. LV, match region
6. LV, inferior wall, subepicardial	6. RV
7. LV, septum, subendocardial	7. Left Atrium
8. LV, septum, subepicardial	8. Right Atrium
9. Apex	
10. RV	
11. Left Atrium	
12. Right Atrium	

Ventricular regions in non-ischaemic hearts (with the exception of apex) came from the same slice of one particular heart, which was a slice from a midventricular section. In ischaemic hearts the area where the samples where taken from was based on the PET results and differed slightly from heart to heart (see Figure 9).

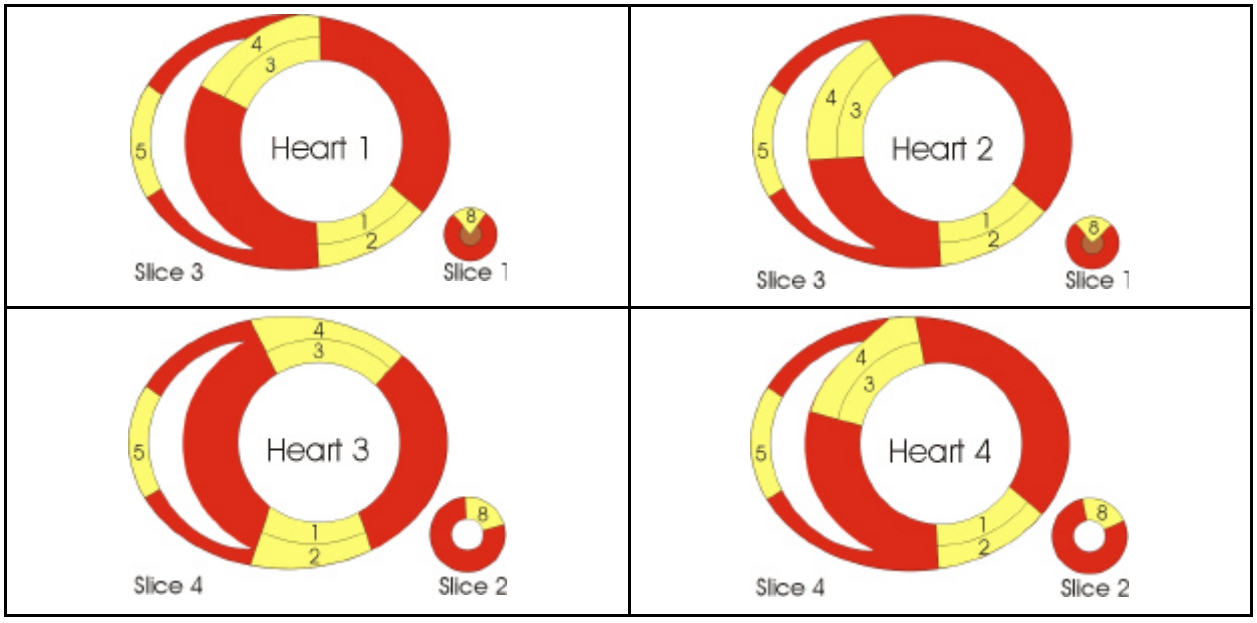

Figure 9 Examined Ventricular Regions of Ischaemic Hearts

2.2.3.1.2 Membrane enrichment

The aim of membrane preparation is to gain a membrane enriched protein fraction from tissue samples. This includes sarcolemma as well as intracellular membranes. Both include glucose transporters, which are typical membrane proteins.

To slow down the reactions of proteases and other hydrolysing enzymes during the preparation all steps were performed at 4°C. A small piece weighing between 0.5 and 0.8 g was cut out of the slices kept at –70°C. It was washed with cold PBS to remove blood. Macroscopical visible vessels and connective tissue were cut off with a razor blade.

A modified homogenisation buffer according to Ryder (Ryder et al., 1999) which was mixed with collagenase (1.1 g/ml) was added to the tissue (about 5 ml/g tissue) (see 2.1.5). The collagenase is added for digestion of connective tissue in the sample (Fischer et al., 1991) with the aim to improve sample handling (exact pipetting).

The tissue was pre-cut with a razor blade and chopped up for about 15 minutes to get a homogenous mash of tissue. Further homogenisation was achieved by an Ultra Turrax (2x 20s, 10 000 rpm) with a medium dispersion tool (10G). At the end cells were sheared by a glass-glass-homogeniser (potter) (10x). Afterwards the sample's volume was documented. The homogenate was then incubated for 15 minutes at 37°C to be in the range of the temperature optimum of the collagenase.

100 µl of this fraction was then diluted with 200 µl of storage buffer (see 2.1.5) and stored at –70°C (CH-fraction). The main part of the sample was centrifuged for 10 minutes (300 x g and 4°C) to remove non-destroyed cells, detritus and nuclei from the supernatant. The pellet was discarded and the supernatant was centrifuged again for one hour in the ultra centrifuge (4°C, 170000 x g). This pellet now contained the entire membrane fraction (plasma membrane, mitochondria, lysosomes, peroxisomes, endoplasmatic reticulum and endo-/exocytotic vesicles)(McNamee, 1989). It was diluted with 200 µl storage buffer and stored frozen at –70°C. After re-thawing it was resuspended with additional 500 µl storage buffer and then kept as the membrane fraction (170000 x g fraction).

2.2.3.2 Protein Determination Assay

50 µg of protein per sample were routinely loaded on a gel. Therefore the protein concentration in the sample had to be estimated. It was determined by the method of Pierce (BCA Assay).

The BCA Assay is a colorimetric assay. The central reaction is the reduction of Cu^{2+} to Cu^{+} by the peptidic bonds of proteins. This bicinchoninic acid chelates Cu^{+} ions with very high specificity and forms a purple coloured water soluble complex.

As the progress of the reaction increases by high temperature and continues over time, the reaction should be read at a defined time and low temperature conditions.

The final Cu^{+} complex has a maximum optical absorbance at 562 nm where the reaction is measured. This absorbance is directly proportional to protein concentration and has a broad linear range between 5-20 µg/ml and 1-2 mg/ml. To calculate the concentration a reference curve for a standard protein has to be obtained.

The assay was performed according to the manufacturer's protocol.

2.2.3.3 SDS-PAGE

SDS-PAGE was performed according to the protocoll introduced by Laemmli (Laemmli, 1970) (ingredients see 2.1.5). It additionally contained the tracking dye bromophenol blue and glycerol to increase the weight of the sample. Thus, it sinks to the ground of the well. At last ß-mercaptoethanol is added to reduce disulfide bonds.

The calculated aliquot of the sample referring to 50 µg protein is mixed with the sample buffer at a ratio of 1:1 but at least with 25 µl. Additionally a molecular weight marker was applied. The rainbow marker RPN 800 was used for this (Amersham Pharmacia Biotech, Freiburg) and shows bands from 250 kDa to 10 kDa in different colours. 15 µl of the marker was mixed with 20 µl sample buffer and applied to the gel with a Hamilton syringe.

Electrophoresis was started with a constant current of 50 mA per gel and a voltage limitation of 390 V for a run lasting about 3.5 hours. To prevent warming of the gel it was cooled to 8 °C in a closed system which pumps the cold water through the system's cooling core during the run.

Following this process, the gel was cut for optimal size (empty lanes, stacking gel and the part below the bromophenol blue of the separating gel were removed) and washed in blotting buffer for 15-30 min to remove SDS, which interferes with the transfer to nictrocellulose.

2.2.3.4 Western Blot

2.2.3.4.1 Transfer

Method

For the transfer a vertical buffer tank system was used. Two whatman filter papers were cut to gel-size + 1 mm on each edge. The edges of the nitrocellulose membrane were 2 mm longer than those of the gel. Nitrocellulose was watered with H_2O bidest and the blotting sponge pads and whatman paper were watered in blotting buffer. The gel and blotting membrane were clamped in grids between the whatman papers and the sponge pads (see Figure 10). The chamber was filled with blotting buffer and the transfer took place over night at 4 °C with a constant voltage of 15V.

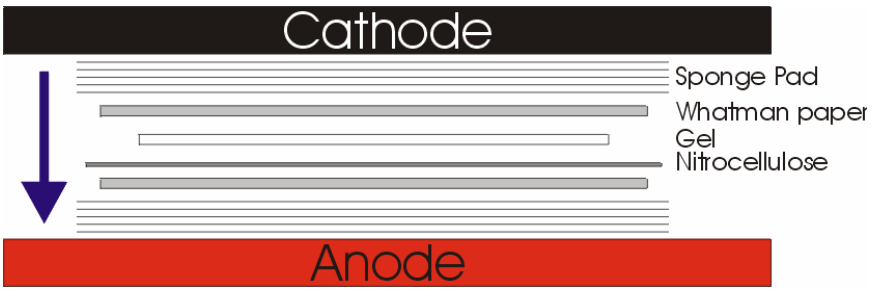

Figure 10 Electrophoretic Tank Blotting

2.2.3.4.2 Ponceau S Staining

Prior to the immunodetection of the proteins the reliability of the blot was documented through reversible ponceau S staining. For staining the membrane was placed in the 1:10 diluted stock solution of ponceau S for 30 s (ingredients see 2.1.4) after washing in PBS (see 2.1.5) for 5 minutes. Surplus dye was removed by H_2O bidest until the red coloured bands were visible. Thus, transfer defects due to air bubbles in the blotting stack, were easy to detect. This was documented with a copier. Then the membrane was destained completely in TBS.

2.2.3.4.3 Blocking

To prevent unspecific antibody binding, the membrane had to be blocked with macromolecular substances, e.g. 5% skimmed milk, which must not take part in the ensuing reactions. This

background-blocking was performed with a blocking buffer (ingredients see 2.1.5) at 37°C for 90 minutes.

2.2.3.5 Specific Detection of Proteins

The detection of the examined proteins utilises the binding of a specific antibody (primary antibody) to the proteins. In a second step a radioactive labeled immunoglobuline G (secondary antibody) binds to the constant region of the primary antibody.

2.2.3.5.1 Primary Antibody

The primary antibodies were diluted in 0.1 % sodium azide containing blocking buffer with dilutions of 1:800 for GLUT1, GLUT4 and hexokinase. Different GLUT3 antibodies were tested with varying dilutions (see 2.1.6).

The nitrocellulose membrane was sealed in a transparent film bag. The antibody solution was added and incubated at room temperature for two hours. The solution was recycled several times. Before incubating with the secondary antibody the membrane was washed (6 x 6 minutes) in TBS in order to remove unbound antibody to get decreased background radiation.

2.2.3.5.2 Secondary Antibody

^{125}I-labeled goat-antibody directed against rabbit was used. The antibody was diluted in blocking buffer. The incubation was performed as described in 2.2.3.5.1. Afterwards the membrane was washed in TBS again (6 x 6 min).

2.2.3.5.3 Phosphor Imager

To visualize and quantify the bands containing the measured enzymes a phosphor imager was used. It uses special screens to which the membrane had to be exposed.

Principle

The screens of the phosphor imager consist of salts containing europium (Eu^{2+}). Exposition to beta particles, X-rays and, as is the case with immunoblotting, gamma rays induces elevation of electrons into a metastable condition. The laser of the phosphor imager supplies further energy and they are elevated even more before they fall back to their stable basic condition while emitting light. This emitted light from the screen is proportionate to the amount of radioactivity in the sample and can be detected by the scanner. The resulting digital image of the phosphor imager allows quantification of subtle signal intensity differences with a specific computer program.

Method

After the last washing step the membrane is dried, sealed in a transparent film and placed in an exposure cassette with the screen for at least 12 hours. Afterwards the screen is scanned by the phosphor imager. The software (latest version: Image Quant 5.1) produced an image of the gel (see Figure 11).where bands could be marked for quantification

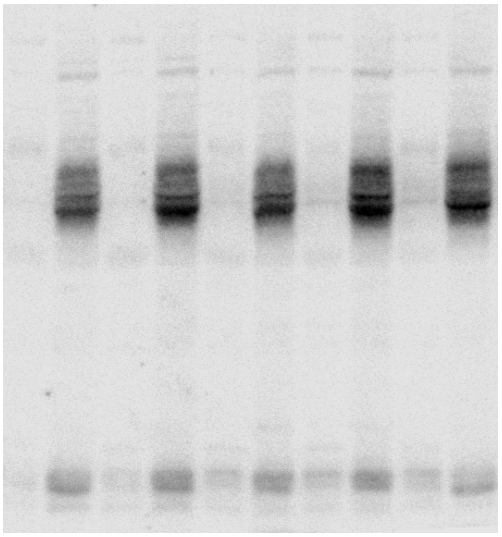

Figure 11 Example of a blot incubated with anti-GLUT4

To compare the samples from different regions and different hearts an internal standard was prepared by pooling 4 membrane preparations from the left ventricle and applying it to each gel. On each of the gels this “standard” sample was on one lane. Thus, it could be assumed that this lane represented - independent from other conditions – a constant amount of each of the enzymes. Therefore, all the samples were comparable by normalizing them to this internal standard and could be quantified relatively.

2.2.4 RNA

2.2.4.1 Handling of RNA

Since RNA is more susceptible to degradation than DNA, the following procedures were conducted under standard conditions recommended for working with RNA.

DEPC water: To destroy RNases 1 l bidest water was treated with 0,1 % (v/v) DEPC over night. This substance is thermolabil and is destroyed by autoclaving the solution twice.

2.2.4.2 Tissue Homogenisation and Extraction of RNA

The samples for homogenisation were taken from the same regions 1 – 7 (8) as for immunoblotting (see **2.2.3.1.1**). Homogenisation and RNA extraction is based on the method introduced by Chomczynski, which uses a patented monophasic solution containing phenol, guanidinium thiocyanate, buffer and solvents.(Chomczynski and Sacchi, 1987)

2.2.4.2.1 Principle of RNA Isolation with TRI Reagent™

The procedure is very effective for isolating all types of RNA molecules from 0,1 to 15 kb in length. The resulting total RNA is intact with little or no contaminating DNA and protein due to the presence of guanidinium thiocyanate, which is a very effective protein denaturant. After centrifugation with chloroform the homogenate is separated into three phases: The aqueous phase containing RNA, the interphase DNA and the organic phase proteins. RNA is extracted from the aqueous phase by precipitation with isopropanol. With this method a typical yield of 1 – 1.5 µg RNA / mg tissue is achieved from (skeletal) muscle tissue.

2.2.4.2.2 Method

Prior to RNA extraction the piece of tissue was minced and homogenised. A piece of 50 to 100 mg tissue was minced in 1 ml TRI Reagent with the Ultra Turrax tool (see 2.1.1) at 24000 rpm for 1 minute. To avoid warming the homogenate was immediately put on ice again (for about 1 minute) and homogenisation completed by sonicating the sample with a frequency of 24 kHz and amplitude of 170 µm for 15 to 30 seconds. The resulting homogenate was either stored at –70°C or used for immediate RNA extraction (= isolation).

At the beginning of RNA extraction the homogenate had to incubate for 10 minutes at room temperature. During this time the denatured proteins could separate and solve from the nucleic acids.

Per millilitre TRI Reagent 0.2 ml chloroform was added and shaken manually for 15 seconds. The mixture was left for 5 minutes and then centrifuged (12000 x g, 15 minutes, 4°C). The aqueous RNA-containing supernatant was precipitated with 0.8 to 1.0 ml isopropanol for 10 minutes at room temperature followed by a further centrifugation step (12000 x g, 15 minutes, 4°C). The resulting pellet was washed superficially with 1 ml 75% ethanol. It was again centrifuged (12000 x g, 10 minutes, 4°C), air-dried at room temperature and resuspended with RNase-free water using the thermomixer (65°C) (see 2.1.1) for 5 minutes.

2.2.4.2.3 Photometrical Determination of RNA Concentration and Purity

The RNA concentration and purity can be determined photometrically. A 1:100 dilution of each sample was placed in a UV-suitable cuvette in order to read the optical density (OD) at 230, 260, 280 and 325 nm. Absorbance readings at 260 nm measure RNA concentration and should be greater than 0.15 to ensure significance. An absorbance of 1 unit at 260 nm corresponds to a concentration of 40 µg of RNA per millilitre of water. From the known RNA concentration the yield (µg RNA per mg tissue) can be calculated. It should be higher than 1 µg RNA / mg tissue.

The ratio between the absorbance at 260 and 280 nm gives an estimate but not a definitive assessment of RNA purity. This ratio is influenced by the pH value. As water is unbuffered, the same RNA sample may show different A_{260}/A_{280} ratios in different types of water, ranging from 1.5 to 1.9. However, it should not be smaller than 1,5. Furthermore, RNA itself can influence the pH value (Quiagen, 1999; Sambrook J. et al., 1989). The 260 nm reading is taken near the top of a broad peak in the absorbance spectrum of nucleic acids, whereas the 280 nm reading is taken on a steep slope. Therefore, small variations in wavelength in the region around 280 nm have a greater effect on the ratio than will variations at 260 nm. Thus, different instruments may give slightly different ratios due to variations in their wavelength accuracy. In this work we always used the same instrument (see 2.1.1).

Absorbance at 230 nm is very close to the absorbance minimum of nucleic acids and nucleotides. An elevated absorbance can be caused by:

- Protein contamination as the wavelength is near the absorbance maximum of peptide bonds
- Organic compounds (e.g. guanidinium thiocyanate). To exclude such a contamination the A_{260}/A_{230} ratio should be higher than 2.0.
- Buffers as Tris, EDTA and other buffer salts (Dadd Andrew, 1996).

Absorbance at 325 nm is mainly due to light scattering effects and indicates particulates in the solution or dust at the surface of cuvettes.(Gallagher Sean R. and Smith John A., 1994) In all RNA samples investigated in this study absorbance at 230 nm and 325 nm was negligible.

However, contamination with ssDNA or dsDNA cannot be excluded photometrically. $A_{260} = 1$ corresponds to 40 µg RNA/ml or ssDNA/ml and also to 50 µg dsDNA/ml. This can only be detected by a negative control in the RT reaction (see 2.2.4.3.2).

At the end the obtained RNA solution was stored at –70°C.

2.2.4.3 Reverse Transcription

2.2.4.3.1 Principle

Isolated RNA was converted into cDNA by reverse transcription. Reverse transcription is catalysed by the enzyme AMV Reverse Transcriptase. It is an RNA-dependent 5'? 3' DNA polymerase. A complementary primer (DNA oligonucleotide) with a 3' hydroxyl group has to be bound to the RNA as substrate. In this work an oligo-dT-primer was used. In contrast to other kinds of primer this one binds to the poly-A-tail, which is specific for mRNA.

Avian Myeloblastosis Virus (AMV) Reverse Transcriptase is one of two commercially available reverse transcriptases besides Moloney murine leukemia virus (Mo-MLV) Reverse Transcriptase.

Both enzymes lack 3'? 5' exonuclease activity on DNA. Thus, during elongation there is no repair, which is necessary about every 500^{th} base because of random integration of a non-complementary nucleotide. On RNA they show RNase H activity (5'? 3' as well as 3'? 5' exoribonuclease activity) which degrades the RNA in RNA:DNA hybrids.

AMV Reverse Transcriptase exerts a relatively strong RNase H activity, which can be disadvantageous when synthesizing long strands because RNase- and polymerase activity compete. But AMV's advantage is its high temperature optimum (42°C). This results in a high efficiency in copying RNA molecules with lots of secondary structures.

2.2.4.3.2 Method

RNase Inhibitor and AMV Reverse Transcriptase were thawed on ice. All other solutions were thawed at room temperature and then kept on ice. Before starting all reagents were

briefly centrifuged. This ensures that the (sometimes very) small volume is collected at the bottom of the tubes.

Because of the very small volume of one single reaction a so-called master mix was prepared according to Table 2.

Table 2 Master mix for reverse transcription

Reagent	Volume per Sample [µl]	Final Concentration
10x Reaction Buffer	2,0	1x
25 mM $MgCl_2$	4,0	5 mM
Deoxynucleotide Mix	2,0	1 mM
Oligo-p$(dT)_{15}$ Primer	2,0	0,04 A_{260} units (1,6 µg)
RNase Inhibitor	1,0	50 units

Per reaction the master mix included 0,8 µl AMV Reverse Transcriptase, which was replaced by sterile water in the case of the negative controls. In each case 1 µg RNA was added to a final volume of 20 µl per reaction. The content was mixed and centrifuged. The tubes were incubated for 10 minutes at room temperature to allow primer annealing to the RNA template. During the following incubation step at 42°C for one hour the cDNA is synthesized by the AMV Reverse Transcriptase. To stop the reaction the samples were heated to 99°C for 5 minutes, which denatures the enzyme. Otherwise AMV Reverse Transcriptase may interfere with subsequent applications. Then the samples were cooled to 4°C and were either used immediately for PCR or stored at -20°C.

For each sample a positive reaction (containing AMV) and a negative control was prepared. The intention of preparing negative controls (“minus AMV”) was to obtain a measurement of the contamination with genomic DNA (ssDNA and dsDNA) in the RNA samples. As mentioned in 2.2.4.2.3 DNA contamination cannot be detected photometrically. However, it may give rise to primer-specific amplification in subsequent PCR reactions. In RNA samples not subjected to reverse transcription (negative control) contaminating genomic DNA accounts for the formation of PCR products. Therefore, if copy numbers were detected in negative controls they were subtracted from the positive samples at the end of data analysis.

2.2.4.4 Polymerase Chain Reaction

PCR was used in order to quantify the initial amount of cDNA of GLUT1, GLUT3 and GLUT4 in each sample. These values were normalised by the house-keeping gene cyclophilin

(Haendler et al., 1987). Since there was no porcine nucleotide sequence of hexokinase type II available, the mRNA content of this enzyme could not be measured and quantified.

2.2.4.4.1 Conventional PCR

PCR is a method introduced by Kary Mullis in 1983. In this work conventional PCR was used to establish this method with pig GLUT1, 3 and 4 mRNA.

In a final volume of 50 µl per reaction the reagents shown in
Table 3 were needed:

Table 3 Components for conventional PCR

Volume		***Final Concentration***
0,5 µl	Taq DNA Polymerase	2,5 units
5,0 µl	10 x PCR buffer	1 x
5,0 µl	Magnesium chloride solution (25 mM)	2,5 mM
19,5 µl	Rnase-free water (no DEPC water)	
8,0 µl	Deoxynucleotides (dNTPs Mix) (5 mM)	0,8 mM
5,0 µl	5'-Primer (10 µM)	1,0 µM
5,0 µl	3'-Primer (10 µM)	1,0 µM
2,0 µl	Sample with the DNA to be amplified	

To start the PCR the chemically modified Taq polymerase (see 2.1.3) was activated at 95°C for 9 minutes. Then 35 cycles of melting (1 min, 95°C) – annealing (2 min, 62°C) and elongation (3 min, 72°C) were performed. This PCR was done to establish and optimise the PCR protocol, i.e. different annealing temperatures between 56°C and 64°C (see 3.3.1.2) and different $MgCl_2$ concentrations were tested.

Assessment of PCR Results With PAGE and Ethidium Bromide Staining

Following conventional PCR, amplification products were checked for their size and homogeneity in an ethidium bromide stained PAGE.

The PCR samples (50 µl) were mixed with 12.5 µl sample buffer (5 x sample buffer, see 2.1.5) and 10 µl were applied to the gel. In addition 5 µl of a base pair marker mixed with 1 µl sample buffer were applied to the gel. The mini-gels were poured into a multiple gel caster (see 2.1.2 nd 2.1.5). Unused gels can be stored in TBE buffer (ingredients see 2.1.5) at 4°C. Electrophoresis was performed with a constant voltage of 80 V and 1 X TBE as the running buffer.

After the run the bands were made visible by ethidium bromide staining, which is an intercalating, orange fluorescent dye at a wavelength of 366 nm. Gels were stained in 0,5 µg ethidium bromide / ml TBE for 20 – 30 minutes and then washed in TBE or H_2O for 20 minutes.

Exposing the gel to ultraviolet light showed the DNA bands. To document the result a picture was taken with a Polaroid camera (see Figure 12):

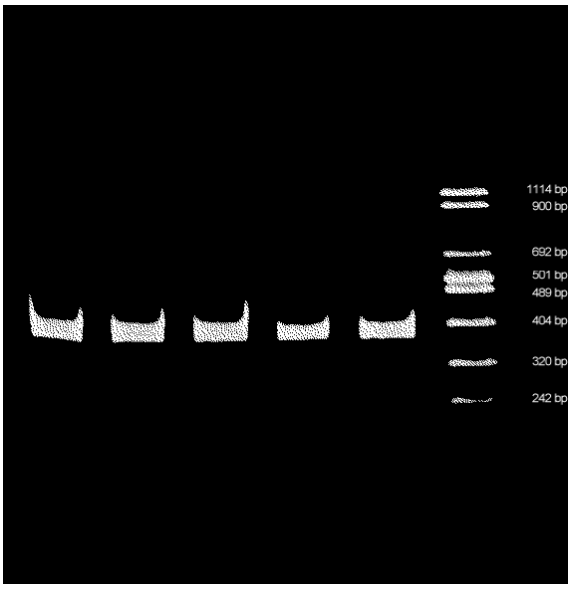

Figure 12 Representative gel showing GLUT1 bands and the marker

2.2.4.4.2 Real-time PCR with the LightCycler Instrument

2.2.4.4.2.1 Principle

In the past RNA quantification was achieved either by Northern blotting or by competitive conventional PCR. Both methods require electrophoretic separation of a radioactive-labelled probe for detection and quantification. In contrast, LightCycler PCR offers the opportunity for target quantification without further handling. This instrument measures a template-specific fluorescence emission from single samples in each cycle during a PCR run. Thus, changes in amplicon concentration can be observed in real-time.

The LightCycler consists of the heating coil, the thermal chamber containing the samples, the drive units and the electronic boards (see Figure 13). Hot or ambient temperature air, introduced into the thermal chamber, regulates the temperature of the samples, which are in thin glass capillaries. They have a high surface-to-volume ratio being responsible for a ramp rate of about 20°C per second. Thus, one cycle takes about 30 seconds in comparison to 6 minutes in a conventional PCR.

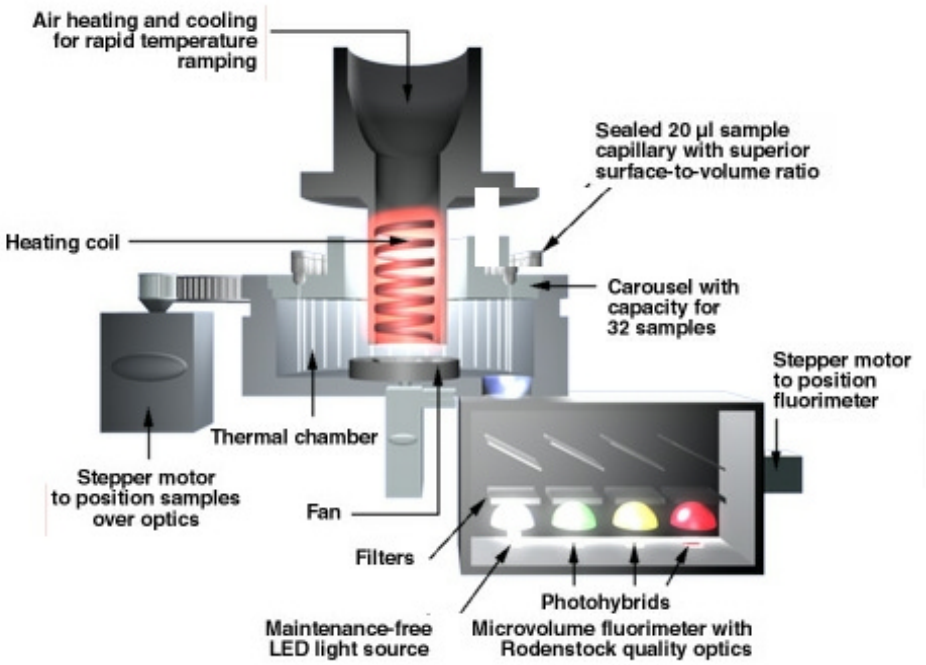

Figure 13 Scheme of the LightCycler Construction (Roche Molecular Biochemicals, 2000)

To generate a detectable fluorescence, two alternative methods exist:

- SYBR Green I as fluorescent dye
- Hybridisation probes tagged with fluorophores

SYBR Green I is an intercalating substance like ethidium bromide. However, it is much less mutagenic and more sensitive (see www.clarechemical.com). The fluorescence signal is proportional to the amount of double strands in the capillary. However, it does not illustrate the amount of a specific sequence.

Hybridisation probes account for high specificity of the signal due to the specific binding of fluorescent probes during the annealing step of each PCR cycle. In addition to the reaction components used for

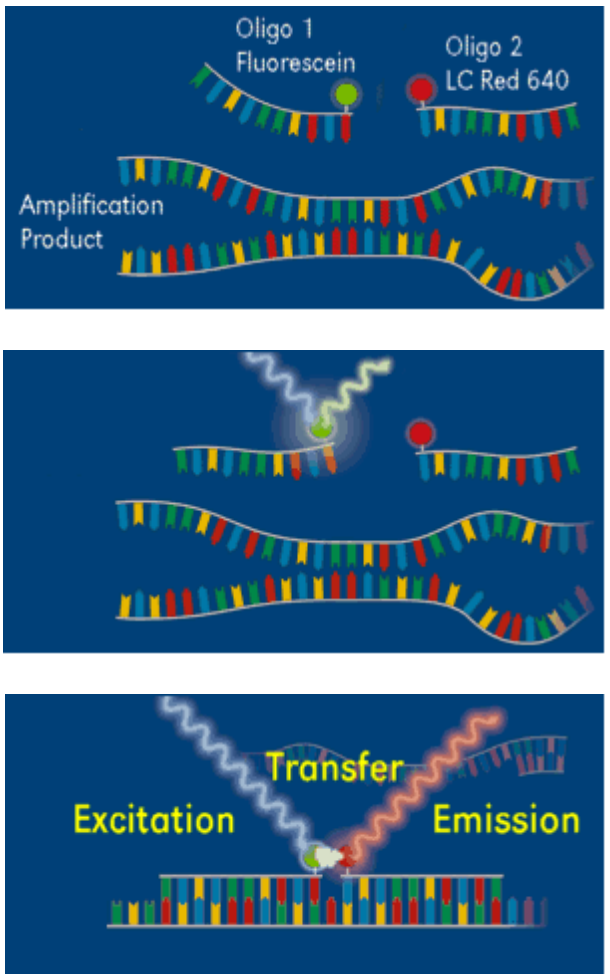

Figure 14 Principle of Hybridisation Probes

conventional PCR, two specially designed, sequence specific oligonucleotides labelled with fluorescent dyes are applied for this detection method (see Figure 14). Oligonucleotide 1 (Oligo 1) carries a fluorescein label at its 3' end whereas oligonucleotide 2 carries LC red 640 at its 5' end. Fluorescein is excited by the LightCycler's Light Emitting Diode (LED) and emits green fluorescent light at a slightly longer wavelength (middle figure). The sequences of the two oligonucleotides are selected such that they hybridise to the amplified DNA fragment in a head to tail arrangement. Hybridisation in this orientation positions the two fluorescence dyes in close proximity to each other. In this case excitation of fluorescein induces excitation of LC Red640 via "fluorescence resonance energy transfer" (FRET), which subsequently emits a red fluorescent light. FRET is highly dependent on the spacing between the two dye molecules. Only if the molecules are in close proximity (1-5 nucleotides in distance) excitation energy is transferred with high efficiency. The light emitted by LC Red 640 is filtered and measured by the LightCycler's optics. This allows specific detection of the amplification product. The increasing amount of measured fluorescence is proportional to the increasing amount of target DNA generated during the ongoing PCR process. Since the signal is only emitted when both oligonucleotides are hybridised, the fluorescence measurement is performed after the annealing step.

For hybprobe design the following points were considered:

- The sequence should be near the 3'-end of the target strand but should not overlap the primer binding-site (see Figure 15)

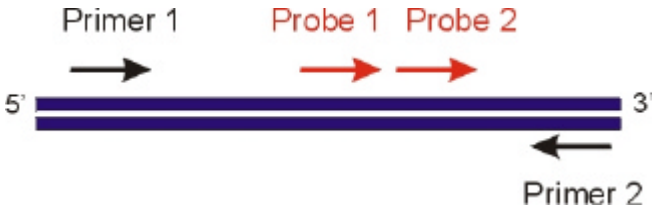

Figure 15 Relative Positions of Primers and HybProbes

- No repetitive or monotonous sequences, as they cause "slipping" of the probes
- No self-complementary sequences, as they may form loops
- No clusters of Gs or Cs at either end of the probe, which might cause too tight a binding of the probe to the target
- No extremely rich content of purines (G or A), as they may hybridise poorly then
- No sequences that may hybridise with primers to prevent primer-probe dimers (Roche Molecular Biochemicals, 2000)

- The melting temperature was to be 5-10°C higher than that of the primers but not more than 20°C higher

When performing a real-time PCR with hybprobes the fluorescence signal changes during the run as demonstrated in Figure 16. It shows three concentrations, which differ by the factor 10, and a negative control (all of them measured twice). The real-time PCR is performed with GLUT4 primers and hybprobes. Since theoretically the copy number is doubled in each cycle the curve equals an exponential curve at the beginning but later shows saturation and therefore, has a sigmoid character. The method to calculate the concentration uses the point when the curve leaves the background noise ("crossing point"). This point is proportional to the initial copy number. The quantity of the fluorescence signal is not used since this would be a measurement under conditions where the samples are in saturation for different periods of time. It would be an endpoint analysis then as employed for the previous quantification methods (see above).

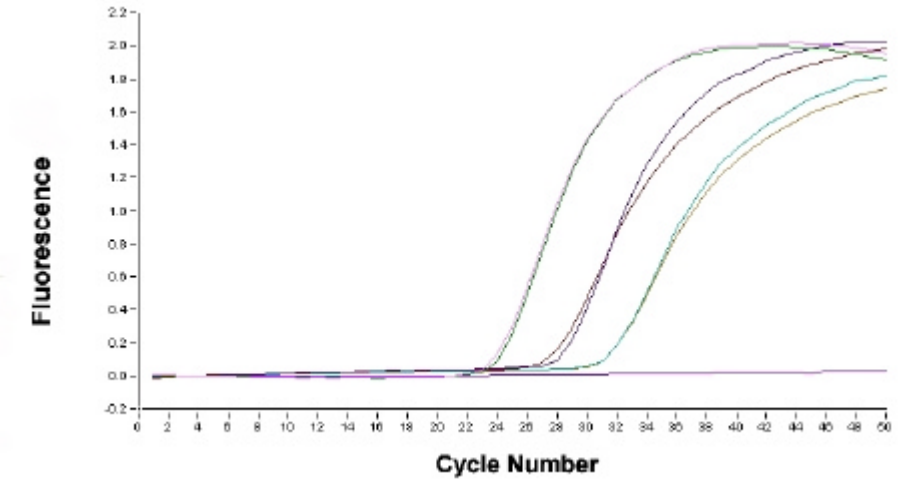

Figure 16 Fluorescence signal obtained with GLUT4 hybridisation probes

The advantage of real-time PCR is that measurement is done in the log-linear phase. After defining the background noise, the specific computer software calculates the initial copy number. Figure 16 also shows that samples with a concentration difference of factor 10 result in crossing points that differ by approximately 3,3 cycles, which equals the theoretical value $\log_2 10$. Figure 17 shows the determination of the crossing points after removing background noise.

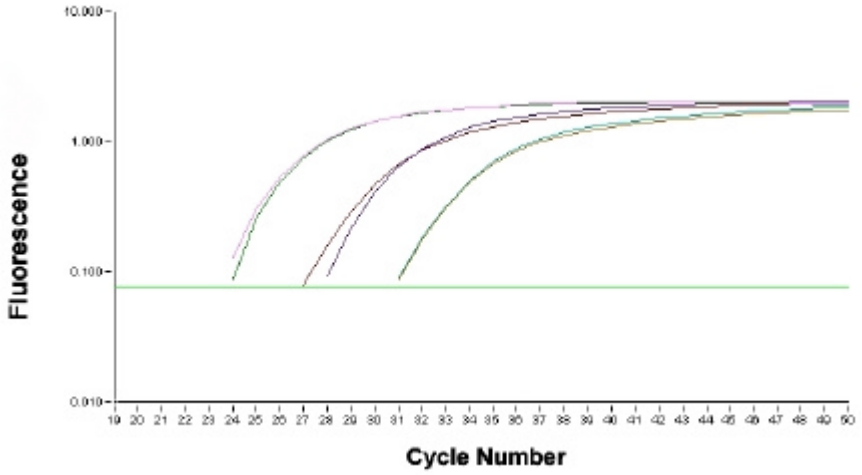

Figure 17 Quantification of the fluorescence signal

2.2.4.4.2.2 Method

SYBR Green(Roche, 1999):

The kit "LightCycler – DNA Master SYBR Green I" (content see 2.1.3) is a ready-to-use reaction mix. Only template DNA, primers and additional $MgCl_2$ had to be added. The Light-Cycler-PCR was performed according to the manufacturer's protocol(Roche, 1999). The used standard was produced by cloning the sequence between each pair of primers into the plasmid pCR 2.1 from invitrogen. For quantification a external standard curve was used. By having a standard sample with known concentration in each run the concentration of the unknown samples could be calculated.

Table **4** shows the conditions for the run with the LightCycler.

Table 4 PCR conditions in a run with SYBR Green

Cycle Program Data	***Value***		
Cycles	50		
Analysis Mode	Quantification		
Temperature Targets	Melting	Annealing	Elongation
Target Temperature (°C)	95	62	72
Incubation time (s)	1	10	18
Temp. Transition Rate (°C/s)	20.0	20.0	20.0
Acquisition Mode	None	None	Single

The acquisition mode shows the point of time of measuring the fluorescence signal (here: one single measurement after elongation when the entire DNA is double stranded).

After 50 cycles of amplification a melting curve analysis was performed in a third step: In a single cycle the DNA was first melted, then cooled down and again very slowly heated (0.1°C/s) to 95°C. During the last segment the signal was measured continuously. At the end the samples were cooled to 40°C (30 seconds).

Hybridisation Probes(Roche, 2001; Roche, 2000):

The used Hybridisation-Probes-Kit from Roche was: "LightCycler – FastStart DNA Master Hybridisation Probes"(Roche, 2001).

In this kit the enzyme is modified with heat-labile blocking groups on some of its amino acid residues. Therefore, elongation during the period where primers can bind non-specifically is inhibited. This enzyme is activated by removing these groups at a high temperature (i.e. pre-incubation step at 95°C for 10 minutes). The experimental conditions were the same as described above for SYBR Green except for a first pre-incubation step to remove the blocking groups, which was 10 minutes at 95°C and the lack of a melting curve(Roche, 2001).

2.3 Data Analysis and Statistics

Data is shown as mean ± standard error of the mean (Mean ± SEM) or as single values as the size of the groups (non-ischaemic and ischaemic) was only four pigs. This was also the reason non-parametric tests were used as oppose to parametric ones: The Mann-Whitney test to compare two groups and the Kruskal-Wallis test to compare more than two groups / regions of the heart. The confidence interval used was 95%.

3 RESULTS

3.1 Coronar Angiography and PET after Seven Days

The coronary angiography showed a closed LAD artery with good collateral flow supply to the distal portions in all four animals.

3.1.1 Gated-PET and left ventricular function evaluation

The results of the parameters concerning global and regional left ventricular function are displayed in Table 5. There was a marked decrease in regional wall motion, denoted by decreased systolic count increase, in all animals with closed LAD. Animal number 3 which displayed open LAD at 7 days showed less severe disturbance in segmental left ventricular wall motion. The mean count increase was significantly reduced in the LAD territory compared to the remote region ($p = 0.0017$), as illustrated in Figure 18.

Table 5 ^{13}**N-ammonia Gated-PET assessment of global and regional LV function**

				CI - Mismatch	
Animal ID	***LVEF (%)***	***EDV (m)***	***ESV (ml)***	***(%)***	***CI - Remote (%)***
1	57.7	56.8	24	-55	10
2	62.4	64.5	24.3	-77	10
3	49.2	86.6	44	-43	15
4	39.7	62.1	37.5	-36	30
Mean	55.1	63.5	29.2	-42.6	16.8
SD	10.7	14.5	11.3	27.5	8.3

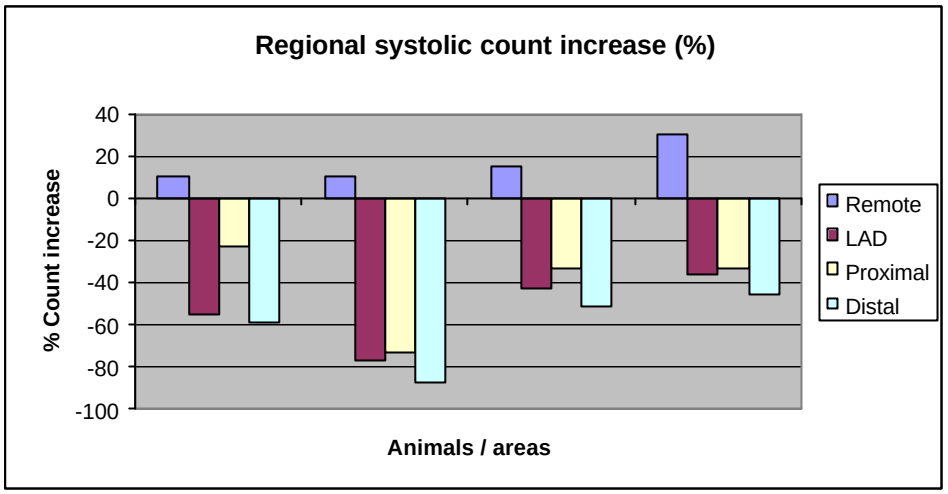

Figure 18 Bar graphic representing the comparative regional count increase (%) in normal remote area and hypoperfused Mismatch areas.

3.1.2 Regional myocardial blood flow by PET N13-ammonia

Table 6 summarises the results of regional myocardial blood flow changes in the Mismatch and Remote area territories.

Table 6 ^{13}N-ammonia assessment of myocardial blood flow

	Mismatch territory (reduced MBF)		*Remote area*
Animal ID	Area (%)	MBF	MBF
1	40	0.629	1.075
2	49	0.674	1.167
3	53	0.498	1.203
4	45	0.602	0.936
Mean	46.8	0.638	1.088
SD	5.6	0.106	0.104

Large areas of reduced perfusion involving 46% of the LV surface were found. The mean MBF in Mismatch territory (0.638 ml/g/min) was reduced at 41% as compared to normal areas outside the Mismatch territory (1.088 ml/g/min), ($p = 0.0001$).

3.1.3 Myocardial rate of glucose uptake (MRGU)

The uptake of FDG was evaluated in fasted condition. An increased uptake of FDG, in comparison to remote areas, was detected inside the hypoperfused Mismatch territory in all animals. The mean myocardial rate of glucose uptake was increased about 10-fold in the Mismatch territory as compared to the remote territory ($p = 0.0108$), Table 7.

Table 7 Values of Myocardial Rate of Glucose Uptake (Patlak)

Animal ID	*Mismatch territory (reduced MBF)*	*Remote area*
1	0.024	0.00027
2	0.03	0.00247
3	0.058	0.00715
4	0.022	0.00021
Mean	0.034	0.00253
SD	0.017	0.00326

3.1.4 Correlation between MBF and MRGU

To further document the increase of glucose uptake in areas of chronic reduction of myocardial blood flow in the investigated animal sample a correlation analysis between MBF and MRGU was performed. The values of each variable were obtained using a 17-segment model of left ventricular regions. There was a significant correlation between these variables ($R = -0.6693$, $p < 0.0001$ – see Figure 19), indicating that chronic reduction in myocardial perfusion is correlated to increase myocardial glucose uptake in fasted condition.

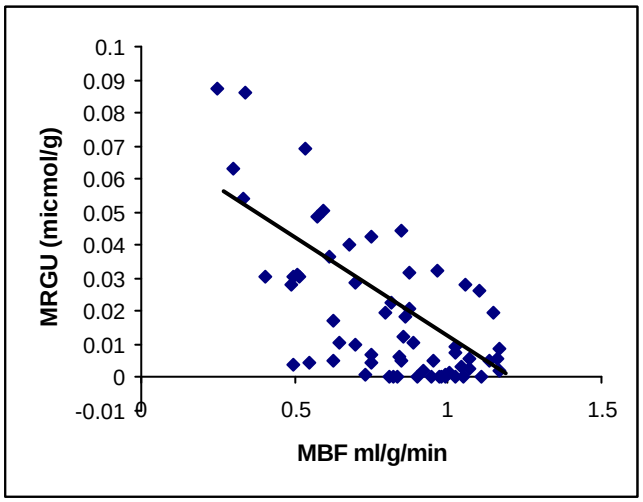

Figure 19 Scatter plot demonstrating the correlation between MBF and MRGU

3.2 Proteins

3.2.1 Optimisation Experiments

3.2.1.1 Membrane Preparation

Earlier versions of the protocol mentioned were varied in order to optimise membrane enrichment. This included homogenisation with a dismembrator, additional sonication with

ultrasound, centrifugation with 200 g instead of 300 g, variation of duration of the Ultra Turrax step and the use of collagenase.

3.2.1.1.1 Dismembrator

A dismembrator was tested in order to replace the cutting step with razor blades and the Ultra Turrax step. A nitrogen-cooled chamber containing the tissue sample was fixed in the instrument and vibration started. The steel ball mashed the frozen tissue resulting in powder-like material. Four vibration periods were tested: 1 x 3 min, 2 x 2 min, 1 x 2 min and 1 x 1 min. Thawing of tissue could not be avoided during the three longer time periods. Only the 1 min use of the dismembrator showed no thawing of the sample.

The protein determination by the BCA assay showed no significant changes compared to razor blade and Ultra Turrax. However, there were smaller amounts of both GLUT in the CH-preparations after dismembrator homogenisation.

These results suggest that tissue mincing by a dismembrator is not as good as the pre-cutting with a razor blade followed by an Ultra Turrax step. Therefore, the last method was used.

3.2.1.1.2 Sonicator

The ultrasound was additionally applied prior to the pottering step with the glass-glass homogeniser (2 x 10 s, 24 kHz, amplitude 170 µm). Protein determination by the BCA assay and GLUT content in the crude homogenate revealed no significant changes in comparison to razor blade and Ultra Turrax.

As the additional use of the sonicator did not show any improvement neither in protein yield nor in content of GLUT1 and GLUT4 this method was not further used.

3.2.1.1.3 200 x g Centrifugation

Instead of the first centrifugation step with 300 x g for 10 minutes (see 2.2.3.1.2) 200 x g were applied to reduce a probable loss of membranes. Protein determination by the BCA assay and GLUT content in the crude homogenate revealed no significant changes in comparison to razor blade and Ultra Turrax.

As the centrifugation with 200 x g did not lead to an improvement neither in protein yield nor in content of GLUT1 and GLUT4 300 x g were kept. Moreover, pipetting of the samples with 200 x g was difficult and less accurate than with 300 x g, because more fiber-like tissue still was in the solution.

3.2.1.1.4 Duration of Ultra Turrax Step

Because pipetting of the samples caused problems in volume accuracy it was tested whether a longer Ultra Turrax step could be advantageous. In variations of the original protocol (2 x 10 s), we also tested 1 x 60 s. Protein determination by the BCA assay and GLUT content in the crude homogenate revealed no significant changes in comparison to razor blade and Ultra Turrax.

These results suggested that the longer duration of the Ultra Turrax step did not decisively improve homogenisation in terms of outcome. However, the outcome is also not diminished and samples were easier to handle. As this was the base for accurate pipetting the step was elongated to 2 x 20 s.

3.2.1.1.5 Collagenase

The fiber-like quality of the connective tissue prevented exact pipetting. To avoid this collagenase was tested to give better tissue homogenisation without significant loss of proteins. The chosen collagenase type CLS II is a mixture of collagenase, clostripain and other proteolytic and tryptic activities. It is recommended for cell isolation in cardiac tissue. Protein determination by BCA assay is shown in Table 8. The protein yield in the samples with collagenase increased nearly two-fold although this value was corrected.

Table 8 Pierce BCA assay in samples with and without collagenase (n=2). * In the samples with Collagenase correction was necessary as the enzyme itself increases the protein content. But with the known amount of collagenase added the protein content of collagenase could be subtracted.

	Yield (mg protein / g tissue)
Without Collagenase	69,0
With Collagenase*	120,7

In addition the difference of GLUT1 and GLUT4 content in the CH of this preparations were investigated. Results show an increased content of both GLUT. Thus, it may be concluded that GLUT proteins are not digested by collagenase.

Table 9 Phosphor Imager quantification of GLUT1 and GLUT4 with and without collagenase (n=2)

	Tool	Mean Volume	Relative Volume
GLUT1	Without Collagenase	1302108,4	1,00
	With Collagenase	1761938,4	1,35
GLUT4	Without Collagenase	1847069,5	1,00
	With Collagenase	2243070,2	1,21

As both protein yield and content of GLUT1 and GLUT4 seemed to increase with the use of collagenase during tissue homogenisation, this step was included in the protocol of this work.

3.2.1.2 SDS-PAGE and Immunoblot

3.2.1.2.1 Specific Detection of Proteins

As shown in 2.1.6 none of the antibodies are specifically directed against "pig" glucose transporters or "pig" hexokinase. Therefore, antibodies used had to be tested for specific binding. For that purpose immunoblotting was performed as described in **2.2.3.5.1** and the resulting bands were compared to bands from species with known specific binding. The molecular weight of the band (position on the gel) and its shape were used as parameters for specifity.

GLUT1

Figure 20 demonstrates that the bands of GLUT1 in the different species were very similar. All three species displayed additional bands beside the main band. For mouse it was shown that these are due to unspecific binding.

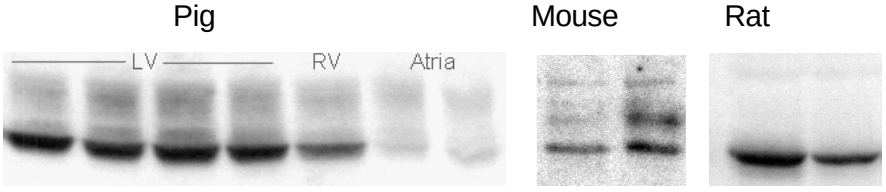

Figure 20 Western blots showing GLUT1 in membrane fractions of pig, mouse and rat heart

As the main protein band shows similar molecular weight and shape for all species tested, the band of pig heart tissue samples was considered to resemble GLUT1 and therefore further quantificated.

GLUT4

Figure 21 shows an immunoblot of GLUT4 for the different species. Protein bands were very similar and had a similar molecular weight. Because of different degrees of glycosylation, two specific bands were visible.

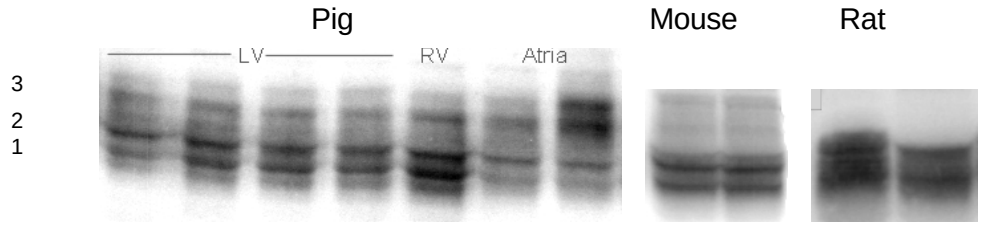

Figure 21 Western blots showing GLUT4 in membrane fractions of pig, mouse and rat heart

In pig tissue an additional band (No. 3) appeared above the specific bands, which was not found in mouse or rat. As it was not clear if this band was specific to GLUT4 it was not included for quantification.

Hexokinase Type II

The initially employed antibody from Linaris did not produce any bands in the western blot although the secondary antibody was directed against goat. However, the second-choice antibody from Chemicon bound to one strong and sharp band with a molecular weight of approximately 100 kDa (see Figure 22) . As this is the weight of hexokinase type II it could be assumed that the band is due to specific binding of the antibody.

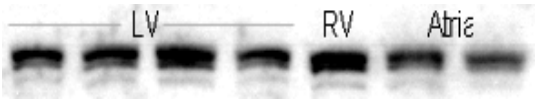

Figure 22 Western Blot showing HKII in crude homogenate of pig

3.2.1.2.2 GLUT3 Detection

Originally GLUT3 protein detection was planned in parallel to mRNA quantification by PCR. For this purpose 3 different antibodies were tested (see 2.1.6).

The first antibody tested (Diagnostic International) produced only faintly visible bands after applying a maximum of contrast on the immunoblot. No clearly specific binding could be detected. Two further antibodies from Chemicon (against human GLUT3) and Alpha Diagnostic (against mouse and rat GLUT3; shown in Figure 23A and Figure 24A) were tested. Beside the pig samples, mouse brain samples were also applied as this tissue could serve as a positive control for the mouse GLUT3 antibody.

Both blots showed multiple bands but it was not clear whether they were specific to GLUT3 or not. Further ensurance for specific binding was achieved by a competition assay (see Figure 23B and Figure 24B). In this method a specific peptide binds to the specific antibody prior to incubation with the antigen. When comparing a normal blot with a competition assay blot all specific bands vanish on the competition assay. All other visible bands are most probably caused by different unspecific antigens and for that reason not utilisable for quantification.

The solution for the competition assay was prepared by preincubation of the antibody with 50-100 µg peptide in 40 µl blocking buffer (1 hour, 4°C). After this hour the rest of the blocking buffer was added and incubated with the nitrocellulose as described.

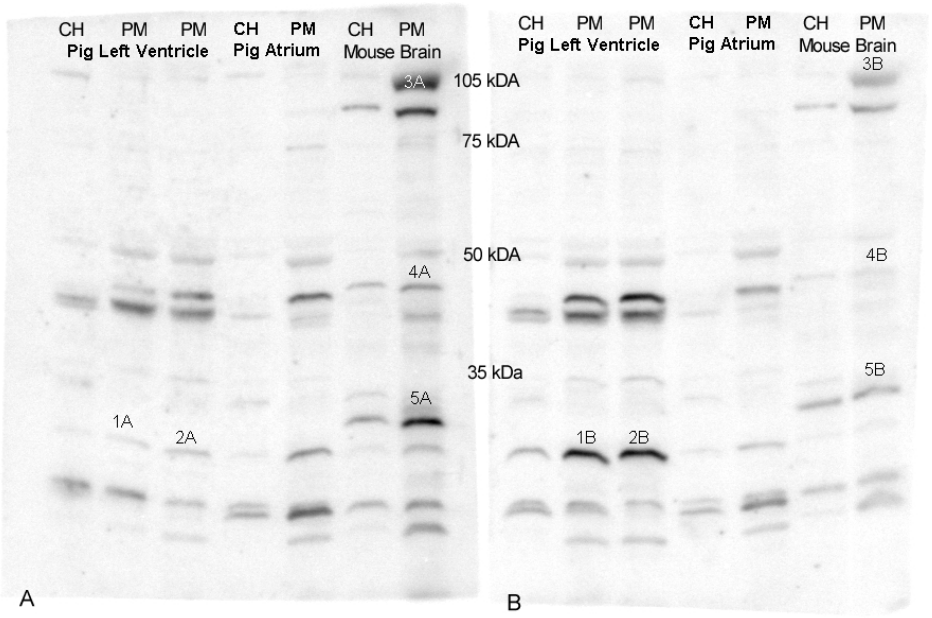

Figure 23 A) Western Blot and B) Competition Assay with Anti-GLUT3 (human) obtained from Chemicon International

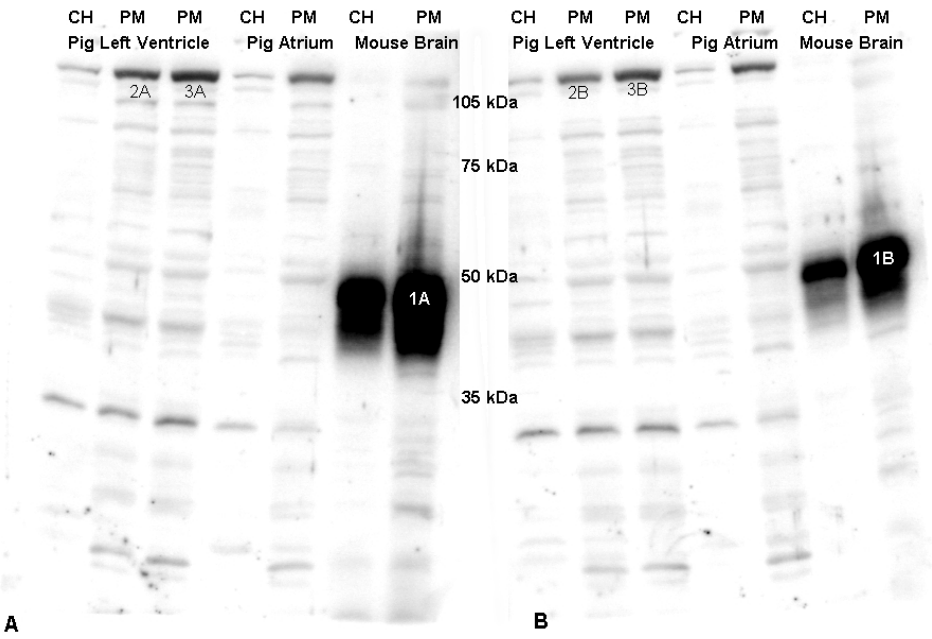

Figure 24 A) Western Blot and B) Competition Assay with Anti-GLUT3 (mouse/rat) obtained from Alpha Diagnostic

The comparison of Figure 23A with Figure 23B reveals that there are no bands in A that vanished or were diminished in B for the pig samples of left ventricle and atrium. Some bands even appear stronger (e.g. band 1A/B and 2A/B). Thus, all these bands are not due to the specific GLUT3 antibody binding. However, mouse brain tissue includes bands, which are diminished in B (e.g. 3A/B, 4A/B and 5A/B) suggesting specific binding. The band in the brain samples at about 100 kDa (3A/B) could probably be a dimer or trimer and there is also a smaller band at about 40 kDa (4A/B), which could be caused by the monomer. No corresponding bands could be detected for the same molecular weight in the pig samples. However, this result does not show if the antibody against human GLUT3 binds to pig GLUT3. It only shows that binding to mouse GLUT3 is specific.

In Figure 24A and Figure 24B the specific binding of the positive control is obvious (1A/B). In A it is an immense band that is highly diminished in B. At a molecular weight of about 105 kDa there are bands visible in the PM fraction of the pig heart samples in A (2A and 3A), which vanish in the competition assay B (2B and 3B). All other bands look the same in A and B and therefore are non-specific. Thus, results with this antibody do not clearly define binding to pig GLUT3.

To clarify if one of the two above mentioned antibodies binds to pig GLUT3 competition assays with both antibodies and their specific peptides were incubated with samples of pig brain. Beside this, a rat heart sample and a heart sample of a GLUT4 knockout mouse were applied to the gel.

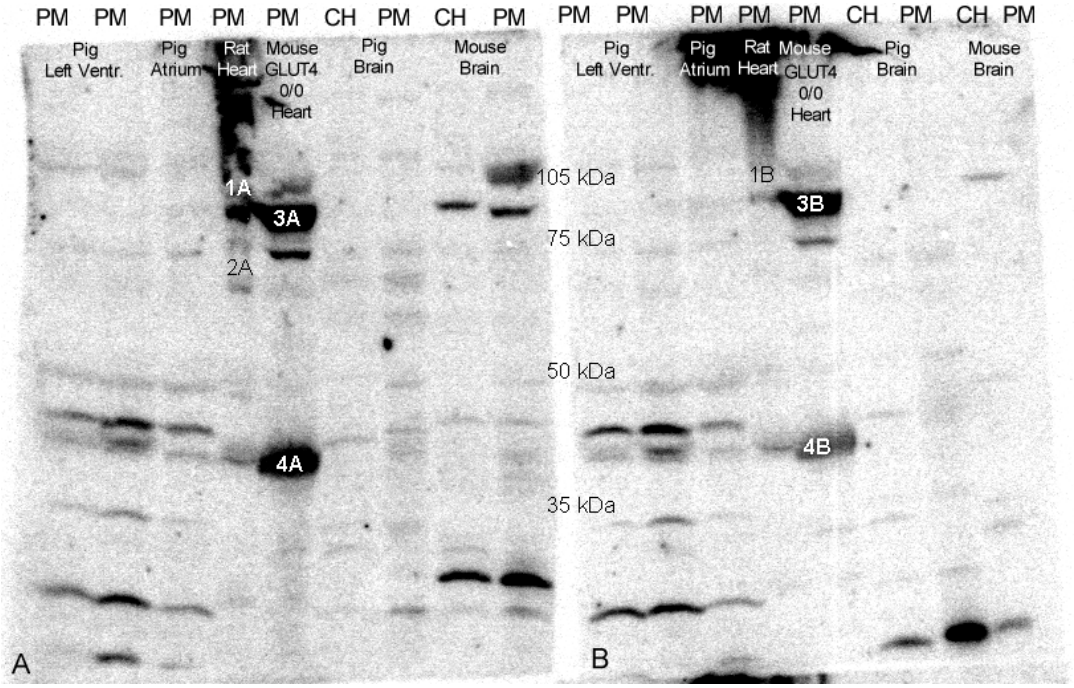

Figure 25 A) Western Blot and B) Competition Assay with Anti-GLUT3 (human) obtained from Chemicon International

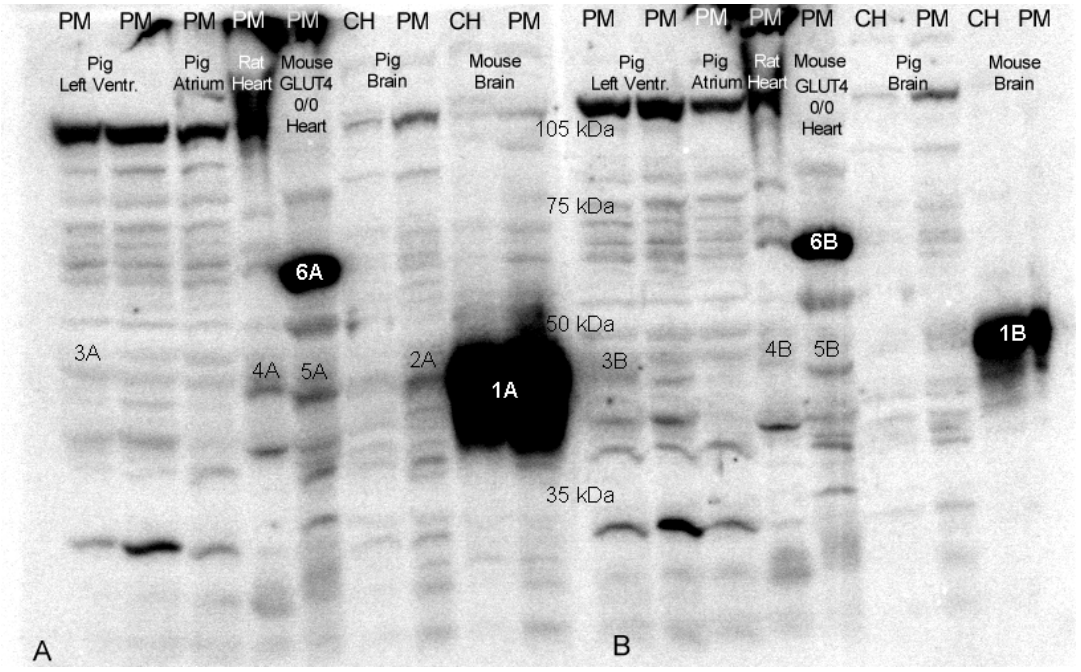

Figure 26 A) Western Blot and B) Competition Assay with Anti-GLUT3 (mouse/rat) obtained from Alpha Diagnostic

When comparing the pig brain samples in Figure 25 A and B (Chemicon) there is no band in either of the blots. As there should be a very high GLUT3 content in the brain this suggests that this antibody does not bind to pig GLUT3 or only to an amount so low that it is beyond the

detection level of this method. Comparing the mouse brain samples in this assay reveals again that mouse GLUT3 can be detected and blocked by the peptide. The heart preparation of rat shows bands at about 80 kDa (1A/B) and a bit lower (75 kDa; 2A without 2B) that might be a dimer in different glycosylated forms. They are blocked in the competition assay. The heart preparation of the GLUT4 knockout mouse displays strong bands in the weight regions of 40 and 80 kDa (3A/B and 4 A/B) that can be blocked by the peptide. This reflects GLUT3 protein and probably suggests upregulation of this GLUT in GLUT4 knockout mice.

Figure 26 A and B show the Immunoblot and competition assay of the same samples as above but incubated with the primary anti-mouse/rat GLUT3 antibody purchased from Alpha Diagnostic. The mouse brain samples that served as the positive control show immense bands that could partly be blocked in the competition assay (1A/B). Moreover, the PM fractions in the pig brain samples show a faint band (2A) that is blocked by the peptide (no 2B). A corresponding band in the pig heart lanes can only be seen very weakly (3A) but did not disappear completely in the competition assay (3B). All other (and stronger appearing) bands in the pig heart samples seem to be due to unspecific binding. The rat heart reveals a specific band at about 40 kDa (4A/B). The GLUT4 knock-out mouse heart has a specific band at about 40 kDa (5A/B) and a further strong band at 70 kDa (6A/B). However, the strong band was not blocked by the peptide and therefore not specific.
In conclusion, of the 3 tested GLUT3 antibodies only the Alpha Diagnostic antibody binds to pig GLUT3 (as shown in brain tissue) but with a very low affinity. The probably minute amounts of GLUT3 which may exist in the pig heart cannot be quantified using one of these antibodies.

3.2.2 Ponceaus S Staining

Ponceau S staining was performed in order to document homogeneous transfer and transfer defects. Figure 27 shows the Ponceau S stain documented with a digital camera.

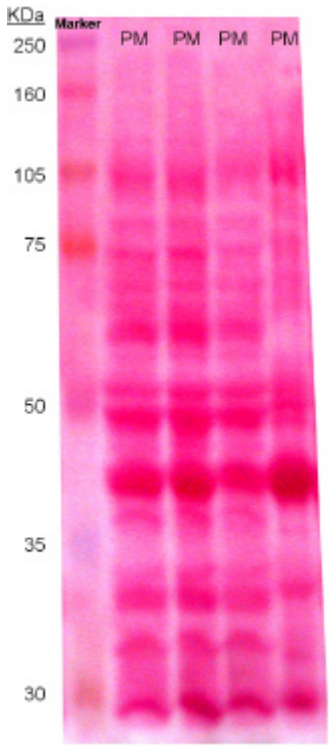

Figure 27 Ponceau S Stain documented with a digital camera

3.2.3 Immunoblot of Glucose Transporters and Hexokinase Type II

3.2.3.1 GLUT1 Protein

3.2.3.1.1 Non-Ischaemic Hearts

Table 10 shows the relative protein expression in each of the twelve regions of the examined hearts. These values are graphically illustrated in Figure 28. The values in the left ventricle showed no difference (P = 0,3623) and neither did the values of both atria (P = 0,6857). Significant differences were found to exist between the right and left ventricles (P = 0,0168), between the right ventricle and atria (P = 0,0040) and between the left ventricle and the atria (P < 0,0001). The left ventricle showed the highest protein expression, while the atria showed the lowest.

Table 10 Means for each region and each heart determined out of 3 measurements

	Heart 1	Heart 2	Heart 3	Heart 4	Mean	SEM (%)
Anterior Wall, endocardial	1,47	1,26	1,30	1,64	**1,42**	6,20
Anterior Wall, epicardial	1,65	1,50	1,47	1,47	**1,52**	2,91
Lateral Wall, endocardial	1,46	1,29	1,32	1,28	**1,34**	3,07
Lateral Wall, epicardial	1,44	1,34	1,41	1,38	**1,39**	1,48
Inferior Wall, endocardial	1,20	1,26	1,27	1,49	**1,31**	4,83
Inferior Wall, epicardial	1,49	1,36	1,13	1,44	**1,35**	5,79
Septum, endocardial	0,72	1,41	1,34	1,61	**1,27**	15,09
Septum, epicardial	0,88	1,16	1,18	1,64	**1,21**	13,12
Apex	1,15	1,26	1,25	1,50	**1,29**	5,79
Right Ventricle	1,24	1,00	1,23	0,96	**1,11**	6,61
Left Atrium	0,55	0,33	0,42	0,51	**0,45**	10,75
Right Atrium	0,43	0,36	0,47	0,42	**0,42**	5,45

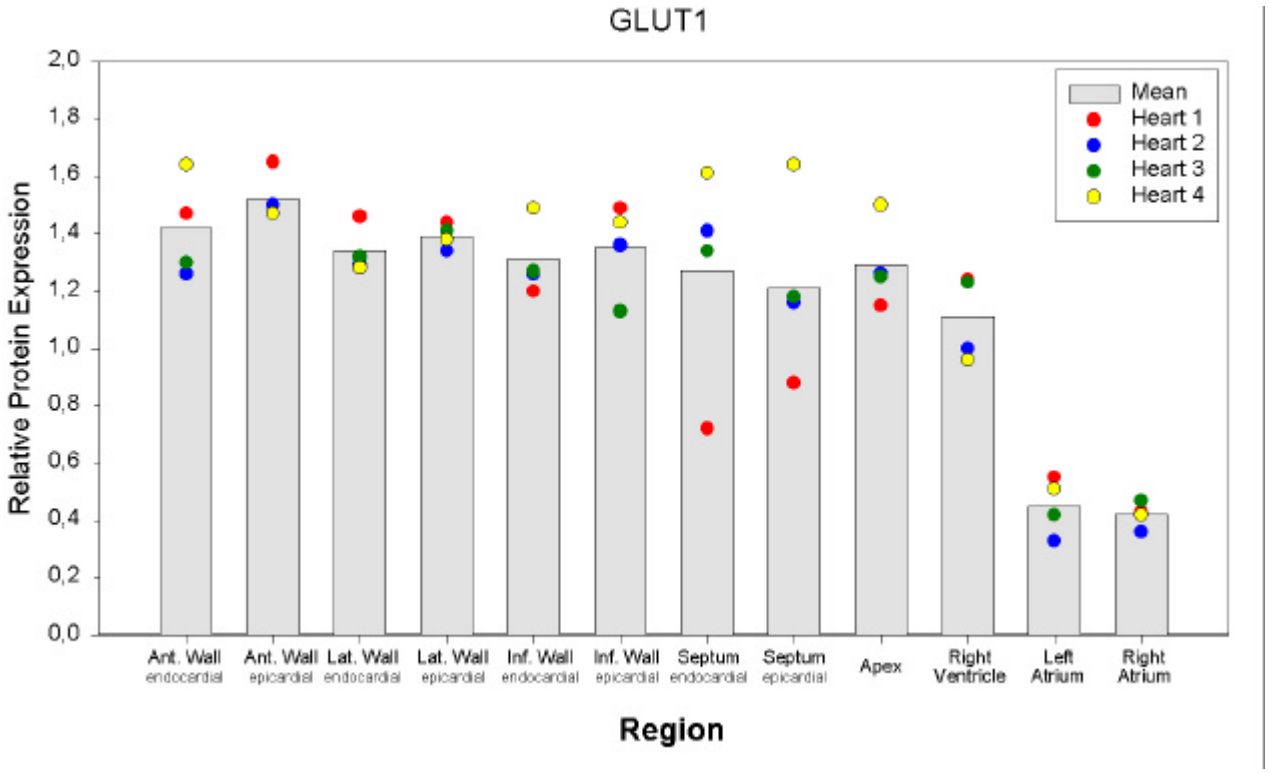

Figure 28 Relative values of GLUT1 protein expression for each region in normal hearts

3.2.3.1.2 *Ischaemic Hearts*

Table 11 shows the relative protein expression in each of the seven regions of the examined hearts. These values are graphically illustrated in Figure 29. The values in the ischaemic regions were significantly lower than in the remote region (P = 0,0003) and were at the level of the expression in the atria. In the right ventricle the expression results varied between the pigs

but was lower than in the remote LV (P = 0,0040), as was the case for RV and LV of non-ischaemic hearts (see 3.2.3.1.1). Moreover, the atria showed a lower GLUT1 content than the remote LV (P = 0,0002) and the RV (P = 0,0162). The values in the remote LV vary somewhat but the values in the ischaemic region and in the atria were consistent.

Using a ratio between the same regions in ischaemic and normal hearts (sum of endo- and epicardial) $\frac{Mean(\text{Re}\,mote_{endocard})_{ischemic} + Mean(\text{Re}\,mote_{epicard})_{ischemic}}{Mean(\text{Re}\,mote_{endocard})_{non-\ ischemic} + Mean(\text{Re}\,mote_{epicard})_{non-\ ischemic}}$ yielded results of 0,64 for the remote region and 0,13 for the Mismatch region. As the SEM increases when using a ratio the interpretation of these values is not definite. However, it suggests that the content of GLUT1 in the injured region of ischaemic hearts (Mismatch) was lower than in the normal hearts.

Table 11 Means for each region and each heart determined out of 3 measurements

	Heart 1	Heart 2	Heart 3	Heart 4	Mean	SEM (%)
Remote, endocardial	0,53	0,93	0,88	0,95	**0,82**	12,16
Remote, epicardial	0,72	0,99	0,82	0,93	**0,87**	6,83
Mismatch, endocardial	0,17	0,24	0,18	0,14	**0,18**	12,00
Mismatch, epicardial	0,21	0,23	0,13	0,18	**0,19**	11,96
Match	0,20	0,19	0,16	0,16	**0,18**	6,29
Right Ventricle	0,33	0,37	0,17	0,33	**0,30**	14,37
Left Atrium	0,20	0,17	0,14	0,13	**0,16**	10,27
Right Atrium	0,19	0,14	0,12	0,15	**0,15**	9,00

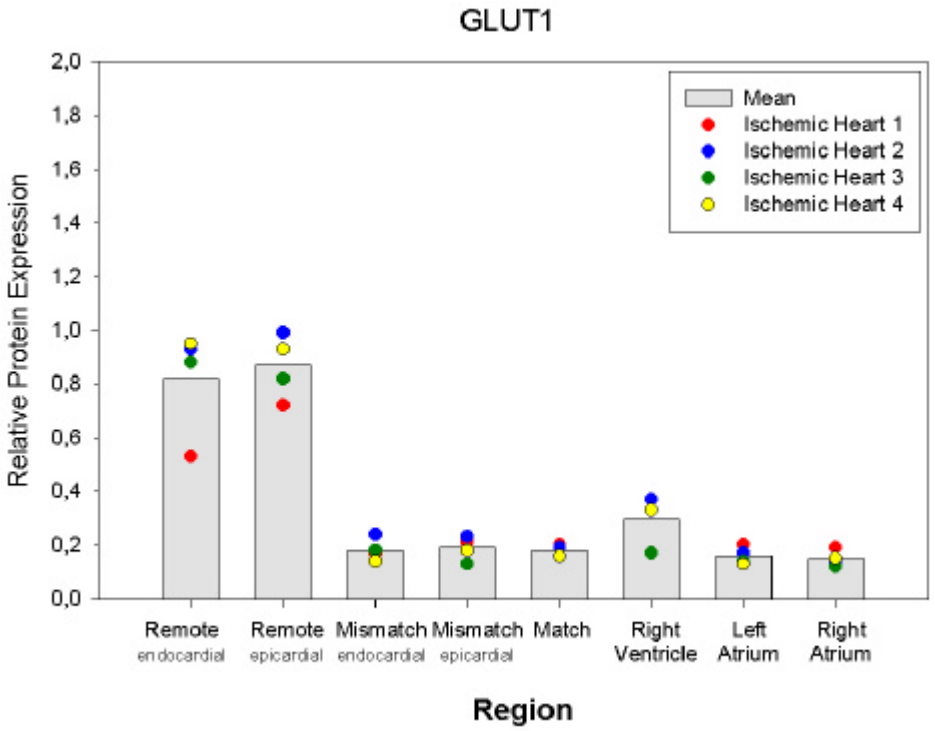

Figure 29 Relative values of GLUT1 protein expression for each region in ischaemic hearts

3.2.3.2 GLUT4 Protein

3.2.3.2.1 Non-Ischaemic Hearts

Table 12 shows the relative protein expression in each of the twelve regions of the examined hearts. These values are graphically illustrated in Figure 30, which shows that the GLUT4 protein expression is homogeneous in the left ventricular regions (P = 0,5668). There is a regional difference in GLUT4 expression between the left and right ventricles (P = 0,0220), which had a higher GLUT4 content. However, there was no difference between LV and atria (P = 0,5206), or between RV and atria (P = 0,3677).

Table 12 Means for each region and each heart determined out of 3 measurements

	Heart 3	Heart 4	Heart 5	Heart 6	Mean	SEM (%)
Anterior Wall, endocardial	1,45	1,08	1,26	1,45	**1,31**	6,70
Anterior Wall, epicardial	1,82	1,19	1,59	1,34	**1,49**	9,28
Lateral Wall, endocardial	1,02	1,53	1,20	0,95	**1,18**	10,99
Lateral Wall, epicardial	1,44	1,76	1,60	1,06	**1,47**	10,25
Inferior Wall, endocardial	1,20	1,14	0,96	1,12	**1,11**	4,56
Inferior Wall, epicardial	1,64	0,91	1,19	1,46	**1,30**	12,30
Septum, endocardial	1,23	1,14	1,53	1,06	**1,24**	8,31
Septum, epicardial	1,12	1,64	1,53	1,13	**1,36**	10,04
Apex	1,07	1,34	1,46	1,10	**1,24**	7,63
Right Ventricle	1,91	1,32	1,66	1,70	**1,65**	7,33
Left Atrium	1,69	0,85	1,64	1,01	**1,30**	16,46
Right Atrium	1,76	1,08	2,19	1,23	**1,56**	16,26

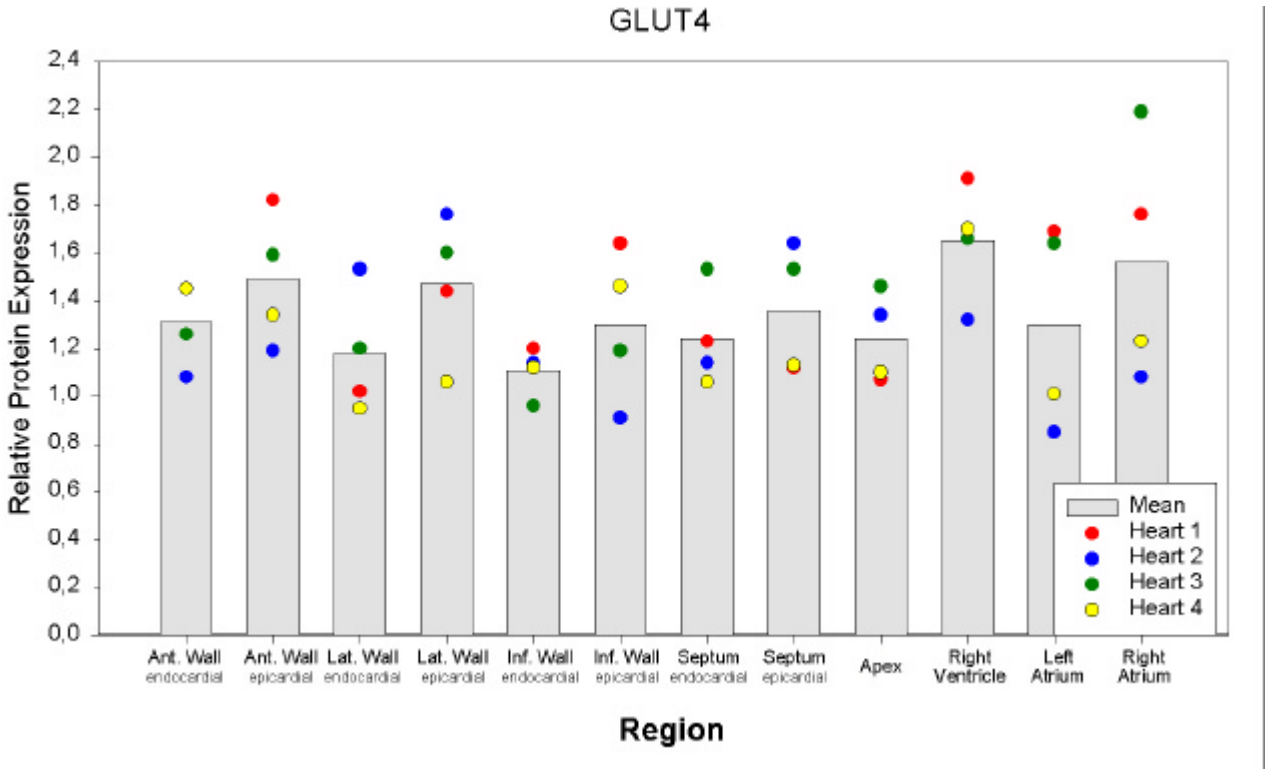

Figure 30 Relative values of GLUT4 protein expression for each region in normal hearts

3.2.3.2.2 *Ischaemic Hearts*

Table 13 demonstrates the relative protein expression in each of the seven regions of the examined hearts. These values are graphically illustrated in Figure 31. The ischaemic regions showed a significantly lower GLUT4 protein expression (P = 0,0003) compared to remote

regions. The right ventricle and the atria had a tendency to a lower content in comparison to the remote regions. However, this was only significant in the case of the atria (P = 0,0281).

Evaluating the ratio of ischaemic and normal hearts for each region as mentioned in 3.2.3.1.2 yielded a value of 0,63 in the remote region and 0,21 in the Mismatch region. This suggests a decreased GLUT4 protein content in the ischaemically injured region in comparison to normal hearts.

Table 13 Means for each region and each heart determined out of 3 measurements

	Heart 1	*Heart 2*	*Heart 3*	*Heart 4*	*Mean*	*SEM (%)*
Remote, endocardial	0,54	0,67	0,74	0,96	**0,73**	12,20
Remote, epicardial	0,60	0,75	0,72	1,05	**0,78**	12,22
Mismatch, endocardial	0,26	0,47	0,22	0,22	**0,30**	20,03
Mismatch, epicardial	0,36	0,38	0,16	0,24	**0,29**	18,29
Match	0,29	0,38	0,25	0,23	**0,29**	11,74
Right Ventricle	0,64	0,70	0,20	0,44	**0,50**	22,54
Left Atrium	0,78	0,47	0,49	0,43	**0,54**	14,67
Right Atrium	0,69	0,40	0,61	0,38	**0,52**	14,81

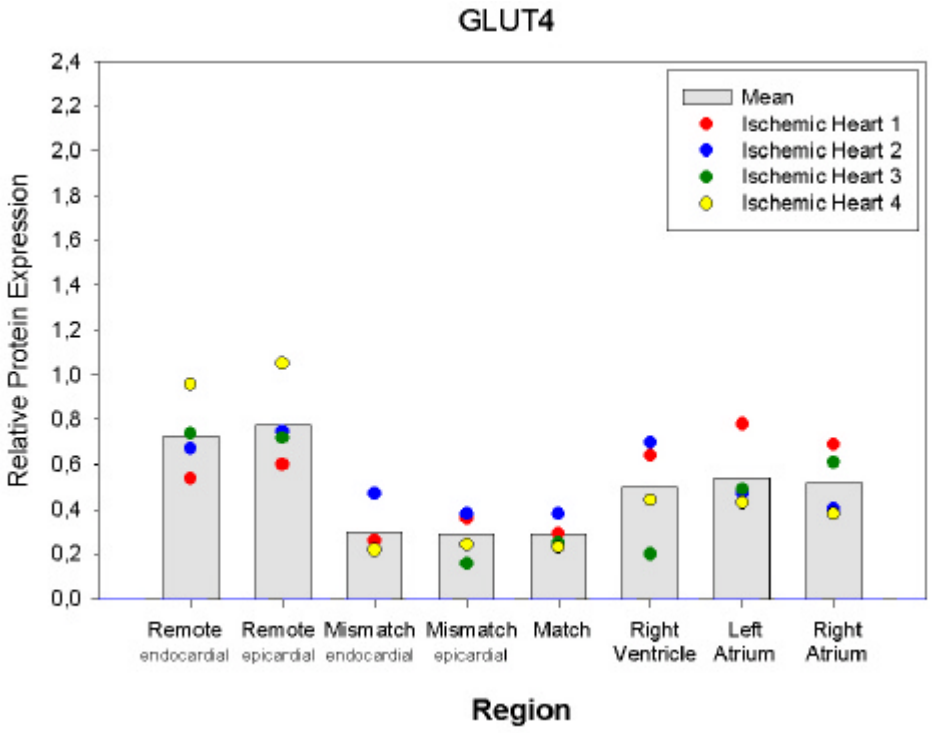

Figure 31 Relative values of GLUT4 protein expression for each region in ischaemic hearts

3.2.3.3 Hexokinase Type II Protein

3.2.3.3.1 Non-Ischaemic Hearts

Table 14 reveals the relative protein expression in each of the twelve regions of the examined hearts. The results are graphically illustrated in Figure 32. The results in the different regions vary from pig to pig. The left ventricle shows a significantly lower expression than the atria (P = 0,0280). However, the four pigs differ significantly from each other (P = 0,0460), which again favours the demonstration of each pig's own results.

Table 14 Means for each region and each heart determined out of 3 measurements

	Heart 3	*Heart 4*	*Heart 5*	*Heart 6*	*Mean*	*SEM (%)*
Anterior Wall, endocardial	0,80	2,45	2,12	2,64	**2,00**	20,77
Anterior Wall, epicardial	0,75	1,98	1,42	2,31	**1,62**	21,09
Lateral Wall, endocardial	1,72	1,65	1,09	1,62	**1,52**	9,53
Lateral Wall, epicardial	0,81	0,74	1,03	0,96	**0,88**	7,57
Inferior Wall, endocardial	1,22	1,24	0,97	1,23	**1,16**	5,55
Inferior Wall, epicardial	0,76	0,77	2,21	1,86	**1,40**	26,75
Septum, endocardial	1,33	1,21	1,31	1,44	**1,32**	3,62
Septum, epicardial	1,42	1,52	0,97	0,89	**1,20**	13,25
Apex	1,07	1,00	0,75	1,33	**1,04**	11,42
Right Ventricle	0,98	2,32	1,52	1,44	**1,56**	17,83
Left Atrium	1,03	4,30	2,20	2,43	**2,49**	27,20
Right Atrium	0,98	2,37	2,15	1,77	**1,82**	16,81

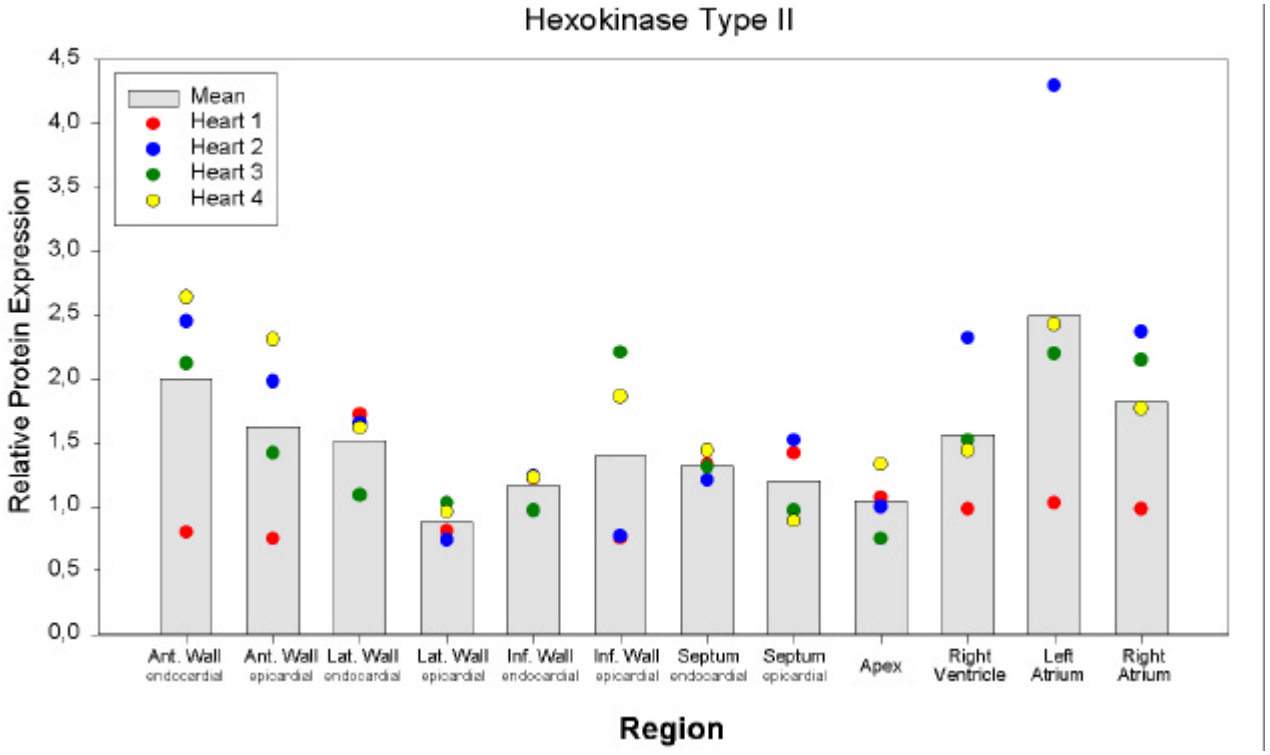

Figure 32 Relative values of hexokinase II protein expression for each region in normal hearts

3.2.3.3.2 Ischaemic Hearts

Table 15 shows the relative protein expression in each of the seven regions of the examined hearts. These values are graphically illustrated in Figure 33. Although the values for each region varied somewhat, there was no difference between the four hearts (P = 0,7966). Comparing ischaemic and remote regions, there seemed to be a slightly increased content of hexokinase in the ischaemic regions, but this was not significant (P = 0,0538). There was also no significant difference between the right ventricle and the remote left ventricle (P = 0,0727). However, the atria had a higher hexokinase protein expression than the remote LV (P = 0,0006) as in the non-ischaemic hearts. Although the two atria showed a different pattern (Figure 33) there was no significance found between them (P = 0,2000).

Evaluating the ratio of ischaemic and normal hearts for each region as mentioned in 3.2.3.1.2 yielded results of 0,65 in the remote region and 0,59 in the mismatch region, suggesting no or only little change in protein expression of hexokinase in the ischaemic region.

Table 15 Means for each region and each heart determined out of 3 measurements

	Heart 1	Heart 2	Heart 3	Heart 4	Mean	SEM (%)
Remote, endocardial	0,78	0,95	0,69	0,89	**0,83**	7,07
Remote, epicardial	0,76	0,92	0,63	1,01	**0,83**	10,27
Mismatch, endocardial	0,98	1,03	0,86	1,59	**1,11**	14,55
Mismatch, epicardial	0,76	1,29	1,14	0,88	**1,02**	11,96
Match	1,44	0,85	1,22	0,85	**1,09**	13,40
Right Ventricle	0,84	1,07	1,53	0,96	**1,10**	13,76
Left Atrium	1,03	0,96	1,16	1,02	**1,04**	4,11
Right Atrium	1,50	0,96	1,57	1,84	**1,47**	12,56

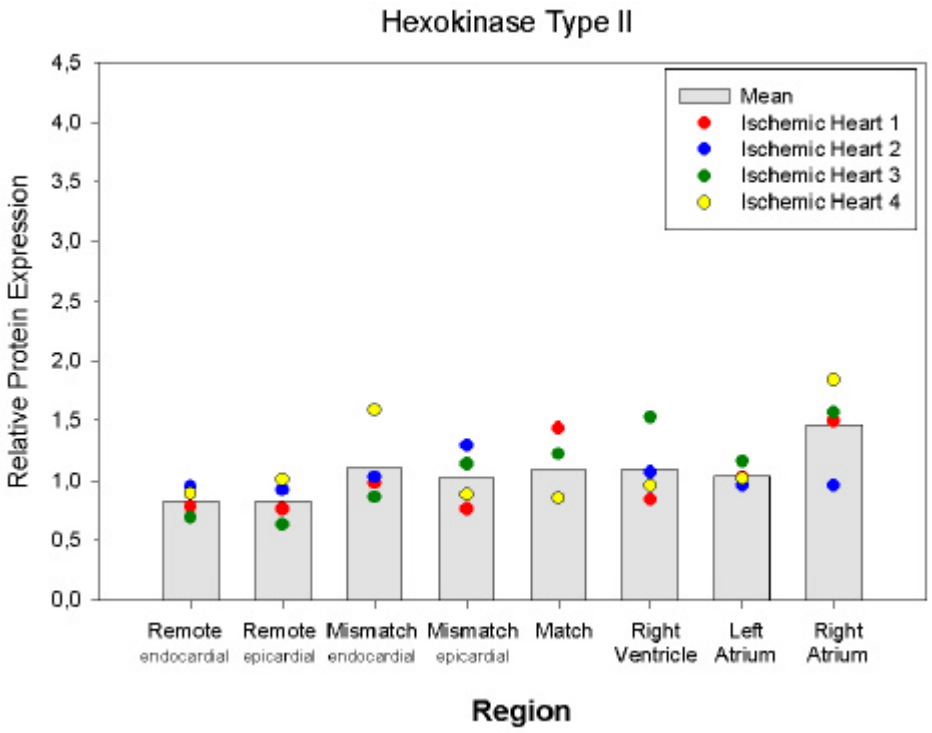

Figure 33 Relative values of hexokinase II protein expression for each region in ischaemic hearts

3.2.3.4 GLUT1/GLUT4 Ratio

3.2.3.4.1 Non-Ischaemic

Table 16 demonstrates the relative GLUT1/GLUT4 ratio in the twelve regions for each normal heart in relation to the standard. Therefore, all values show the difference in GLUT1 and GLUT4 distribution in relation to the standard (which was obtained from LV). Thus, the LV

regions have values around 1. The results are graphically illustrated in Figure 34. The right ventricle showed a lower ratio than the left (P = 0,0035) and a higher ratio than the atria (P = 0,0040). This suggests that the GLUT4 content in RV and atria is higher than in the LV. The ratios in the two atria did not differ (P = 0,3429).

Table 16 GLUT1/GLUT4 ratio for each region and each heart determined out of 3 measurements

	Heart 3	*Heart 4*	*Heart 5*	*Heart 6*	*Mean*	*SEM (%)*
Anterior Wall, endocardial	1,02	1,16	1,03	1,13	**1,09**	6,63
Anterior Wall, epicardial	0,91	1,26	0,92	1,09	**1,05**	15,87
Lateral Wall, endocardial	1,42	0,84	1,10	1,35	**1,18**	13,72
Lateral Wall, epicardial	1,00	0,76	0,88	1,31	**0,99**	27,43
Inferior Wall, endocardial	1,00	1,11	1,32	1,33	**1,19**	34,30
Inferior Wall, epicardial	0,90	1,49	0,96	0,98	**1,08**	32,82
Septum, endocardial	0,59	1,23	0,87	1,52	**1,05**	38,77
Septum, epicardial	0,78	0,70	0,77	1,46	**0,93**	38,29
Apex	1,07	0,94	0,85	1,36	**1,06**	21,09
Right Ventricle	0,65	0,76	0,74	0,57	**0,68**	13,10
Left Atrium	0,32	0,39	0,25	0,50	**0,37**	28,93
Right Atrium	0,24	0,33	0,21	0,34	**0,28**	22,41

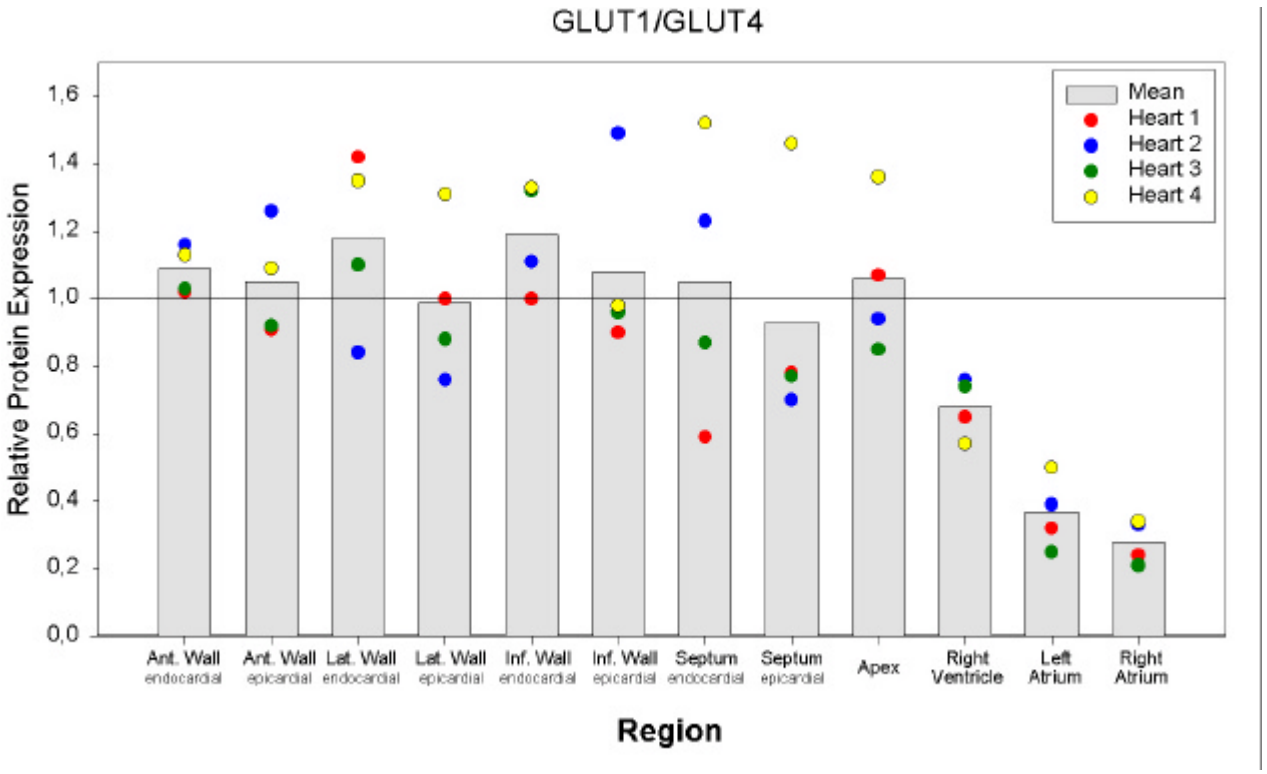

Figure 34 GLUT1/GLUT4 protein ratio for each region in non-ischaemic hearts

3.2.3.4.2 Ischaemic

Table 17 shows the GLUT1/GLUT4 ratio in the seven regions for each ischaemic heart. The values are illustrated in Figure 35. Compared to the non-ischaemic heart (see 3.2.3.4.1) the ratio in the non-ischaemic LV (remote region) was also around 1 or higher. However, in the ischaemic regions the ratio was decreased, suggesting that GLUT4 is expressed at a higher rate than GLUT1 in these regions (P = 0,0003). As for the non-ischaemic hearts, the right ventricle and the atria had ratios below 1 and thus showed a significantly lower ratio than the remote region (P = 0,0040 for the RV and P = 0,0002 for the atria). However, the ratio in the ischaemic regions was still higher than in the right ventricle (P = 0,0044) and in the left atrium (P = 0,0044).The atria themselves differed (P = 0,0286), but there was no distinction between ischaemic regions and the right atrium (P = 0,8555).

Table 17 GLUT1/GLUT4 ratio for each region and each heart determined out of 3 measurements

	Heart 1	Heart 2	Heart 3	Heart 4	Mean	SEM (%)
Remote, endocardial	0,98	1,40	1,19	0,99	**1,14**	17,55
Remote, epicardial	1,20	1,32	1,15	0,89	**1,14**	15,95
Mismatch, endocardial	0,63	0,51	0,81	0,61	**0,64**	19,15
Mismatch, epicardial	0,58	0,61	0,81	0,74	**0,69**	15,84
Match	0,51	0,53	0,85	0,74	**0,66**	25,34
Right Ventricle	0,26	0,36	0,29	0,30	**0,30**	13,77
Left Atrium	0,27	0,35	0,20	0,39	**0,30**	27,27
Right Atrium	0,70	0,51	0,64	0,70	**0,63**	13,96

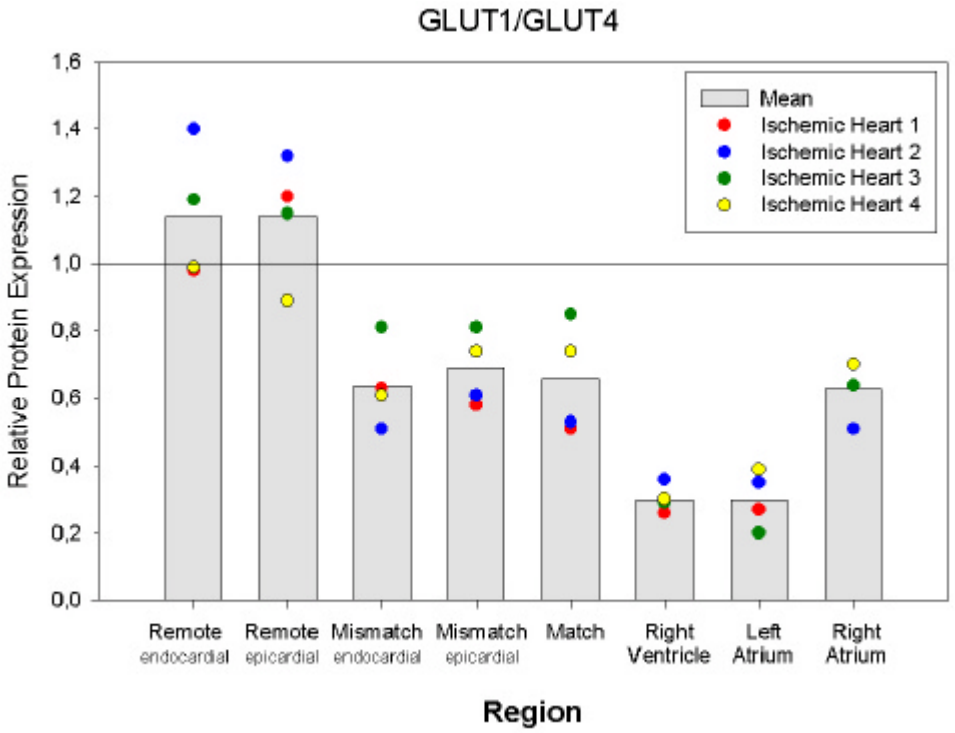

Figure 35 GLUT1/GLUT4 protein ratio for each region in ischaemic hearts

3.2.3.5 Summary

3.2.3.5.1 Non-Ischaemic

Table 18 is an overall view summarising results of the immunoblot with samples of the normal hearts. The highest GLUT1 content was found in the LV compared to the RV and the atria. In contrast, the GLUT4 content was higher in the RV while both atria were consistent with LV or RV. Hexokinase protein expression showed no regional difference at all.

Table 18 Summary of statistics in the non-ischaemic hearts.

ns: Not significant difference

⊙: Significant difference

Hearts: Difference between the single hearts

LV ⇔ RV: Difference between left and right ventricle

LV ⇔ Atria: Difference between left ventricle and atria

RV ⇔ Atria: Difference between right ventricle and atria

LV: Endo- ⇔ epicardial: Difference between the endo- and epicardial regions in LV

LV: Anterior ⇔ Posterior: Difference between the Anterior and Posterior region in LV

	Hearts	*LV ⇔ RV*	*LV ⇔ Atria*	*RV ⇔ Atria*	*LV: Endo- ⇔ epicardial*	*LV: Anterior ⇔ Posterior*
GLUT1	ns	⊙	⊙	⊙	ns	ns
GLUT4	ns	⊙	ns	ns	ns	ns
Hexokinase	⊙	ns	⊙	ns	ns	ns
GLUT1/GLUT4	ns	⊙	⊙	⊙	ns	ns

3.2.3.5.2 Ischaemic

Table 19 is an overall view summarising the results of the immunoblot with samples of the ischaemic hearts. Both GLUT1 and GLUT4 displayed a decreased protein content in the ischaemic regions. Hexokinase protein expression was not changed under ischaemic conditions.

Table 19 Summary of statistics in the ischaemic hearts.

ns: Not significant difference

⊙: Significant difference

Hearts: Difference between the single hearts

Remote ⇔ Ischaemic: Difference between remote regions of the left ventricle and ischaemic regions

Remote ⇔ RV: Difference between remote left ventricle and the right ventricle

Remote ⇔ Atria: Difference between the remote left ventricle and the atria

	Hearts	*Remote ⇔ Ischaemic*	*Remote ⇔ RV*	*Remote ⇔ Atria*
GLUT1	ns	⊙	⊙	⊙
GLUT4	ns	⊙	ns	⊙
Hexokinase	ns	ns	ns	⊙
GLUT1/GLUT4	ns	⊙	⊙	⊙

3.3 RNA

3.3.1 Optimisation Experiments

3.3.1.1 Tissue Homogenisation and Extraction of RNA

Performing an RNA extraction allows the choice of emphasising purity or yield. To emphasise purity chloroform extraction can be performed twice (the second time only with 0.12 ml chloroform per millilitre TRI) before adding isopropanol. In order to test the influence of this second step on purity or yield both variants were tested (see Table 20).

Table 20 Differences in purity and yield after RNA extraction done once or twice

Extraction	*Mean (A_{260}/A_{280})*	*SD (A_{260}/A_{280})*	*Mean (Yield) [µg RNA / mg tissue]*	*SD (Yield)*
Twice (n=13)	1,57	28,7 %	0,47	31,6 %
Once (n=62)	1,63	4,7 %	0,90	45,4 %

This shows that the ratio A_{260}/A_{280} is not influenced, but the yield is significantly higher after extracting only once (P=0.0006).

3.3.1.2 Conventional PCR

In order to establish a PCR protocol specific to porcine sequences, first-choice primers were designed (TibMolbiol) and tested under a low stringent annealing condition of 56°C. To detect even small amounts of DNA, 60 PCR cycles were performed.

Since the first-choice primers did not lead to amplification, the alternative primers were designed and tested. For comparison a PCR run with both pairs of primers (2 x 2 primers) was performed to increase the probability of primer binding. This run could then be compared to a run with the "first-choice" primers and to a run with the alternative primers. As the run with the 2 x 2 primers showed the same result as the PCR with alternative primers, which showed amplification, these primers were used in the experiments from then on. In addition, more stringent conditions with annealing temperatures of 60°C, 62°C and 64°C could be tested. This showed an optimal result with an annealing temperature of 62°C.

Further Optimisation experiments, e.g. adaptation of magnesium chloride concentration were performed with the LightCycler.

3.3.1.3 LightCycler PCR

3.3.1.3.1 Standard Curve

For quantitation, the LightCycler's software used a standard curve obtained from samples with known concentration of the respective amplicon sequence. To acquire a representative standard curve, plasmids containing the sequence of interest were analysed.
These plasmid solutions had the following concentrations: 5×10^2, 5×10^3, 5×10^4, 5×10^5 and 5×10^6 copies per µl. Since 2 µl DNA sample was added per capillary the concentration range in these capillaries corresponded to copies of cDNA in the samples. Figure 36 demonstrates a typical standard curve for GLUT1.

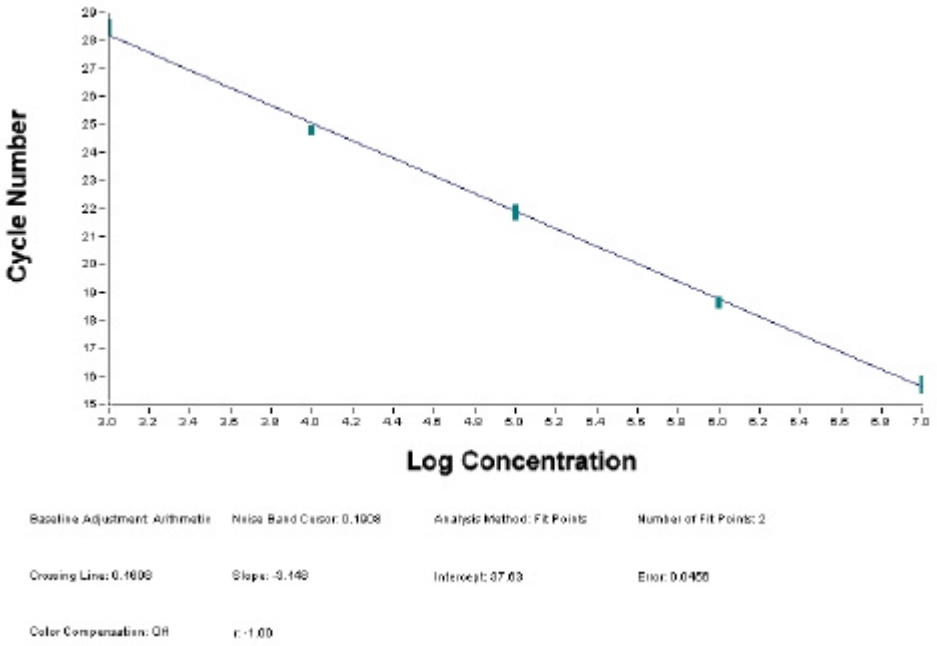

Figure 36 Standard curve for GLUT1

3.3.1.3.2 Magnesium Chloride Concentration

For every new PCR protocol the optimum $MgCl_2$ concentration must be determined experimentally. Different concentrations (2 mM, 3 mM, 4 mM, 5 mM, 6 mM) were tested with a pooled cDNA sample from different RNA preparations and plasmids. The parameters used to determine the "best" $MgCl_2$ were:

- Intensity of the fluorescence signal, because a low signal is harder to distinguish from background noise.
- Efficiency of the taq polymerase.

Comparing the different $MgCl_2$ concentrations the best efficiency and the highest signal were obtained with a concentration of 5 mM. Figure 37 shows a GLUT1 PCR with 3 mM, 4 mM and 5 mM $MgCl_2$ indicating the same result.

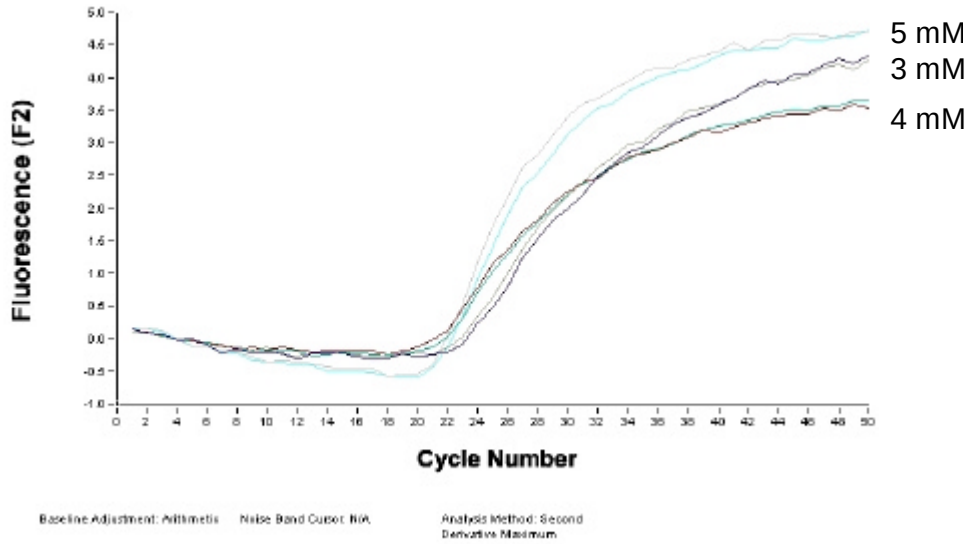

Figure 37 LightCycler PCR with 10^6 plasmids and different $MgCl_2$ concentrations

3.3.1.3.3 Polymerase Efficiency With Plasmids and cDNA

Accurate quantification requires close to identical amplification efficiencies for cDNA samples and plasmid standards. To ensure that amplification efficiencies were the same, the slope of a standard curve was compared to the slope of a dilution series of a pooled cDNA sample from different RNA preparations (pool, 0,1 x pool and 0,01 x pool). This showed that there is no marked difference between the efficiency of the Taq Polymerase processing plasmids and cDNA.

3.3.1.3.4 Cross Reactions

As the glucose transporters belong to a larger family of glucose transport proteins they show high homology. PCR reactions were checked for cross-reactions between target sequences, primers and hybprobes of different GLUTs.

A PCR was run with every possible combination of plasmids, primers and hybprobes (see Table 21).

Table 21 Combinations of plasmids, primers and hybprobes applied to test for cross-reactions

Plasmid (10^6copies)	Primer	HybProbe
GLUT1	GLUT1	GLUT1
GLUT1	GLUT1	GLUT3
GLUT1	GLUT1	GLUT4
GLUT1	GLUT3	GLUT1
GLUT1	GLUT3	GLUT3
GLUT1	GLUT3	GLUT4
GLUT3	GLUT1	GLUT1
…and so on		

Only the samples in which plasmids, primers and hybprobes belonged to the same gene gave rise to PCR products. All other combinations did not lead to amplification.

3.3.2 LightCycler PCR

3.3.2.1 Cyclophilin mRNA

3.3.2.1.1 Non-ischaemic Hearts

Table 22 shows the absolute cyclophilin mRNA expression (per µg total RNA) in each of the twelve regions for the examined hearts. These values are graphically illustrated in Figure 38. The results for one region of the different hearts varied. Therefore, the pattern of cyclophilin mRNA expression in the investigated regions differed significantly between the four hearts (P = 0,0058). There was no difference between the LV and RV (P = 0,2792) but there was between LV and the atria (P = 0,0443). Also, the RV showed a lower expression than the atria (P = 0,0283). The endocardial regions of the LV had a higher expression than the epicardial (P = 0,0122).

Table 22 Means for each region and each heart determined out of 3 x 2 measurements

	Heart 1	Heart 2	Heart 3	Heart 4	Mean	SEM (%)
Anterior wall, endocardial	135667	494650	198167	302400	**282721**	27,79
Anterior wall, epicardial	66180	208283	143558	228200	**161555**	22,63
Lateral wall, endocardial	35883	345200	152200	211100	**186096**	34,57
Lateral wall, epicardial	24874	87173	95908	68778	**69184**	22,86
Inferior wall, endocardial	362583	540767	325267	438067	**416671**	11,41
Inferior wall, epicardial	226567	257783	123602	296633	**226146**	16,39
Septum, endocardial	140600	271600	202367	535950	**287629**	30,24
Septum, epicardial	65180	237333	143067	248683	**173566**	24,89
Apex	186740	185683	103797	393050	**217318**	28,40
Right Ventricle	82315	180817	186597	143417	**148286**	16,17
Left Atrium	112467	487900	240317	619583	**365067**	31,55
Right Atrium	454100	194960	335667	604417	**397286**	21,90

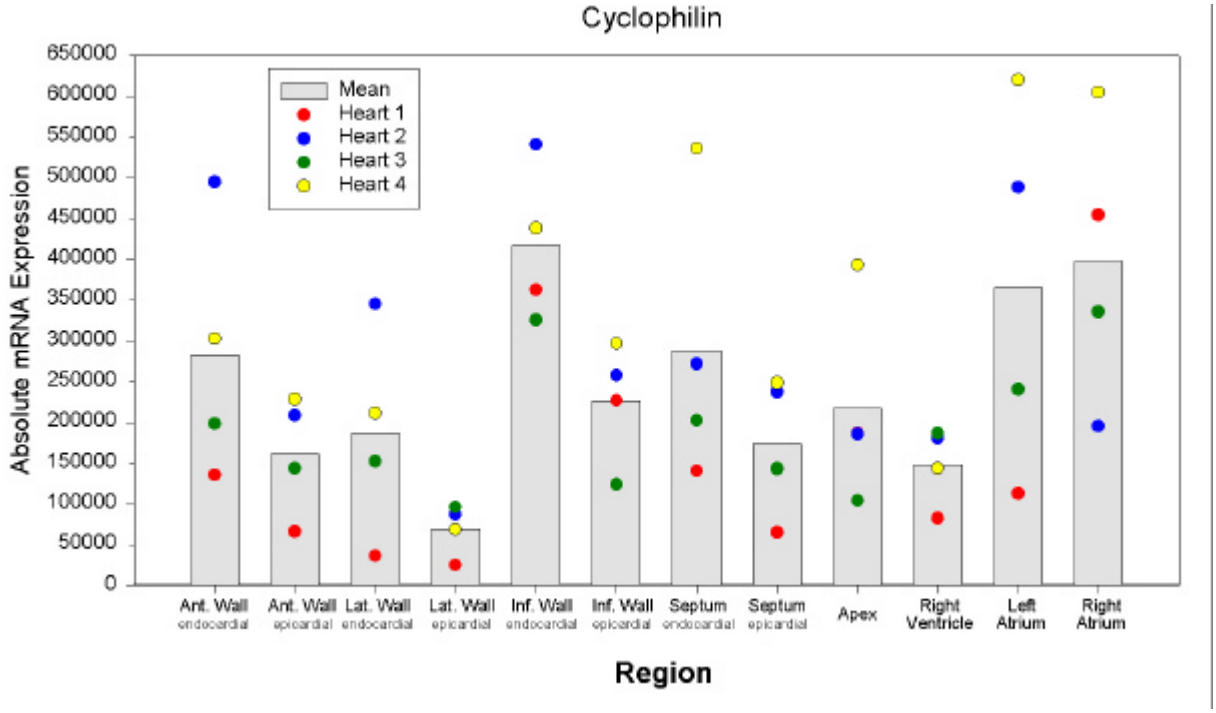

Figure 38 Absolute values of Cyclophilin mRNA expression for each region in normal hearts

3.3.2.1.2 Ischaemic Hearts

Table 23 demonstrates the absolute cyclophilin mRNA expression (per µg total RNA) in each of the seven regions for the examined hearts. These values are graphically illustrated in Figure 39, which shows that there were differences between the four hearts in these regions (P =

0,0067). The ischaemic regions had a higher cyclophilin expression than the remote regions (P = 0,0279).

The ratio between the sum of the means of the remote region in normal and the sum in ischaemic hearts (i.e. $\frac{Mean(\text{Re } mote_{endocard})_{ischemic} + Mean(\text{Re } mote_{epicard})_{ischemic}}{Mean(\text{Re } mote_{endocard})_{non-\ ischemic} + Mean(\text{Re } mote_{epicard})_{non-\ ischemic}}$) was 2,89. The value for the ratio calculated in the Mismatch region yielded 10,68. Considering the high SEM this suggests that cyclophilin expression was increased in ischaemic hearts – even more in the injured region than in the remote regions.

Table 23 Means for each region and each heart determined out of 3 x 2 measurements

	Heart 1	Heart 2	Heart 3	Heart 4	Mean	SEM (%)
Remote, endocardial	1228083	446040	641280	1304600	**905001**	23,53
Remote, epicardial	1218567	436820	1087667	1066900	**952488**	18,39
Mismatch, endocardial	3131333	493320	2675833	2828167	**2282163**	26,46
Mismatch, epicardial	3612333	1396200	2127667	2706000	**2460550**	19,03
Match	2783500	809360	117935	2034333	**1436282**	41,70
Right Ventricle	916183	154980	2349833	1020917	**1110478**	41,06
Left Atrium	1774333	707800	1192600	1832000	**1376683**	19,30
Right Atrium	1513500	938420	1056283	1213550	**1180438**	10,55

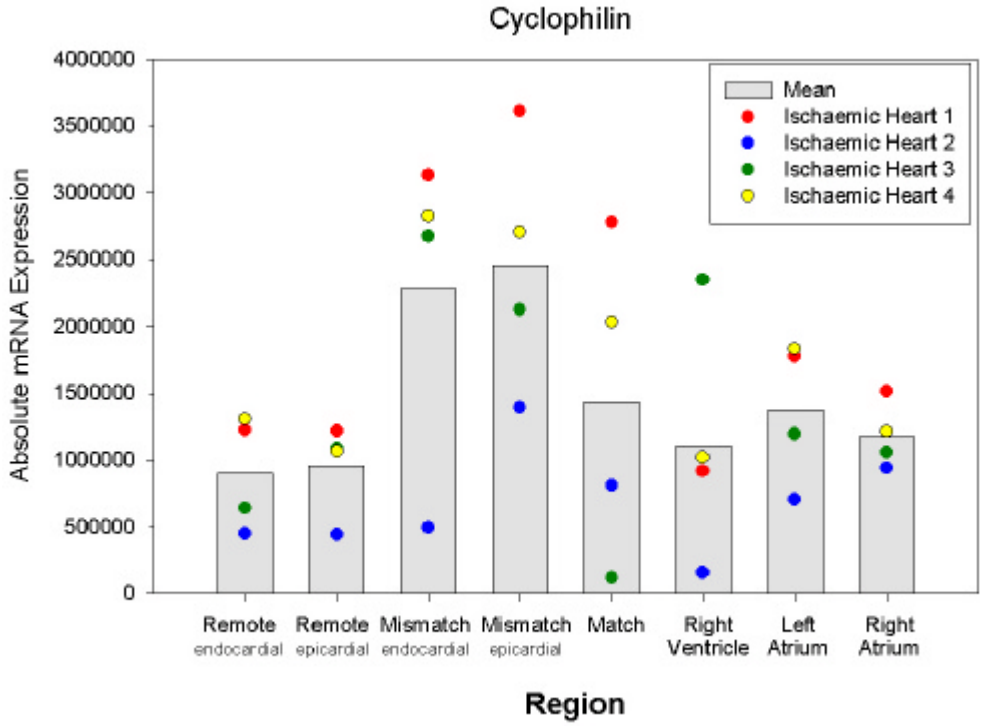

Figure 39 Absolute values of Cyclophilin mRNA expression for each region in ischaemic hearts

3.3.2.2 GLUT1 mRNA

3.3.2.2.1 Non-Ischaemic Hearts

Table 24 shows the absolute GLUT1 mRNA expression (per µg total RNA) in each of the twelve regions for the examined hearts. These values are graphically illustrated in Figure 40. There was a significant difference between the endo- and epicardial parts of the LV (P = 0,0151). In contrast no significant difference could be detected between the two atria (P = 0,6857) and also between the atria and the RV (P = 0,2828). The epicardial LV had the same GLUT1 expression level as the RV and the atria, but the endocardial LV had a significantly higher expression than the atria (P = 0,0044) but not than the RV (P = 0,0528).

Table 24 Means for each region and each heart determined out of 3 x 2 measurements

	Heart 1	Heart 2	Heart 3	Heart 4	Mean	SEM (%)
Anterior wall, endocardial	1923,2	13450,0	3064,3	3514,2	**5487,9**	48,74
Anterior wall, epicardial	751,7	3505,3	1238,7	1754,5	**1812,5**	33,12
Lateral wall, endocardial	604,7	14575,0	1219,3	2323,3	**4680,6**	70,87
Lateral wall, epicardial	286,5	1604,0	1047,1	1203,7	**1035,3**	26,64
Inferior wall, endocardial	5616,5	17730,0	3710,5	10029,2	**9271,5**	33,59
Inferior wall, epicardial	2166,0	3623,5	2273,2	3431,7	**2873,6**	13,23
Septum, endocardial	1117,50	14730,00	2329,33	12656,33	**7708,3**	45,28
Septum, epicardial	347,15	9751,75	2005,75	2980,00	**3771,2**	54,79
Apex	1056,87	3902,00	519,97	3986,40	**2366,3**	38,78
Right Ventricle	1134,0	1899,5	1480,1	1432,1	**1486,4**	10,60
Left Atrium	419,4	1737,8	356,4	3402,0	**1478,9**	48,40
Right Atrium	1255,8	773,1	322,3	1404,9	**939,0**	26,18

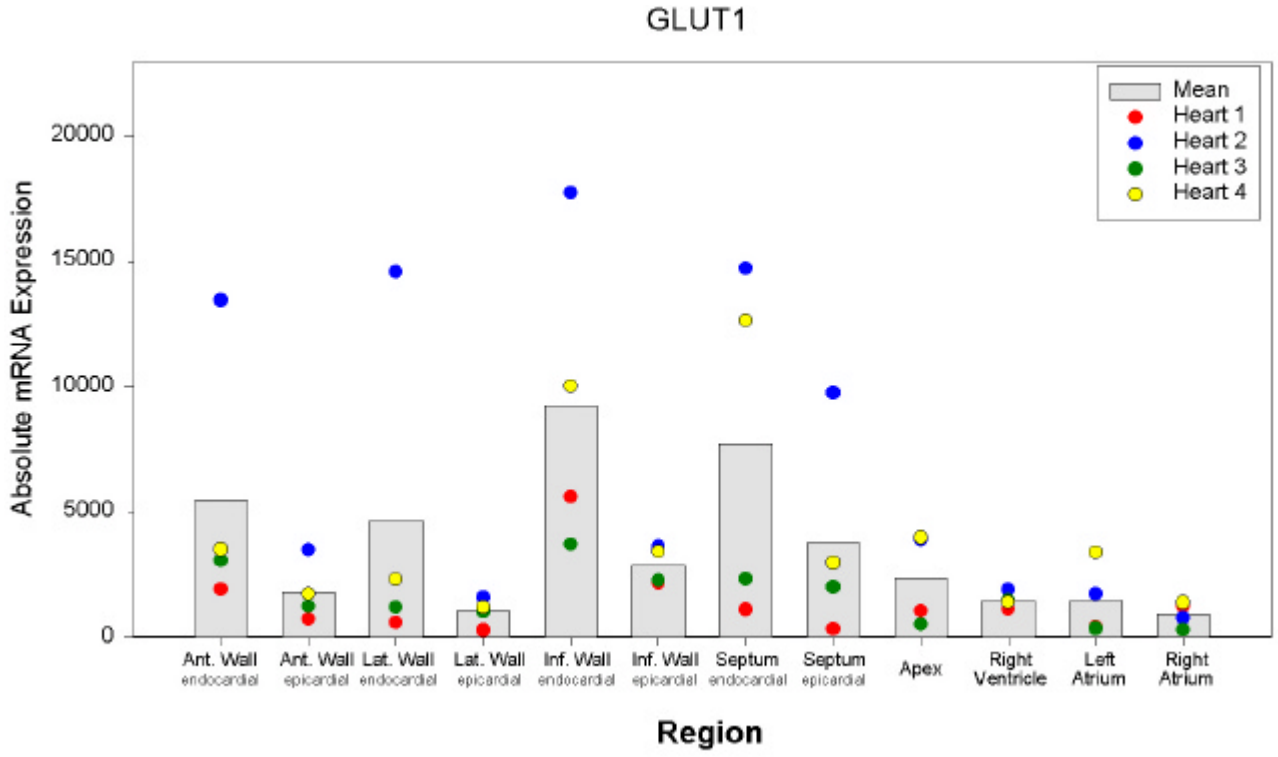

Figure 40 Absolute values of GLUT1 mRNA expression for each region in normal hearts

3.3.2.2.2 Ischaemic Hearts

Table 25 demonstrates the absolute GLUT1 mRNA expression (per µg total RNA) in each of the seven regions for the examined hearts. These values are graphically illustrated in Figure 41, which shows that the results for individual hearts varied in all regions. Therefore, the SEM

was quite high, but there was no significant difference between the hearts (P = 0,4872). Moreover, there was no significant difference between the remote and ischaemic regions (P = 0,3750). However, the remote regions had a significantly higher expression than the atria (P = 0,0070), like the endocardial regions in the normal hearts (see 3.3.2.2.1). But they did not differ from the RV (P = 0,4606).

Evaluating the ratio between ischaemic and normal hearts (as mentioned in 3.3.2.1.2) yielded 1,36 for the remote region. Considering the SEM this is a value around 1 suggesting similar expression of GLUT1 in the remote regions of ischaemic and normal hearts. This ratio yielded a value of 3,51 for the Mismatch region, suggesting an increased GLUT1 expression in the regions of ischaemia.

Table 25 Means for each region and each heart determined out of 3 x 2 measurements

	Heart 1	*Heart 2*	*Heart 3*	*Heart 4*	*Mean*	*SEM (%)*
Remote, endocardial	4440,8	5646,0	5037,2	18040,0	**8291,0**	39,31
Remote, epicardial	4801,7	8088,0	9309,5	10644,3	**8210,9**	15,23
Mismatch, endocardial	15218,3	4817,8	17191,7	12747,0	**12493,7**	21,73
Mismatch, epicardial	22444,0	7127,6	8184,3	14860,0	**13154,0**	26,90
Match	10189,7	5587,0	582,7	6760,2	**5779,9**	34,41
Right Ventricle	2980,3	3022,4	11627,0	8083,3	**6428,3**	32,77
Left Atrium	3343,5	3465,8	2989,0	5533,0	**3832,8**	15,02
Right Atrium	3702,5	7889,8	3157,0	3027,7	**4444,2**	26,05

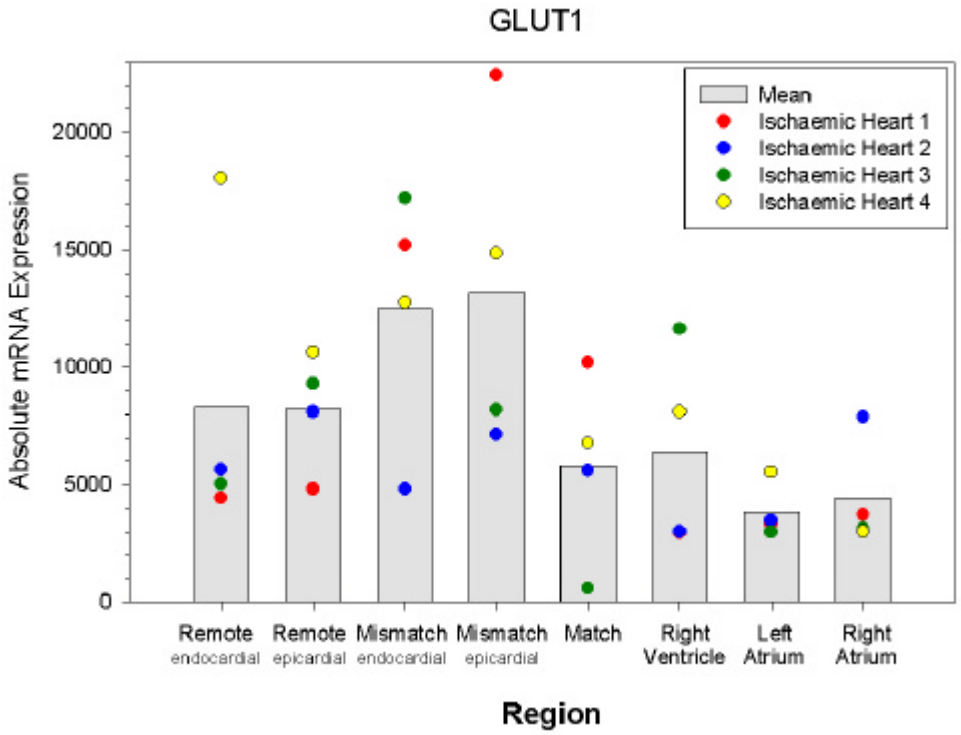

Figure 41 Absolute values of GLUT1 mRNA expression for each region in ischaemic hearts

3.3.2.3 GLUT1/Cyclophilin Ratio

3.3.2.3.1 Non-Ischaemic Hearts

Table 26 displays the relative GLUT1 mRNA expression in each of the twelve regions for the examined hearts. These values are graphically illustrated in Figure 42 and show that LV and RV do not differ significantly (P = 0,0871). Both ventricles had a higher GLUT1/Cyclophilin ratio than the atria (P < 0.0001). Although the ratio was slightly higher in the endocardial than in the epicardial parts (especially because of heart 2), this was not significant (P = 0,1632).

Table 26 Means for each region and each heart determined out of 3 x 2 measurements

	Heart 1	Heart 2	Heart 3	Heart 4	Mean	SEM (%)
Anterior wall, endocardial	0,0142	0,0272	0,0155	0,0116	**0,0171**	20,18
Anterior wall, epicardial	0,0114	0,0168	0,0086	0,0077	**0,0111**	18,46
Lateral wall, endocardial	0,0169	0,0422	0,0080	0,0110	**0,0195**	39,88
Lateral wall, epicardial	0,0115	0,0184	0,0109	0,0175	**0,0195**	10,02
Inferior wall, endocardial	0,0155	0,0328	0,0114	0,0229	**0,0206**	22,74
Inferior wall, epicardial	0,0096	0,0141	0,0184	0,0116	**0,0134**	14,21
Septum, endocardial	0,0079	0,0542	0,0115	0,0236	**0,0243**	43,24
Septum, epicardial	0,0053	0,0411	0,0140	0,0120	**0,0181**	43,54
Apex	0,0057	0,0210	0,0050	0,0101	**0,0105**	35,38
Right Ventricle	0,0138	0,0105	0,0079	0,0100	**0,0105**	11,47
Left Atrium	0,0037	0,0036	0,0015	0,0055	**0,0036**	23,00
Right Atrium	0,0028	0,0040	0,0010	0,0023	**0,0025**	24,78

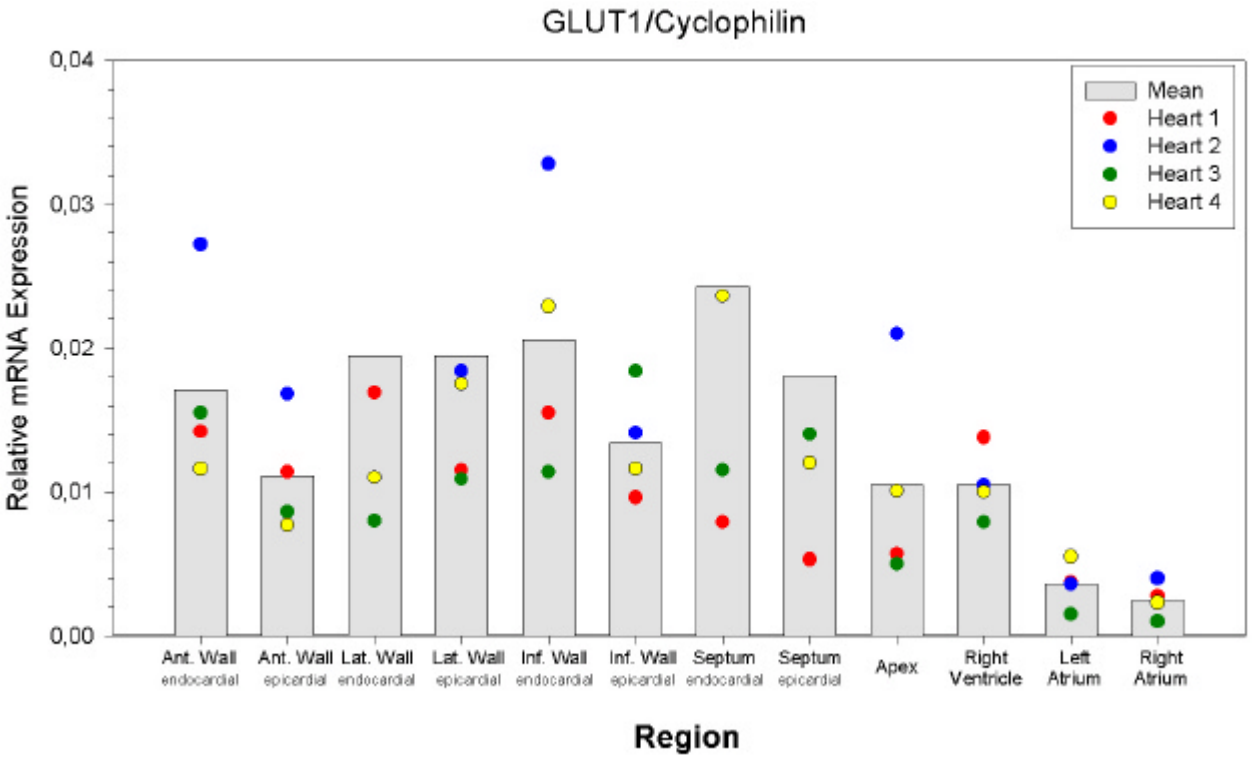

Figure 42 Relative values of GLUT1 mRNA expression for each region in normal hearts

3.3.2.3.2 Ischaemic Hearts

The relative GLUT1 mRNA expression in each of the seven regions for the examined hearts is summarised in Table 27. These values are graphically illustrated in Figure 43. In most of the regions heart 2 had the highest GLUT1/Cyclophilin ratio and caused a high SEM in the remote

epicardial region, in the right ventricle and right atrium. The pattern of GLUT1/Cyclophilin mRNA expression in the investigated regions varied significantly for the four hearts (P = 0,0119). Also, remote and ischaemic regions differed (P = 0,0492) in terms of a higher ratio in the remote LV. As in the non-ischaemic heart, the atria had a smaller ratio than the non-ischaemic LV (remote regions) (P = 0,0030). All other regions did not differ significantly.

The ratio between ischaemic and normal hearts (as mentioned in 3.3.2.1.2) evaluates at 0,58 for the remote region and 0,41 for the Mismatch region. In contrast to the evaluation of absolute GLUT1 mRNA expression (see 3.3.2.2.2) this suggests that the expression in the ischaemic heart was only about half the expression in normal hearts.

Table 27 Means for each region and each heart determined out of 3 x 2 measurements

	Heart 1	*Heart 2*	*Heart 3*	*Heart 4*	*Mean*	*SEM (%)*
Remote, endocardial	0,0036	0,0127	0,0079	0,0138	**0,0095**	24,72
Remote, epicardial	0,0039	0,0185	0,0086	0,0100	**0,0102**	29,69
Mismatch, endocardial	0,0049	0,0098	0,0064	0,0045	**0,0064**	18,78
Mismatch, epicardial	0,0062	0,0051	0,0038	0,0055	**0,0052**	9,60
Match	0,0037	0,0069	0,0049	0,0033	**0,0047**	17,22
Right Ventricle	0,0033	0,0195	0,0049	0,0079	**0,0089**	41,12
Left Atrium	0,0019	0,0049	0,0025	0,0030	**0,0031**	21,11
Right Atrium	0,0024	0,0084	0,0030	0,0025	**0,0041**	35,41

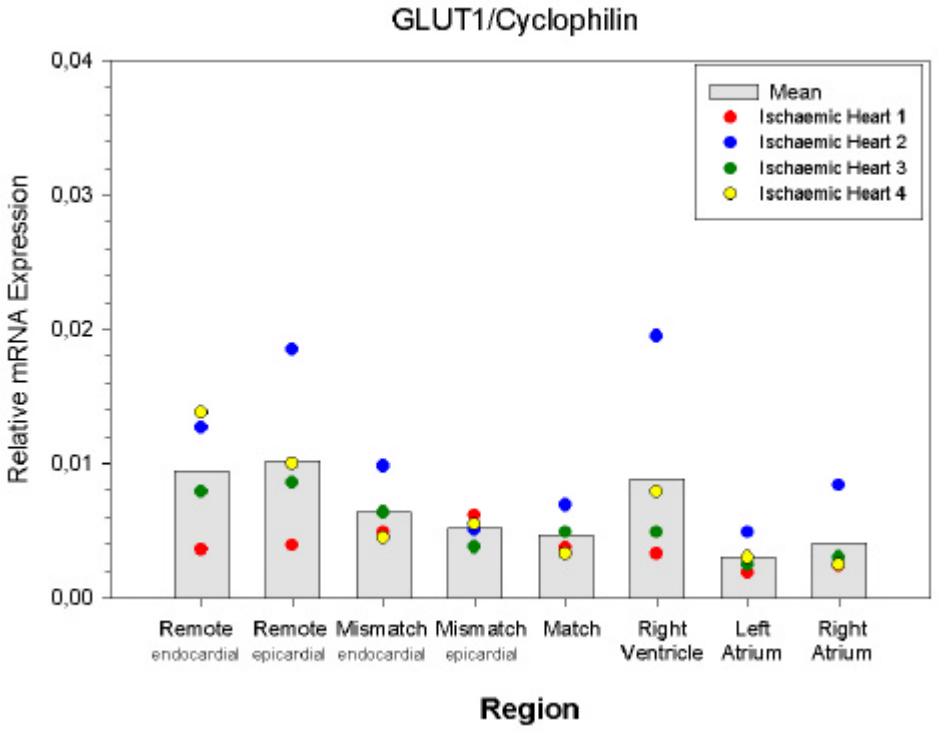

Figure 43 Relative values of GLUT1 mRNA expression for each region in ischaemic hearts

3.3.2.4 GLUT3 mRNA

3.3.2.4.1 Non-Ischaemic Hearts

Table 28 shows the absolute GLUT3 mRNA expression (per µg total RNA) in each of the twelve regions for the examined hearts. These values are graphically illustrated in Figure 44. The endocardial regions in the LV had a significantly higher expression of GLUT3 than the epicardial (P = 0,0479). They also showed a significantly higher expression than atria (P = 0,0054) and the RV (P = 0,0160). The epicardial regions had the same expression level as the atria (P = 0,1185) and the RV (P = 0,3694). The GLUT3 mRNA expression was not homogeneous in the LV: The inferior wall showed a higher mRNA content than the lateral (P = 0,0104) and anterior (P = 0,0148) walls.

Table 28 Means for each region and each heart determined out of 3 x 2 measurements

	Heart 1	Heart 2	Heart 3	Heart 4	Mean	SEM (%)
Anterior wall, endocardial	1029,4	2550,0	885,4	1329,2	**1448,5**	26,14
Anterior wall, epicardial	614,1	934,2	649,3	916,0	**778,4**	10,93
Lateral wall, endocardial	679,5	3845,4	570,2	480,5	**1393,9**	58,70
Lateral wall, epicardial	314,2	987,8	824,1	499,4	**656,4**	23,26
Inferior wall, endocardial	2162,7	3570,5	1195,8	4224,5	**2788,4**	24,50
Inferior wall, epicardial	2053,2	1591,0	940,5	1697,8	**1570,6**	14,78
Septum, endocardial	938,87	4065,20	1092,50	3256,50	**2338,3**	33,44
Septum, epicardial	420,77	3048,00	1273,45	807,14	**1387,3**	41,83
Apex	963,15	2133,80	660,90	1429,28	**1296,8**	24,73
Right Ventricle	675,9	779,2	882,7	805,5	**785,8**	5,44
Left Atrium	449,5	702,7	410,1	849,9	**603,0**	17,37
Right Atrium	928,3	680,6	678,4	689,3	**744,2**	8,25

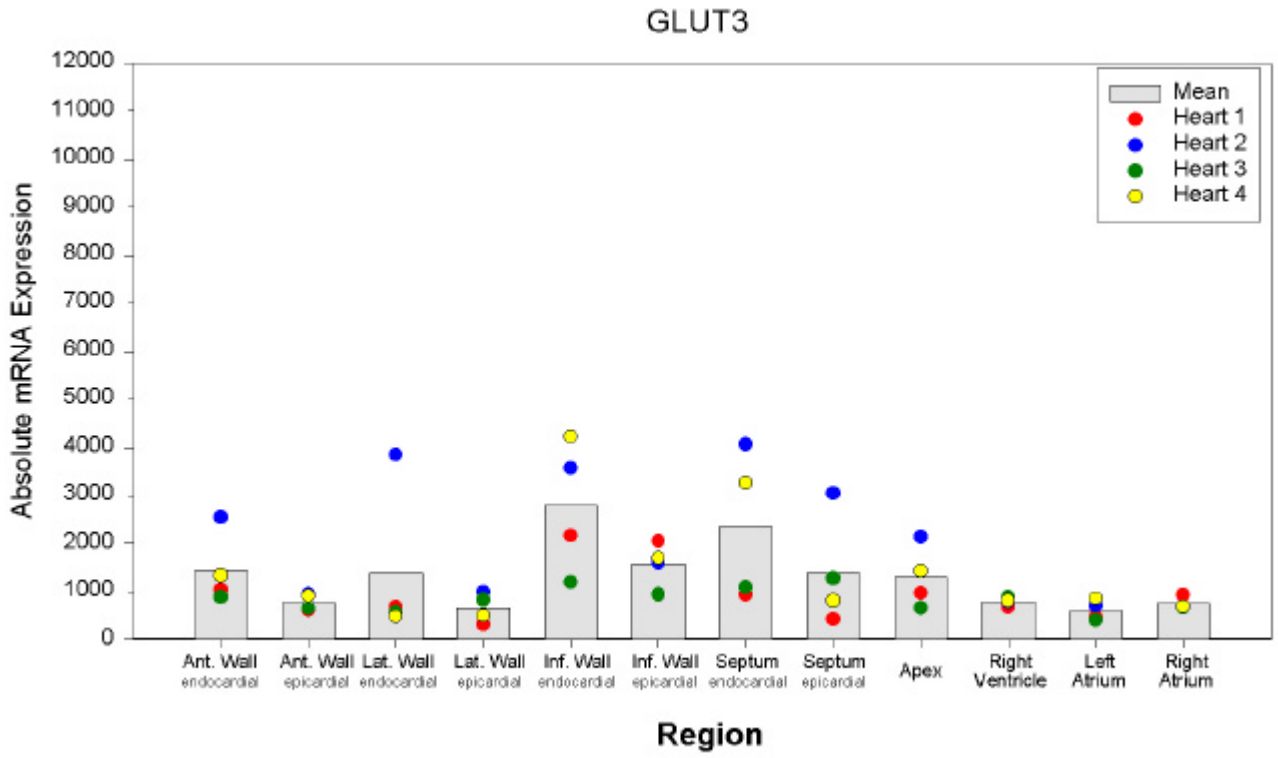

Figure 44 Absolute values of GLUT3 mRNA expression for each region in normal hearts

3.3.2.4.2 Ischaemic Hearts

Table 29 shows the absolute GLUT3 mRNA expression (per µg total RNA) in each of the seven regions for the examined hearts. These values are graphically illustrated in Figure 45. The

pattern of GLUT3 mRNA expression in the investigated regions differed significantly for the four hearts (P = 0,0140). Also, they showed a significant difference between ischaemic and remote regions (P = 0,0098). In the ischaemic region of the epicardial Mismatch the values were widely spread (especially heart 1 had an extraordinary high value in comparison to the other hearts). However, after exclusion of this high single value, the difference is even more significant (P = 0,0020). Between atria and RV there was no detectable difference in the expression level of GLUT3 (P = 0,8081). In contrast to the non-ischaemic heart there was no significant difference between the remote LV and the RV (P = 0,1535) and atria (P = 0,0830), respectively.

Evaluating the ratio between ischaemic and normal hearts (as mentioned in 3.3.2.1.2) yielded 2,23 for the remote region and 2,84 for the Mismatch region. Considering the SEM this suggests an increased GLUT3 expression in the remote as well as in the injured region of ischaemic hearts.

Table 29 Means for each region and each heart determined out of 3 x 2 measurements

	Heart 1	*Heart 2*	*Heart 3*	*Heart 4*	*Mean*	*SEM (%)*
Remote, endocardial	4136,3	3253,5	3002,0	9275,7	**4916,9**	29,96
Remote, epicardial	5148,5	3742,2	3097,8	7224,8	**4803,3**	19,02
Mismatch, endocardial	2536,8	607,3	1160,6	2029,2	**1583,4**	27,28
Mismatch, epicardial	11226,0	1428,8	1117,7	5222,4	**4748,7**	49,53
Match	2629,3	1274,0	105,3	577,9	**1146,6**	47,92
Right Ventricle	3316,5	1511,3	2341,5	3915,3	**2771,2**	19,15
Left Atrium	4733,3	3271,6	2374,5	3121,2	**3375,1**	14,62
Right Atrium	4294,3	1759,8	2480,7	1566,0	**2525,2**	24,62

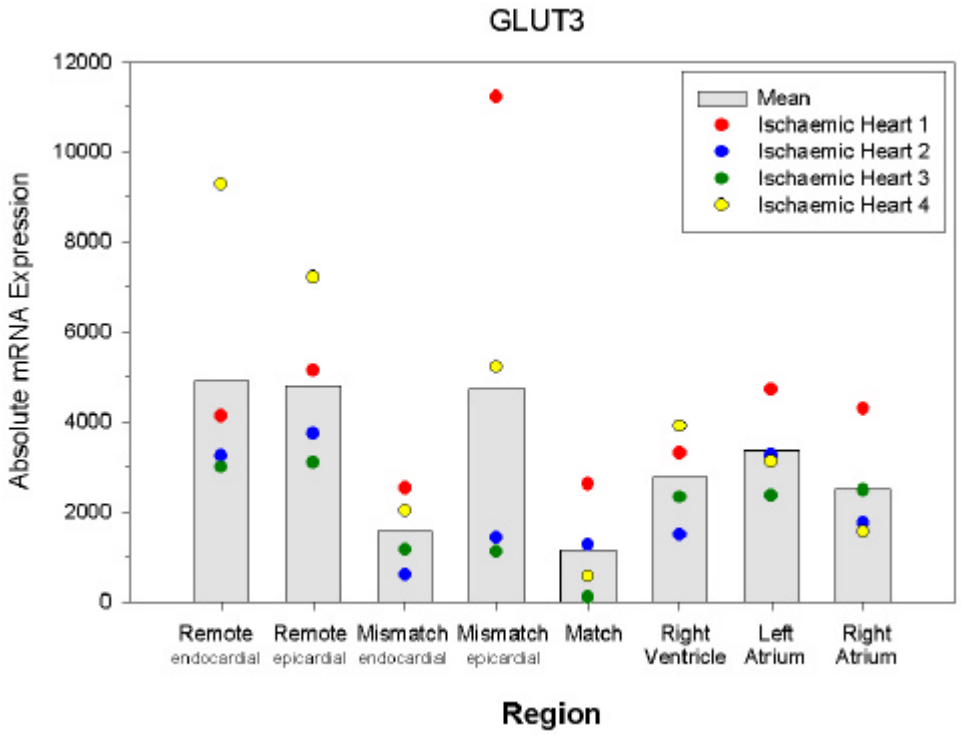

Figure 45 Absolute values of GLUT3 mRNA expression for each region in ischaemic hearts

3.3.2.5 GLUT3/Cyclophilin Ratio

3.3.2.5.1 Non-Ischaemic Hearts

Table 30 demonstrates the relative GLUT3 mRNA expression in each of the twelve regions for the examined hearts. These values are graphically illustrated in Figure 46. Although the values were spread for each region, the hearts did not differ significantly (P = 0,0529). The atria showed a lower GLUT3/Cyclophilin ratio than the ventricular regions (P < 0,0001), which did not differ (P = 0,3784).

Table 30 Means for each region and each heart determined out of 3 x 2 measurements

	Heart 1	Heart 2	Heart 3	Heart 4	Mean	SEM (%)
Anterior wall, endocardial	0,0076	0,0052	0,0045	0,0044	**0,0054**	13,86
Anterior wall, epicardial	0,0093	0,0045	0,0045	0,0040	**0,0056**	22,24
Lateral wall, endocardial	0,0189	0,0111	0,0037	0,0023	**0,0090**	42,45
Lateral wall, epicardial	0,0126	0,0113	0,0086	0,0073	**0,0090**	13,64
Inferior wall, endocardial	0,0060	0,0066	0,0037	0,0096	**0,0065**	19,00
Inferior wall, epicardial	0,0091	0,0062	0,0076	0,0057	**0,0071**	10,59
Septum, endocardial	0,0067	0,0150	0,0054	0,0061	**0,0083**	27,11
Septum, epicardial	0,0065	0,0128	0,0089	0,0032	**0,0079**	25,75
Apex	0,0052	0,0115	0,0064	0,0036	**0,0067**	25,57
Right Ventricle	0,0082	0,0043	0,0047	0,0056	**0,0057**	15,31
Left Atrium	0,0040	0,0014	0,0017	0,0014	**0,0021**	29,45
Right Atrium	0,0020	0,0035	0,0020	0,0011	**0,0022**	22,39

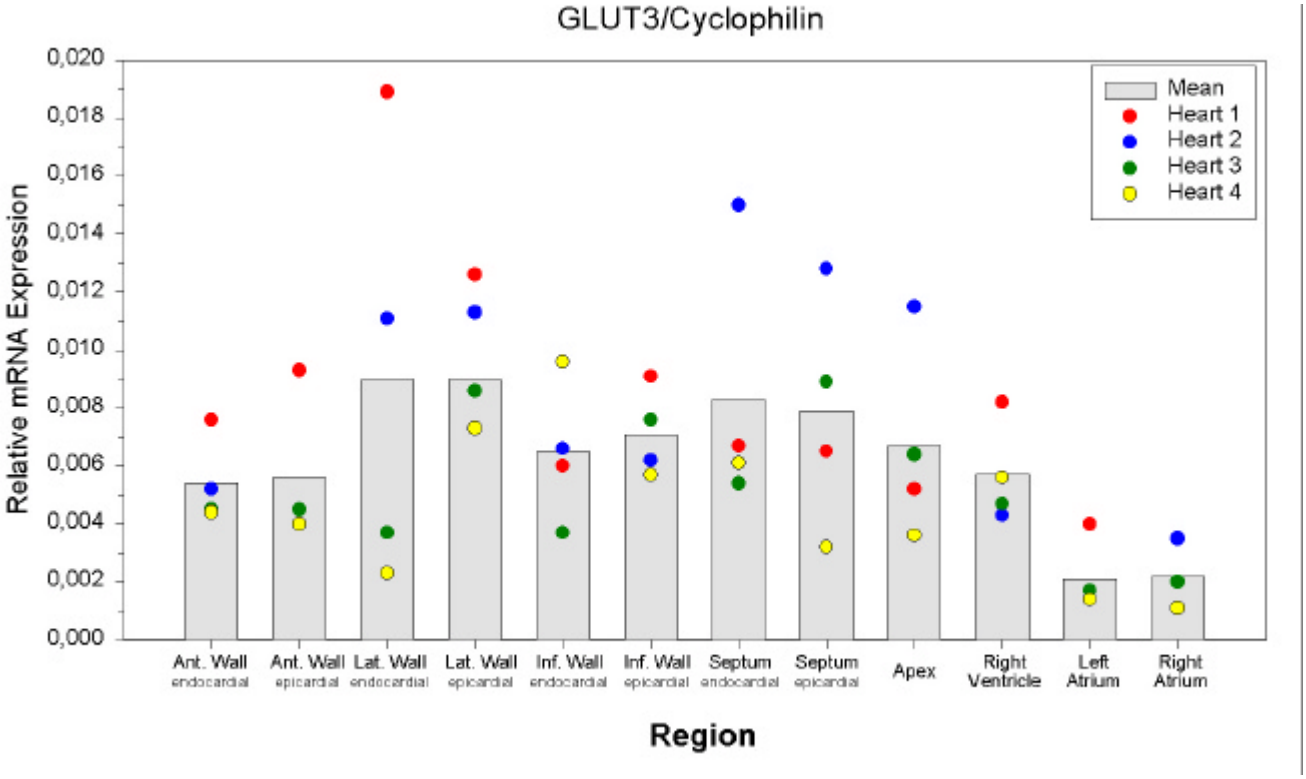

Figure 46 Relative values of GLUT3 mRNA expression for each region in normal hearts

3.3.2.5.2 Ischaemic Hearts

The relative GLUT3 mRNA expression in each of the seven regions for the examined hearts is listed in Table 31. These values are graphically illustrated in Figure 47. Although the regional

expression levels were spread, the pattern of GLUT3/Cyclophilin expression in the investigated regions did not differ significantly (P = 0,3723). In the remote regions we observed a significantly higher GLUT3/Cyclophilin ratio than in the ischaemic areas (P = 0,0003). As in the normal hearts, the non-ischaemic LV (remote regions) showed a higher ratio than the atria (P = 0,0011) but not than the RV (P = 0,5697).

Comparing ischaemic and normal hearts (as mentioned in 3.3.2.1.2) the ratio is 0,82 for the remote region and 0,22 for the Mismatch region. The value for the remote region was around 1 indicating that there is no difference between the two groups of hearts. However, the results suggest a decreased GLUT3 expression in the Mismatch region of ischaemic hearts, which is in contrast to the results of 3.3.2.4.2.

Table 31 Means for each region and each heart determined out of 3 x 2 measurements

	Heart 1	*Heart 2*	*Heart 3*	*Heart 4*	*Mean*	*SEM (%)*
Remote, endocardial	0,0034	0,0073	0,0047	0,0071	**0,0056**	17,04
Remote, epicardial	0,0042	0,0086	0,0028	0,0068	**0,0056**	22,83
Mismatch, endocardial	0,0008	0,0012	0,0004	0,0007	**0,0008**	20,68
Mismatch, epicardial	0,0031	0,0010	0,0005	0,0019	**0,0016**	34,45
Match	0,0009	0,0016	0,0009	0,0003	**0,0009**	28,53
Right Ventricle	0,0036	0,0098	0,0010	0,0038	**0,0046**	40,65
Left Atrium	0,0027	0,0046	0,0020	0,0017	**0,0027**	23,93
Right Atrium	0,0028	0,0019	0,0023	0,0013	**0,0021**	15,83

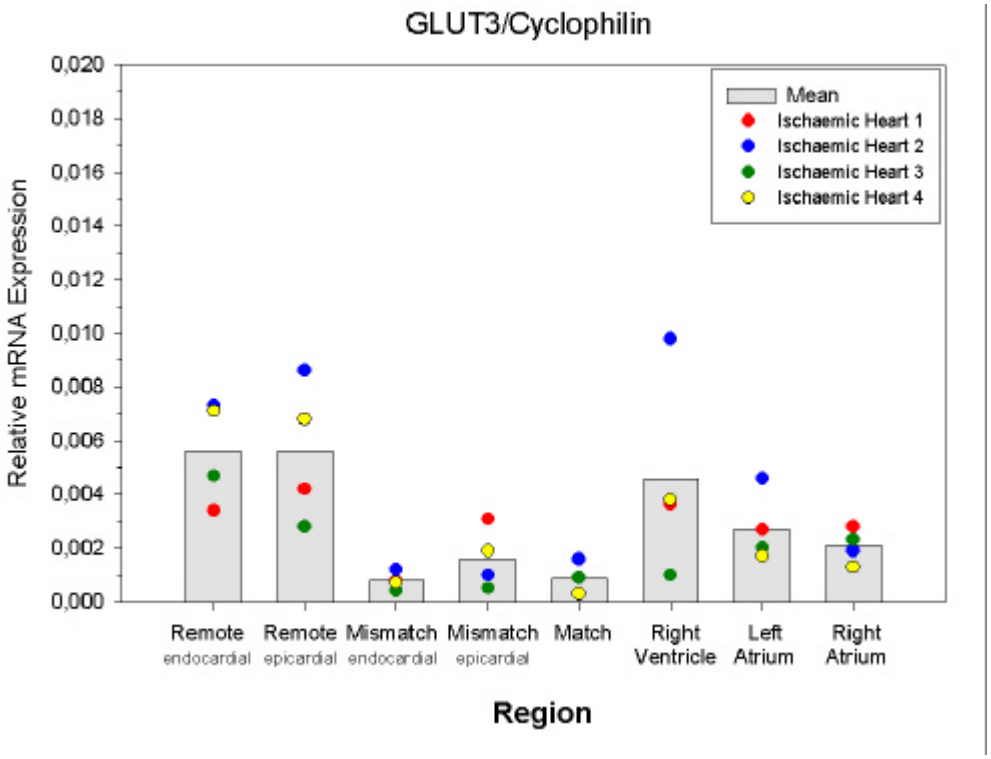

Figure 47 Relative values of GLUT3 mRNA expression for each region in ischaemic hearts

3.3.2.6 GLUT4 mRNA

3.3.2.6.1 Non-Ischaemic Hearts

Table 32 shows the absolute GLUT4 mRNA expression (per µg total RNA) in each of the twelve regions for the examined hearts. These values are graphically illustrated in Figure 48. The high GLUT4 expression in the LV, especially in the endocardial parts, was mainly due to a spread in values (heart 2 and 4 showed high values there). Therefore, there was a significant dissimilarity between the four hearts ($P = 0,0083$). The difference between endocardial and epicardial regions was not significant ($P = 0,0864$). However, there was a significantly higher expression in the LV in comparison to the atria ($P < 0,0001$) and the RV ($P = 0,0127$), respectively. The difference between RV and atria is not significant ($P = 0,1091$). The left ventricular regions displayed no siginificant difference ($P = 0,1053$).

Table 32 Means for each region and each heart determined out of 3 x 2 measurements

	Heart 1	Heart 2	Heart 3	Heart 4	Mean	SEM (%)
Anterior wall, endocardial	6162,3	24157,5	7159,3	10914,4	**12098,4**	34,28
Anterior wall, epicardial	3693,8	10446,8	3990,0	6746,8	**6219,3**	25,21
Lateral wall, endocardial	8748,5	53292,0	11462,0	9704,0	**20801,6**	52,13
Lateral wall, epicardial	3418,0	13475,0	9479,0	11116,3	**9372,1**	22,91
Inferior wall, endocardial	14401,7	34156,7	10027,8	28638,0	**21806,0**	26,24
Inferior wall, epicardial	8469,3	13321,7	6735,3	14570,0	**10774,1**	17,47
Septum, endocardial	7161,50	69932,00	11274,67	51901,67	**35067,5**	43,90
Septum, epicardial	4318,17	37320,00	13656,00	19816,67	**18777,7**	37,03
Apex	12355,00	21880,00	8533,67	17313,33	**15020,5**	19,36
Right Ventricle	3925,0	6757,0	3775,5	4228,0	**4671,4**	15,02
Left Atrium	1148,4	5124,3	1998,6	4041,0	**3078,1**	29,66
Right Atrium	2250,8	3324,0	3110,0	3814,0	**3124,7**	10,45

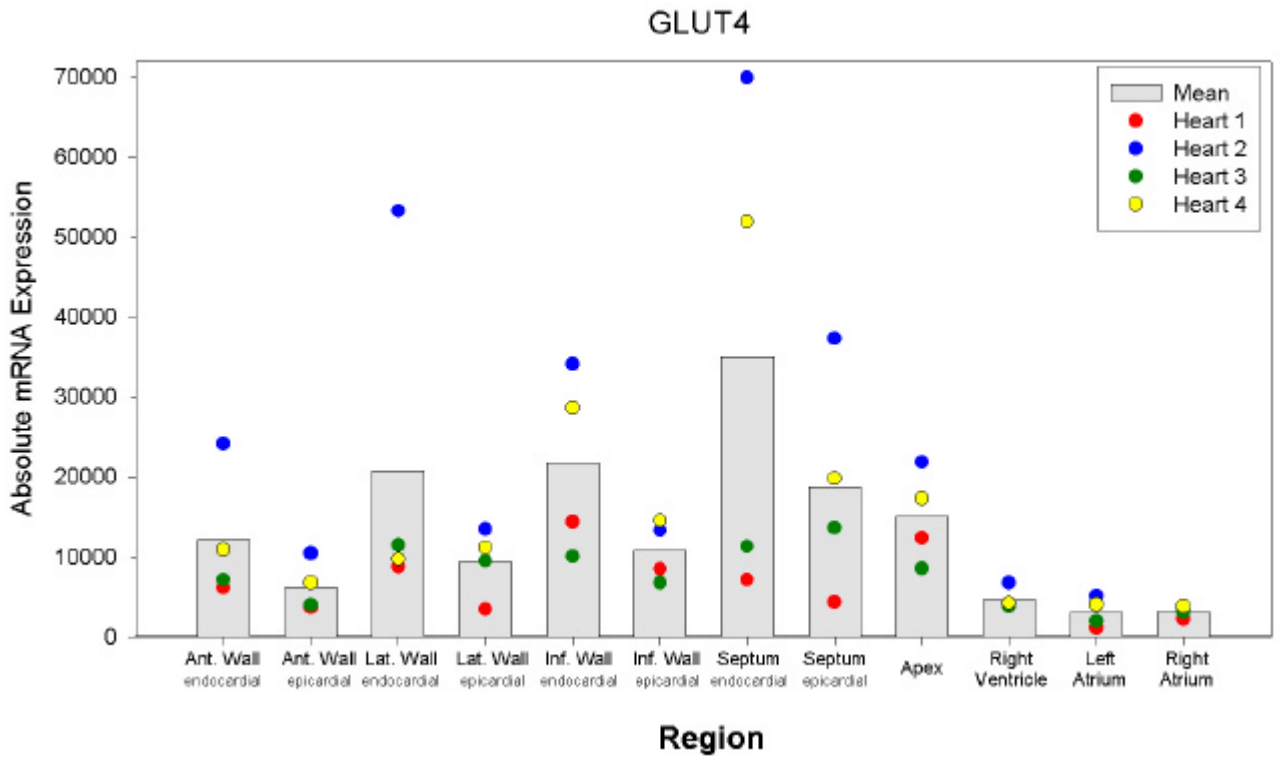

Figure 48 Absolute values of GLUT4 mRNA expression for each region in normal hearts

3.3.2.6.2 *Ischaemic Hearts*

Table 33 shows the absolute GLUT4 mRNA expression (per µg total RNA) in each of the seven regions for the examined hearts. These values are graphically illustrated in Figure 49. The

values spread in the remote regions, mainly due to heart 4, which exhibited a higher GLUT4 expression level. But the pattern of GLUT4 mRNA expression in the investigated regions did not differ significantly between the four hearts (P = 0,2891). The ischaemic regions showed a decreased GLUT4 expression in comparison to remote LV (P = 0,0005). There was no disparity between the non-ischaemic LV and the RV (P = 0,1535) but one was observed between remote LV and atria (P = 0,0499). As in the normal heart there was no difference between RV and atria (P = 0,9333).

The ratio between ischaemic and normal hearts (as mentioned in 3.3.2.1.2) is 1,90 for the remote region and 0,56 for the Mismatch region. Thus, GLUT4 expression was increased in remote regions of ischaemic hearts in comparison to the same region in normal hearts while the expression was decreased in the ischaemically injured region.

Table 33 Means for each region and each heart determined out of 3 x 2 measurements

	Heart 1	*Heart 2*	*Heart 3*	*Heart 4*	*Mean*	*SEM (%)*
Remote, endocardial	25483,3	11874,0	14058,0	61055,0	**28117,6**	40,46
Remote, epicardial	27568,3	24866,0	31493,3	51375,0	**33825,7**	17,76
Mismatch, endocardial	5196,5	1808,2	1406,8	3226,8	**2909,6**	29,44
Mismatch, epicardial	18453,3	1971,8	278,9	8523,2	**7306,8**	56,37
Match	1733,6	5711,0	5,7	1333,4	**2195,9**	55,94
Right Ventricle	15758,3	13590,0	5172,5	25548,3	**15017,3**	27,88
Left Atrium	31743,3	11904,0	17275,0	21010,0	**20483,1**	20,47
Right Atrium	15971,7	8897,6	11169,6	10424,8	**11615,9**	13,15

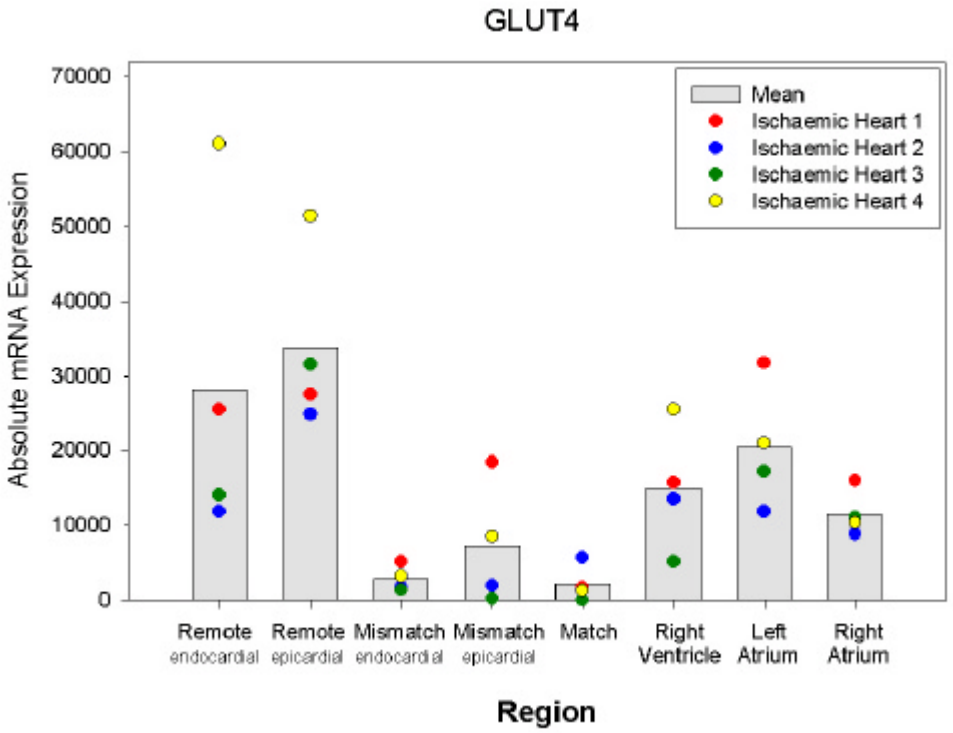

Figure 49 Absolute values of GLUT4 mRNA expression for each region in ischaemic hearts

3.3.2.7 GLUT4/Cyclophilin Ratio

3.3.2.7.1 Non-Ischaemic Hearts

Table 34 shows the relative GLUT4 mRNA expression in each of the twelve regions for the examined hearts. These values are graphically illustrated in Figure 50. The left ventricular regions showed a non homogenous expression as the lateral wall and septum had a higher expression than the inferior and anterior walls (P = 0,0003). The mean value of the LV regions showed a higher GLUT4/Cyclophilin ratio than the atria (P < 0,0001) and the RV (P = 0,0157). There was no significant difference between the two atria (P = 0,6857).

Table 34 Means for each region and each heart determined out of 3 x 2 measurements

	Heart 1	Heart 2	Heart 3	Heart 4	Mean	SEM (%)
Anterior wall, endocardial	0,0454	0,0488	0,0361	0,0361	**0,0416**	7,82
Anterior wall, epicardial	0,0558	0,0502	0,0278	0,0296	**0,0408**	17,44
Lateral wall, endocardial	0,2438	0,1544	0,0753	0,0460	**0,1299**	34,15
Lateral wall, epicardial	0,1374	0,1546	0,0988	0,1616	**0,1299**	10,82
Inferior wall, endocardial	0,0397	0,0632	0,0308	0,0654	**0,0498**	17,23
Inferior wall, epicardial	0,0374	0,0517	0,0545	0,0491	**0,0482**	7,80
Septum, endocardial	0,0509	0,2575	0,0557	0,0968	**0,1152**	42,10
Septum, epicardial	0,0662	0,1572	0,0955	0,0797	**0,0997**	20,17
Apex	0,0662	0,1178	0,0822	0,0440	**0,0776**	20,03
Right Ventricle	0,0477	0,0374	0,0202	0,0295	**0,0337**	17,31
Left Atrium	0,0102	0,0105	0,0083	0,0065	**0,0089**	10,41
Right Atrium	0,0050	0,0170	0,0093	0,0063	**0,0094**	28,79

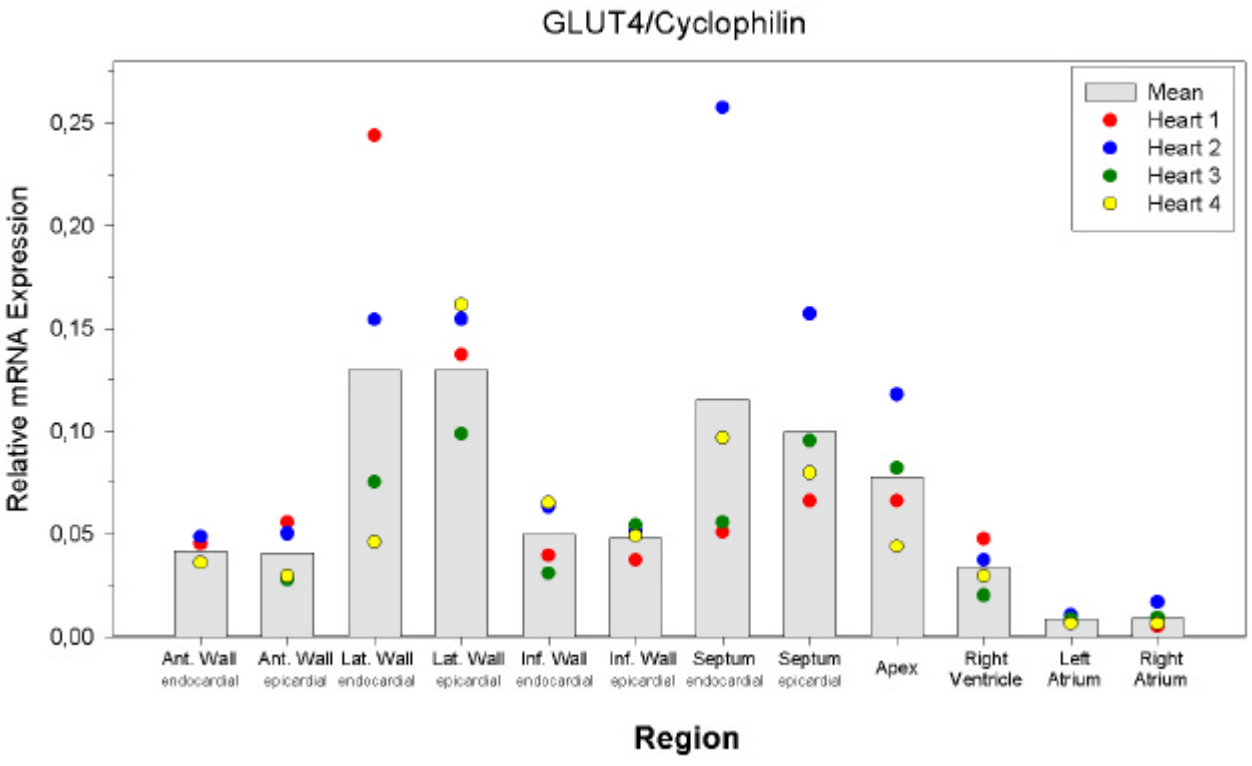

Figure 50 Relative values of GLUT4 mRNA expression for each region in normal hearts

3.3.2.7.2 Ischaemic Hearts

Table 35 demonstrates the relative GLUT4 mRNA expression in each of the seven regions for the examined hearts. These values are graphically illustrated in Figure 51. The ischaemic

regions showed a lower GLUT4/Cyclophilin ratio than the remote LV (P = 0,0003). As in the non-ischaemic heart the remote regions displayed a higher relative GLUT4 expression than the atria (P = 0,0002), but they showed no significant difference compared to the RV (P = 0,4606) (as in the normal hearts, too). The results of the RV were spread widely, causing a high standard deviation and SEM. Especially heart 2 showed a high value, but there was no difference between the four hearts in relation to the expression pattern in all the regions (P = 0,5507). Nevertheless, the statistic evaluation (apart from small changes in the P value) does not change if the values of heart 2 are excluded

The ratio between ischaemic and normal hearts (as mentioned in 3.3.2.1.2) was 0,70 for the remote region and 0,05 for the Mismatch region. So the expression was not changed in the remote region (considering the high SEM) while it was decreased in the ischaemic region in comparison to the same region in normal hearts.

Table 35 Means for each region and each heart determined out of 3 x 2 measurements

	Heart 1	*Heart 2*	*Heart 3*	*Heart 4*	*Mean*	*SEM (%)*
Remote, endocardial	0,0208	0,0266	0,0219	0,0468	**0,0290**	20,88
Remote, epicardial	0,0226	0,0569	0,0290	0,0482	**0,0392**	20,51
Mismatch, endocardial	0,0017	0,0037	0,0005	0,0011	**0,0017**	38,90
Mismatch, epicardial	0,0051	0,0014	0,0001	0,0031	**0,0025**	44,10
Match	0,0006	0,0071	0,0000	0,0007	**0,0021**	79,18
Right Ventricle	0,0172	0,0877	0,0022	0,0250	**0,0330**	57,00
Left Atrium	0,0179	0,0168	0,0145	0,0115	**0,0152**	9,38
Right Atrium	0,0106	0,0095	0,0106	0,0086	**0,0098**	4,87

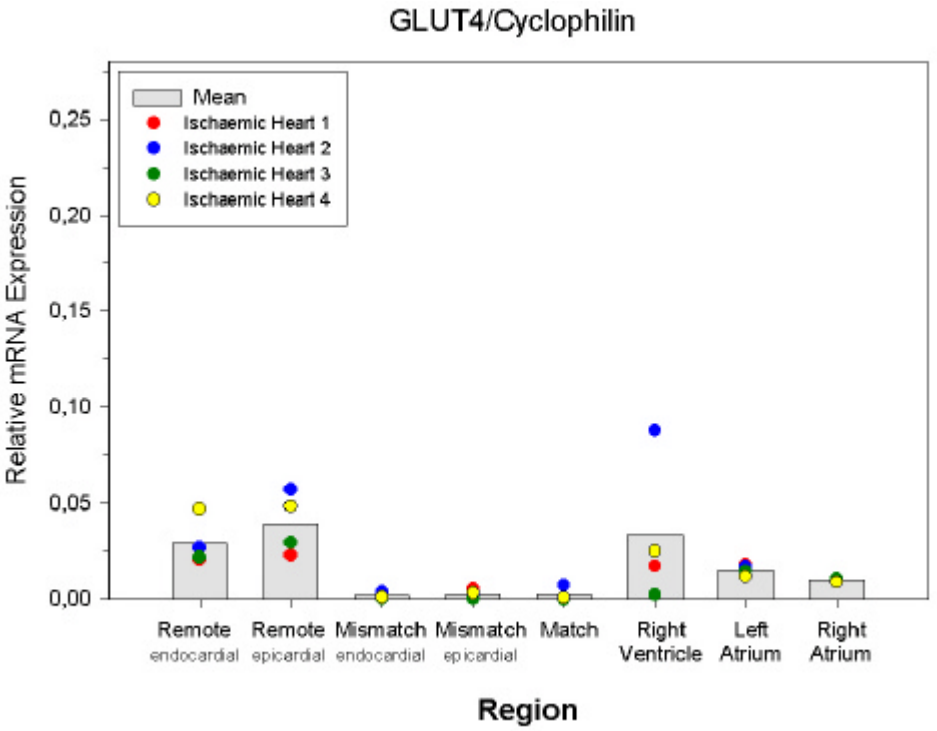

Figure 51 Relative values of GLUT4 mRNA expression for each region in ischaemic hearts

3.3.2.8 GLUT1/GLUT4 Ratio

3.3.2.8.1 Non-Ischaemic Heart

Table 36 shows the GLUT1/GLUT4 mRNA ratio in the twelve regions for each heart. These values are graphically illustrated in Figure 52. All ratios were smaller than one, indicating that GLUT4 expression was predominant. The regional expression pattern showed no significant differences between the hearts (P = 0,5573). The inferior wall revealed a significantly higher expression than the lateral wall (P = 0,0019) and septum (P = 0,0011), respectively. The lateral wall also demonstrated a lower expression level than the anterior wall (P = 0,0030).

Table 36 GLUT1/GLUT4 ratio for each region and each heart determined out of 3 x 2 measurements

	Heart 1	Heart 2	Heart 3	Heart 4	Mean	SEM (%)
Anterior wall, endocardial	0,31	0,56	0,43	0,32	**0,40**	14,10
Anterior wall, epicardial	0,20	0,34	0,31	0,26	**0,28**	10,53
Lateral wall, endocardial	0,07	0,27	0,11	0,24	**0,17**	28,92
Lateral wall, epicardial	0,08	0,12	0,11	0,11	**0,11**	7,17
Inferior wall, endocardial	0,39	0,52	0,37	0,35	**0,41**	9,36
Inferior wall, epicardial	0,26	0,27	0,34	0,24	**0,28**	8,02
Septum, endocardial	0,16	0,21	0,21	0,24	**0,20**	8,87
Septum, epicardial	0,08	0,26	0,15	0,15	**0,16**	23,47
Apex	0,09	0,18	0,06	0,23	**0,14**	28,54
Right Ventricle	0,29	0,28	0,39	0,34	**0,33**	7,89
Left Atrium	0,37	0,34	0,18	0,84	**0,43**	33,17
Right Atrium	0,56	0,23	0,10	0,37	**0,32**	30,79

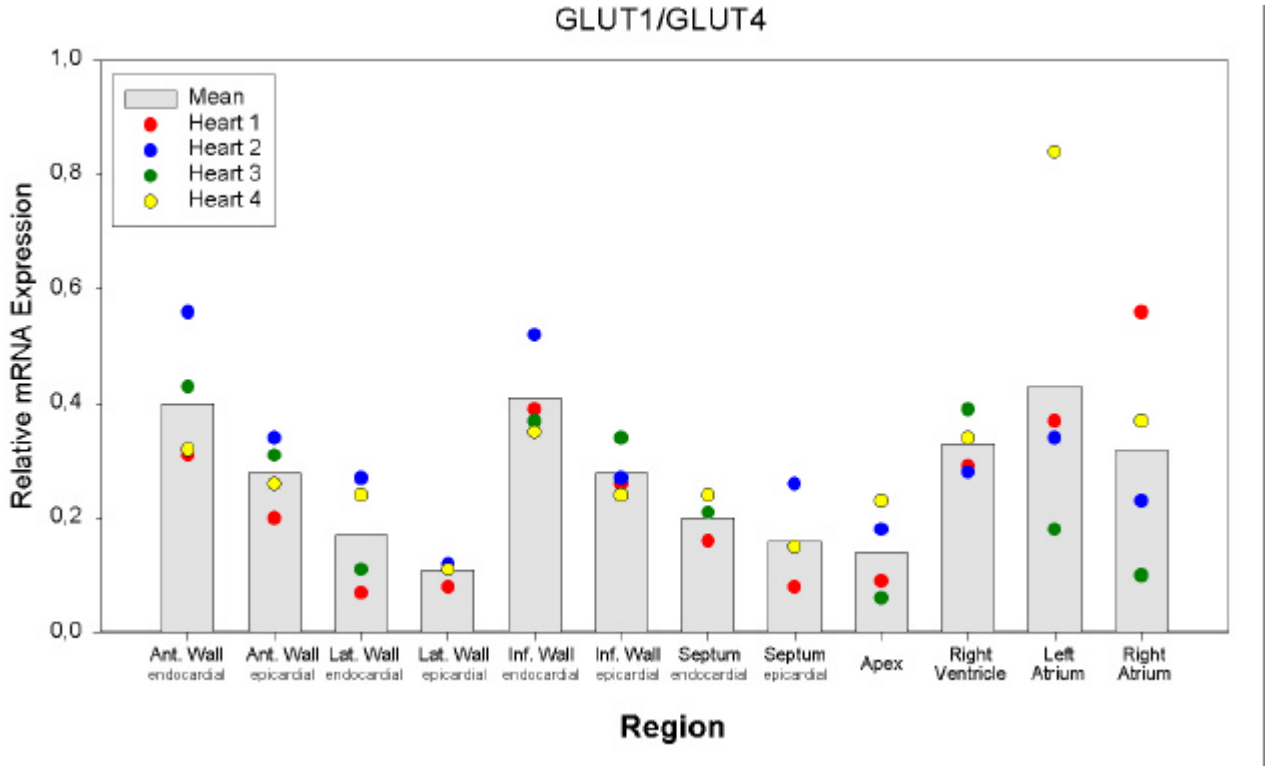

Figure 52 GLUT1/GLUT4 mRNA ratio for each region in non-ischaemic hearts

3.3.2.8.2 Ischaemic Heart

Table 37 shows the GLUT1/GLUT4 mRNA ratio in the eight regions for each heart. These values are graphically illustrated in Figure 53, which has a logarithmic y-axis to visualize the broad range of values. In the ischaemic regions the ratio was above 1 (except heart 2, apex: 0,98), in the non-ischaemic regions the ratio was less than 1 (except heart 3, RV: 2,25). Hence, in normal regions GLUT4 mRNA expression was predominant (as shown in non-ischaemic hearts (see 3.3.2.8.1)), whereas in ischaemic regions GLUT1 expression prevails (P = 0,0003). In spite of the broad range of values the regional expression pattern of the hearts did not differ significantly (P = 0,3690). There was also no difference between the apex and the other ischaemic regions (P = 05697). As in the non-ischaemic hearts there was no difference between the remote left ventricle and the right ventricle (P = 0,8081) and the atria, respectively (P = 0,3823).

Table 37 GLUT1/GLUT4 ratio for each region and each heart determined out of 3 x 2 measurements

	Heart 1	Heart 2	Heart 3	Heart 4	Mean	SEM (%)
Remote, endocardial	0,17	0,48	0,36	0,30	**0,33**	19,28
Remote, epicardial	0,17	0,33	0,30	0,21	**0,25**	14,26
Mismatch, endocardial	2,93	2,66	12,22	3,95	**5,44**	41,84
Mismatch, epicardial	1,22	3,61	29,34	1,74	**8,98**	75,81
Match	5,88	0,98	102,55	5,07	**28,62**	86,19
Right Ventricle	0,19	0,22	2,25	0,32	**0,74**	67,48
Left Atrium	0,11	0,29	0,17	0,26	**0,21**	20,44
Right Atrium	0,23	0,89	0,28	0,29	**0,42**	36,69

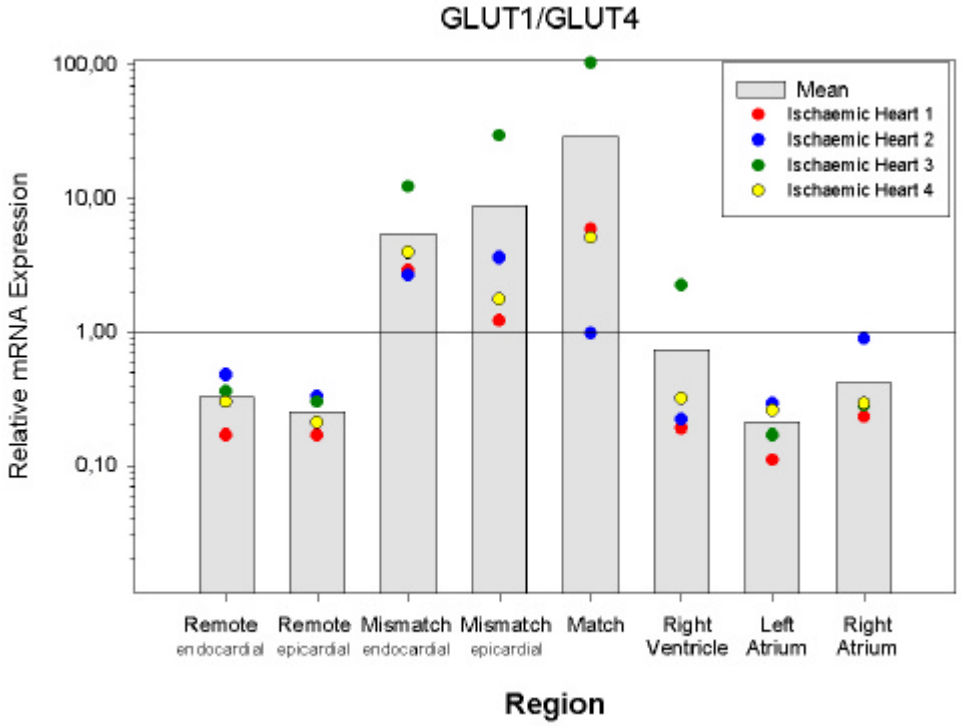

Figure 53 GLUT1/GLUT4 mRNA ratio for each region in ischaemic hearts

3.3.2.9 Summary

3.3.2.9.1 Non-ischaemic Heart

Table 38 shows an overall view to summarise the results of the LightCycler PCR of the normal hearts. GLUT1 displayed higher expression in the endocardial regions than in the epicardial. GLUT3 showed a decrease in expression from LV to RV to atria. The expression of GLUT4 was highest in the left ventricle while right ventricle and atria had a lower expression. After normalisation to cyclophilin the results changed: In this case both ventricles had a higher (normalised) expression than the atria for all three GLUTs.

Table 38 Summary of statistics in the non-ischaemic hearts.

-: not tested
ns: Not significant difference
⊙: Significant difference
⊙ (endo): Only the endocardial LV shows the significance
Hearts: Difference between the single hearts
LV ⇳ RV: Difference between left and right ventricle
LV ⇳ Atria: Difference between left ventricle and atria
RV ⇳ Atria: Difference between right ventricle and atria
LV: Endo- ⇳ epicardial: Difference between the endo- and epicardial regions in LV
LV: Remote ⇳ Mismatch: Difference between the remote and Mismatch region in LV

	Hearts	*LV ⇳ RV*	*LV ⇳ Atria*	*RV ⇳ Atria*	*LV: Endo- ⇳ epicardial*	*4 LV-Regions*
Cyclophilin	⊙	ns	⊙	⊙	⊙	-
GLUT1	⊙	ns	⊙(endo)	ns	⊙	-
GLUT1/Cyclophilin	⊙	ns	⊙	⊙	ns	ns
GLUT3	⊙	ns	⊙	ns	⊙	⊙
GLUT3/Cyclophilin	ns	ns	⊙	⊙	ns	ns
GLUT4	⊙	⊙	⊙	ns	ns	ns
GLUT4/Cyclophilin	ns	⊙	⊙	⊙	ns	⊙
GLUT1/GLUT4	Ns	ns	ns	ns	ns	⊙

3.3.2.9.2 Ischaemic Heart

Table 39 is an overall view summarising the results of the LightCycler PCR of the ischaemic hearts. GLUT1 expression showed no significant difference between remote and ischaemic

left ventricle. However, the expression of GLUT3 and GLUT4 was decreased in ischaemic regions. The housekeeping gene cyclophilin (which should not change under the conditions of the experiment) showed a higher expression in the ischaemic regions. After normalisation to this housekeeping gene all three GLUTs had a decreased expression in the ischaemic regions. However, circumventing normalisation to cyclophilin, the ratio GLUT1/GLUT4 showed the relation between these two transporters and clearly demonstrates: In ischaemic regions GLUT4 becomes predominant.

Table 39 Summary of statistics in the ischaemic hearts.

-: not tested
ns: Not significant difference
⊙: Significant difference
⊙ (endo): Only the endocardial LV shows the significance
Hearts: Difference between the single hearts
Remote ⇔ Ischaemic: Difference between remote regions of the left ventricle and ischaemic regions
Remote ⇔ RV: Difference between remote left ventricle and the right ventricle
Remote ⇔ Atria: Difference between the remote left ventricle and the atria

	Hearts	*Remote ⇔ Ischaemic*	*Remote ⇔ RV*	*Remote ⇔ Atria*
Cyclophilin	⊙	⊙	ns	ns
GLUT1	ns	ns	ns	⊙
GLUT1/Cyclophilin	⊙	⊙	ns	⊙
GLUT3	⊙	⊙	ns	ns
GLUT3/Cyclophilin	ns	⊙	ns	⊙
GLUT4	ns	⊙	ns	⊙
GLUT4/Cyclophilin	ns	⊙	ns	⊙
GLUT1/GLUT4	ns	⊙	ns	ns

4 DISCUSSION

Ischaemic heart disease is still the disease with the highest mortality rate. However, due to a better understanding of the pathophysiology of coronary heart disease, this rate is dropping. The aim of this study was to elucidate the long-term regulation of protein and mRNA levels of GLUT1, 3, 4 and Hexokinase Type II by immunoblotting and RT-PCR. This was done using a pig model with a seven-day ischaemia produced by introduction of a modified stent graft into the LAD. With the help of PET regions with increased FDG uptake and hypoperfusion (hibernating myocardium) the expression levels could be determined under these special conditions. The results gained are discussed below, initially establishing the limitations of the methods used before going into detail. GLUT1 and 4 are mentioned first as they are the transporters, which play the most important role in normal and ischaemic hearts. Then the discussion goes into already available literature about the regulation of their expression. This is followed by the discussion of GLUT3 and hexokinase, about which we know little detail under the chosen experimental conditions in comparison to the other elements.

4.1 Methodological limitations

4.1.1 Degree of ischaemia

Ischaemia was produced by introducing a modified stent graft into the LAD just distal to the first diagonal branch of domestic pigs. However, due to anatomical variation the ischaemic regions differed in size from pig to pig, although the stent was closed in each pig after one week. Also, the rate of occlusion of the stent from the initial 75% to 100% stenosis varied. A further factor was that the extent of collateral development was not uniform in all pigs. Therefore, the degree of injury differed inter-individually and the comparison of the four data sets does not always display changes to the same extent, although the direction constantly stayed the same.

4.1.2 PET, Tissue Acquisition

Results indicate that this newly established experimental model can produce consistently regional contractile dysfunction in areas with coronary artery occlusion and supplied by collateral coronary circulation seven days after intervention. It also demonstrated the association of severe regional reduction of resting myocardial blood flow and corresponding metabolic changes in myocardial energy substrate uptake with increased utilization of

glucose. These are changes typically described in the dedifferentiation process occurring in myocardial hibernation.

In the ischaemic hearts the regions for tissue acquisition were determined by PET studies. The left ventricle was virtually sliced into five pieces along the short axis as it was done practically with the excised heart. With the additional help of the long axes the exact region of hypoperfusion and increased or decreased FDG uptake could be determined. However, the virtual slices had a constant thickness that could hardly be realised practically. Therefore, it is possible that the removed tissue sample not only contained the region of interest but could also be "contaminated" with tissue showing unchanged glucose metabolism. A further possibility of error is that sometimes the "hot spot" in FDG scans was localised between two slices or was quite small. We tried to compensate for this by varying the thickness of the slices in order to get the "hot spot" in one slice.

After localising a region with increased FDG uptake and collecting samples, it has to be kept in mind that this signal can be caused by two completely different mechanisms: 1) Cardiomyocytes in the state of hibernation and 2) invasion of inflammatory cells showing an increased FDG uptake. Therefore, conventional histology was done on a few dip samples with increased FDG uptake, which showed areas of inflammation. To distinguish between an increased FDG uptake into cardiomyocytes caused by ischaemia and uptake of FDG into cells caused by inflammation an immunohistochemistry has to be done. Through this we were able to reveal the localisation of glucose transporters (cardiomyocytes or inflammatory cells).

When comparing the ischaemic hearts with normal hearts one has to be aware that the two groups of pigs were of different age groups (normal pigs: 6 months, ischaemic pigs: 4 months) and received different feeding. Normal pigs were fattened as they were intended for the slaughterhouse. Pigs going for intervention were normally fed and got medication during the week after implantation. Both groups were probably exposed to stress on the day of sacrification. Therefore, exposure of the heart to catecholamines is possible. This has to be considered during examination of ischaemic regions in comparison to the same regions of the normal hearts.

A possibility to omit such an effect is comparing ischaemic regions with normal (remote) regions of the same heart. Then age, feeding and exposure to catecholamines is equal. However, ischaemia with hypokinesia of the affected wall also may change metabolism in the rest of the heart. The remote LV has to compensate the reduced wall motion of the

ischaemic region. If compensation is not complete the left atrium is affected, as it has to deal with a higher volume causing hypertrophy. The next step of a failing compensation is hypertrophy of the volume-stressed RV and later even the right atrium gets involved with increasing preload. Remodelling of the heart and adaptation to the altered pressure conditions can also change expression of proteins playing a role in metabolism like GLUT or HKII. Therefore, comparing ischaemic with remote regions may also be inherently imprecise.

4.1.3 Antibody Binding, Quantification

The affinity of each of the antibodies binding to their specific antigen is not known. Therefore, it was not possible to obtain relative amounts of the examined proteins compared to each other (e.g. “heart tissue has a GLUT distribution of x% GLUT1, y% GLUT3, etc.”). As it was also not possible to obtain a purified polypeptide to apply to the gels an absolute quantification could not be achieved. Results of the immunoblots were quantitated in comparison to the standard sample applied to each gel. Also, the GLUT1/GLUT4 ratio is no absolute ratio of these transporters. It rather shows the difference of the examined region in GLUT1 or GLUT4 content in comparison to the mentioned standard sample obtained from LV regions.

4.1.4 Housekeeping Gene Cyclophilin

The appropriate choice of an internal standard is critical for quantitative RNA analyses. Normally, housekeeping genes are used to cancel the effects of slightly different treatment of all the samples, for example different efficiency of the highly unstable enzyme AMV Reverse Transcriptase. By normalising the result of the examined RNA in a sample to the result of the housekeeping gene in the same sample these effects would disappear. For this, the ideal housekeeping gene should have constant expression levels under different experimental conditions. Thus, there should be no difference in its expression in ischaemic and non-ischaemic hearts or regions. However, this is a theoretical characteristic that hardly can be reached in practice.

In this study a housekeeping gene, cyclophilin, was used, as it was already established for ischaemia (Brosius, III et al., 1997b). The cyclophilins form a family of cyclosporin A binding proteins (17 kDa) with peptidyl prolyl cis trans isomerase activity. This activity is blocked by the immunosuppressive drug cyclosporin A (Harding and Handschumacher, 1988). Cyclophilins are ubiquitous proteins located in both the cytosol and mitochondria. In mammalian tissues four distinct isoforms are found in different intracellular compartments e.g. cytosol (cyclophilin A), endoplasmic reticulum (cyclophilin B and C) and mitochondria

(cyclophilin D) (Doyle et al., 1999). The physiological functions are not well understood, but cyclosporin binding seems to prevent T-cell activation. These events are believed to be responsible for the immunosuppressive action of cyclosporin A (Doyle et al., 1999). Cyclophilin B is located in vesicles and can be secreted into the extracellular fluid where it binds to T-lymphocytes. This indicates a proinflammatory and chemokine-like activity which may also play a role in inflamed regions during ischaemia. Cyclophilins are also suggested to function as cytokines in the pathophysiology of sepsis (Tegeder et al., 1997).

For this study cyclophilin was chosen based upon the observation by Brosius et al. that its expression is not changed by ischaemia in human hearts. It was shown that cyclophilin levels were not specifically altered by ischaemia or other clinical changes in the myocardial samples by using parallel PCR reactions with 2 other control cDNAs (ß-actin and GAPDH). cDNAs from hibernating and normal segments were taken from two patients. Relative amounts of the 3 control cDNAs remained the same, validating the use of cyclophilin as control cDNA for normalisation (Brosius, III et al., 1997b).

However, in this study cyclophilin was not uniformly expressed in the different regions of even a normal pig heart. In the ischaemic hearts it showed significantly different regional expression in different hearts. This could possibly be due to different severities of the ischaemia in the hearts (see 4.1.1). Moreover, expression was significantly higher in ischaemic regions than in remote regions. These results seem to go along with the studies revealing increased cyclophilin mRNA content after hypoxia (Andreeva et al., 1997). Probably not only the hypoxic component of ischaemia leads to the up-regulation of the expression. A second responsible mechanism may be the proinflammatory effect of cyclophilin (Sherry et al., 1992). As mentioned in 4.1.2 inflammed areas were found in the ischaemic regions of this work, which could also cause the up-regulation of cyclophilin expression.

Zhong et al. examined different common housekeeping genes (glyceraldehyde phosphate dehydrogenase (GAPDH), ß-actin, 28S rRNA and cyclophilin) in cell cultures under hypoxic conditions. In contrast to the work of Brosius et al., levels of GAPDH, beta-actin and cyclophilin varied widely with hypoxia. Cyclophilin displayed hypoxia-induced changes in expression from –22,8 to + 7,5% in different cell lines. ß-actin and GAPDH showed the same or even higher changes. Only 28S rRNA remained stable among cell lines under hypoxia (Zhong and Simons, 1999). These results are reasonable as it also has been shown that mitochondrial cyclophilin may play a role in ischaemia. Its inhibition by cyclosporin A retards progression of mitochondrial dysfunction induced in vitro (not in vivo) by calcium overload

and other factors potentially relevant to ischaemic cell injury (Nazareth et al., 1991). It was also shown that cyclophilins are heat and stress inducible proteins in eukaryotic myogenic cells (shown in embryonic rat heart derived myocytes). Their level is significantly increased after heat stress and hypoxia (Andreeva et al., 1997).

However, another study examined glucose transporter expression in rat hearts exposed to hypobaric hypoxia which used GAPDH as a housekeeping gene as well as normalisation to total RNA (Sivitz et al., 1992). GAPDH was displayed as extremely unsuitable in hypoxia studies (Zhong and Simons, 1999) (see above) but in the study done by Sivitz the results do not vary widely in comparison to the results just normalised to total RNA. In summary, these studies demonstrate the yet unsatisfied search for an independent housekeeping gene.

Therefore, a further possibility of normalisation without using a housekeeping gene is relating the mRNA results to µg of total RNA. This method does not exclude the effect of different efficiencies of the Reverse Transcriptase but results of each sample are related to the same amount of total RNA, in this case 1 µg. Thus, the results are comparable. In our study both methods were used.

4.2 GLUT1

GLUT1 and GLUT4 are the most important glucose transporters in cardiomyocytes. Therefore, other studies also examined the effect of different states and degrees of ischaemia on the expression of GLUT1. Most of them reported an increased level of protein and mRNA in rats (Rosenblatt-Velin et al., 2001), (Remondino et al., 2000), (Sivitz et al., 1992), (Tardy-Cantalupi et al., 1999), dogs (Brosius, III et al., 1997a), human patients (Brosius, III et al., 1997b) and pigs (Feldhaus and Liedtke, 1998).

The results of the relative protein content in the normal heart revealed more GLUT1 in examined regions of the left ventricle than of the right or atria. This distribution was similar in the ischaemic hearts, but unexpectedly, the ischaemic regions showed a decreased GLUT1 protein content. Moreover, compared to the “normals” the overall GLUT1 content seems to be decreased in the ischaemic hearts. With respect to literature it was surprising that in the ischaemically injured LAD regions (mismatch) the ratio of ischaemic to non-ischaemic content was far below 1 (0,14) on account of a highly decreased GLUT1 protein content in these regions in comparison to remote regions and the corresponding regions of normal hearts.

Looking at the mRNA results of the normal heart normalised to µg of total RNA showed a significantly higher mRNA content in endocardial regions compared to all other regions. A further discrepancy between total mRNA and protein was due to the inhomogeneity of the hearts. The regional mRNA distribution showed a significant difference between the examined hearts, which was not the case with proteins. This could be due to an acute and fast reaction to individual factors. Such factors could be feeding, insulin level, stress or other unknown factors. As slaughterhouse pigs have almost identical feeding (and therefore probably also similar insulin levels) and comparable stress there may be further factors responsible. However, this short-term reaction may play no further role in protein translation due to posttranscriptional regulation. Additionally, diurnal variations(Young et al., 2001) could be excluded because in slaughterhouse the pigs are sacrificed each day on the same time. In ischaemic hearts the expression in the injured regions tended to be even higher than in the remote, in contrast to protein results.

Normalisation to cyclophilin changed the results. Then the difference between endo- and epicardial was not significant anymore. The atria revealed a lower expression than both ventricles. In ischaemic hearts the remote regions showed a higher ratio than the ischaemic ones. In this case the increased cyclophilin expression in the ischaemic regions changes the results. The higher expression decreases the ratio in ischaemic regions. Therefore, normalisation to cyclophilin is not used anymore since cyclophilin does not fulfil the criteria for a housekeeping gene. Considering this, the ratio of ischaemic to non-ischaemic GLUT1 mRNA content was far above 1 in LAD regions (3,51) indicating a highly increased GLUT1 mRNA expression in ischaemic regions in comparison to remote regions and corresponding regions of normal hearts. Interestingly, these results are contrary to the protein results. The reason for this discrepancy may be due to elevated degradation of the GLUT1 polypeptides while the mRNA expression remains increased probably pointing to a compensatory mechanism. Obviously, posttranscriptional regulation occurs after infarction, which is part of structural processes.

However, it seems unlikely that the increase in GLUT1 mRNA is due to cell loss and increased extracellular matrix like in fibrosis. This would not increase GLUT1 mRNA levels. Also, inflammation is probably not responsible for this effect. If results were highly influenced by GLUT1 expression in inflammatory cells the GLUT1 protein content would be increased too, as shown in cultures with human monocytes differentiating into macrophages. Due to differentiation a progressively increased GLUT1 protein content was demonstrated in Western blot analysis (Malide et al., 1998). Another study demonstrated that activation of human peripheral blood lymphocytes leads to increased GLUT1 protein content (Chakrabarti

et al., 1994). This goes along with the finding that the inflammatory mediator interleukin-1 augments GLUT1 expression (Bird et al., 1990). Apart from inflammation this interleukin-effect could also be one of the factors mediating the increased GLUT1 expression in cardiomyocytes. It has been shown that ischaemia stimulates stress-activated protein kinase pathways in the kidney (Kyriakis et al., 1994), (Pombo et al., 1994). The activation of these pathways has been shown to increase GLUT1 expression in L6 muscle cells (Taha C. and Klip, 1996). And interleukin-1 and tumour necrosis factor are further factors stimulating these pathways (Cornelius et al., 1990), (Bird et al., 1990), (see above). In this regard, it has been shown that tumour necrosis factor levels are elevated in myocardial ischaemia and infarction (Basaran et al., 1993). Thus, such factors may be responsible for the increased GLUT1 mRNA expression in ischaemia.

The mentioned obvious difference in protein and mRNA content is not an uncommon characteristic of the glucose transporter gene product (Estrada et al., 1994), (Bourey et al., 1990), (Okuno et al., 1993). The underlying mechansisms may be regulation of the translation step or changes in the stability of the protein (Estrada et al., 1994).

In rats with large myocardial infarction after LAD ligation, progression from compensated remodelling to overt heart failure is associated with up-regulation of GLUT1 in both the peri-infarction region and the septum (Rosenblatt-Velin et al., 2001). The same study showed an increase of GLUT1 mRNA in the peri-infarcted region and in the septum 24 hours after LAD ligation. 8 weeks after infarction mRNA expression returned to baseline values. At 20 weeks after infarct-induction, myocardial GLUT1 mRNA content was increased again in both regions. The results of our 7-day pig study confirm their results after 1 day. It was also reported that at all time points investigated there was no significant change of expression in the free right-ventricular wall (Rosenblatt-Velin et al., 2001). This is in contrast to our study, where the mRNA content of RV was increased in ischaemic hearts and probably resulted from an increased glucose demand in a volume overloaded RV. The protein levels in the same study were increased 24 hours after surgery in the peri-infarcted region compared to sham operated hearts but did not differ significantly between infarcted and sham-operated hearts 8 weeks after surgery. In contrast, our protein content was decreased after 7 days. However, their time course was different to ours and we did not measure 20 weeks after infarction where they demonstratred a more than doubled GLUT1 protein in both the peri-infarction region and in the septum in hearts with heart failure. In hearts without heart failure no change in protein was found. Similar results have been demonstrated in a further study, where one day after LAD ligation in rats GLUT1 mRNA increased markedly. After 1 week it returned to baseline, and did not change appreciably thereafter. Protein level was increased

one day after infarction and had returned to normal after 2 days (Remondino et al., 2000). Tardy-Cantalupi showed that even after 20 min ligation of the LAD followed by one to seven days with reperfusion the GLUT1 mRNA was increased (almost doubled after 1 day). Their increase almost disappeared after 7 days. Therefore, even a short period of ischaemia may alter the expression of GLUT1 (Tardy-Cantalupi et al., 1999). Surprisingly and in contrast to our 7-day pig study remote regions and sham-operated hearts in their study had a similar GLUT1 mRNA signal. The protein content was slightly increased after one day reperfusion and significantly after 3 three days (Tardy-Cantalupi et al., 1999). There is also a study showing almost the same results as ours. They examined rat hearts under conditions of hypobaric hypoxia and revealed that after two days GLUT1 mRNA levels were increased (2 – 3-fold) in RV and LV. After 14 day levels were increased 1,5 to 2-fold. The increased RV mRNA content is complementary to the elevation in the LV as the hypobaric hypoxia affects the whole heart. Protein levels did not change in LV and RV after 2 days (as in our study) but increased in RV 3-fold and in LV 1,5-fold after 14 days (Sivitz et al., 1992). Thus, we did perhaps not wait long enough after intervention to demonstrate an elevation of GLUT1 protein.

Two studies done by Brosius with humans and dogs also showed an increased GLUT1 mRNA in ischaemic regions. Their dog-study demonstrated no regional differences in LV GLUT1 expression in normal hearts, which is contrary to our study. Average GLUT1 mRNA in ischaemic hearts was 3,4-fold higher after six hours of LAD occlusion when compared to sham-operated hearts. The highest levels tended to be in the remote regions. As in our study, there were no consistent differences in GLUT1 expression of subendocardial and subepicardial regions of the ischaemic heart. In their study protein levels were increased in parallel. Average GLUT1 polypeptide expression in ischaemic hearts was elevated 1,7-fold compared to surgical controls and normal hearts. There was no significant regional variation (Brosius, III et al., 1997a). Also a human study revealed that GLUT1 mRNA was increased 2,0-fold in regions of hibernating myocardium in humans with coronary artery disease as well as in persistently hypoxic rat neonatal cardiomyocytes in primary culture (Brosius, III et al., 1997b). For non-ischaemic hearts a recent study performed on a heterogenous group of humans showed a lower GLUT1 mRNA content in the atria compared to the ventricles, confirming our results although they found no transmural differences (Sharma et al., 2003).

A highly comparable pig study to ours was done by Feldhaus. There, mRNA expression in a pig with 60% reduction of MBF for 40 min revealed a ratio $LAD_{ischaemic\ heart}/LAD_{normal\ heart}$ = 1,38 and $LAD_{ischaemic\ heart}$/LCX (remote) $_{ischaemic\ heart}$ = 1,10, respectively. In our study the increase of mRNA in the ischaemic region was much higher: $LAD_{ischaemic\ heart}/LAD_{normal\ heart}$ = 3,51 and

$LAD_{ischaemic\ heart}$/LCX(remote) $_{ischaemic\ heart}$ = 1,55. However, in our study ischaemia was longer and more severe. In addition they investigated 60% ischaemia for 40 min followed by 40 min reperfusion revealing a ratio $LAD_{ischaemic\ heart}/LAD_{normal\ heart}$ of 2,20 and $LAD_{ischaemic\ heart}$/LCX(remote) $_{ischaemic\ heart}$ of 1,34, respectively (Feldhaus and Liedtke, 1998). The Feldhaus study also included a condition of chronic hibernation, induced by 4 days of reduction of LAD flow by 50%. This yielded GLUT1 mRNA ratios of $LAD_{ischaemic\ heart}/LAD_{normal\ heart}$ = 0,76 and $LAD_{ischaemic\ heart}$/LCX(remote) $_{ischaemic\ heart}$ = 0,85, respectively. This indicates a decreased GLUT1 mRNA expression in hibernating regions. However, their group size comprised of one pig for each group and it seems questionable whether and how they proved the existence of hibernating regions at all. Without mentioning the criteria of hibernation in the animal investigated here they defined this group as “hibernation” on account of a former publication (Liedtke et al., 1995). However, Depre also showed a decrease in GLUT1 mRNA in patients with severe heart failure by 73% (ischaemic or non-ischaemic cardiomyopathy) (Depre et al., 1998b).

In summary, there are numerous studies with other species describing an increased GLUT1 mRNA expression in ischaemic regions. Interestingly, none of them found a decreased GLUT1 protein content. However, none of them had similar ischaemic conditions. In our study PET revealed an elevated FDG uptake in the ischaemically injured regions that cannot be due to an increased total amount of GLUT1 protein. Therefore, if GLUT1 partly plays a role in the increased FDG uptake then a possible explanation is translocation. This has been shown by Young in a canine heart during regional ischaemia (Young et al., 1997), (Young et al., 1999) and Egert in ischaemic rat hearts (Egert et al., 1999b). It was demonstrated that there is a predominant sarcolemmal GLUT1 localisation that is mildly increased in the ischaemic heart.

4.3 GLUT4

Apart from GLUT1, GLUT4 is the most important GLUT in myocardium. The studies that dealt with GLUT4 expression in ischaemic hearts so far mainly showed a decreased expression under ischaemic conditions lasting for several days in rats (Remondino et al., 2000), (Rosenblatt-Velin et al., 2001), (Sivitz et al., 1992), pigs (Feldhaus and Liedtke, 1998) and failing human hearts (Razeghi et al., 2001).

The protein distribution of the normal pigs in our study revealed that the GLUT4 content in the RV was higher than in the left. In the ischaemic hearts the protein content was significantly decreased in all ischaemic regions.

In contrast to protein results GLUT4 mRNA levels in the normal hearts of our study revealed a higher expression in the LV in relation to RV and atria. In principle this did not change in the case of ischaemic. But the difference between remote LV and RV was just a tendency and not statistically significant. As discussed with GLUT1 (see 4.2) the mRNA distribution showed significant differences between the examined heart in contrast to protein results. The ischaemic regions, however, showed a decreased expression compared to remote regions and to normal hearts. Normalisation to cyclophilin did not change results much. But as mentioned in 4.2 normalisation to cyclophilin is not reliable.

To compare these results to other studies working with ischaemic pig hearts is difficult as they are rare and did not produce comparable severities of ischaemia. McFalls produced repetitive myocardial ischaemia in pigs, which was achieved by occluding the proximal LCX for 10 min twice per day for 4 days. This produced no difference in total GLUT4 protein content (McFalls et al., 2002), mRNA content was not measured. However, it seems to be critical to compare 10 min of ischaemia with the 7 day ischaemia of our model. In a recent publication McFalls examined the GLUT4 protein content in hibernating swine myocardium and found it increased(McFalls et al., 2003). The aforementioned study done by Feldhaus with one pig per group examined GLUT4 mRNA expression and demonstrated no change after 40 min with reduction of MBF by 60%. If these 40 min of ischaemia were followed by 40 min of reperfusion the GLUT4 mRNA expression increased. The one pig with chronic hibernation produced by four days reduction of MBF by 50% yielded a slightly decreased mRNA content in the ischaemic region. This pig possibly matches the conditions of our study (four days compared to seven days of hibernation), although reliability is quite low due to the small group (one pig) (Feldhaus and Liedtke, 1998). However, this study shows corresponding results to ours.

All other studies working with hearts in related pathological conditions are performed in rodents. Rosenblatt-Velin examined the effect of LAD ligation after 24 hours, 8 weeks and 20 weeks in rats. 24 hours after ligation protein and mRNA levels of GLUT4 were decreased in the affected areas compared to sham-operated animals. Both returned to baseline values after 8 weeks. This matches our study's results. Both mRNA and protein levels were clearly decreased, which corresponds more closely to their 24-hour-result. As they do not have a 7-day-value one can only make the assumption that the trend to decreased expression after one day becomes more defined after 7 days due to an ongoing degradation with decreased synthesis of new GLUT4 protein, which returns to normal values after 8 weeks due to compensatory mechanisms. The Rosenblatt-Velin study also had 20-weeks-values which revealed mRNA reductions in the peri-infarcted region and also in the right ventricular free

wall in rats with heart failure whereas no significant change was observed in rats without heart failure. GLUT4 protein content decreased in the peri-infarction area after 20 weeks but did not change in the septum of rats with heart failure. In hearts without heart failure there was no change (Rosenblatt-Velin et al., 2001). Another rat study with LAD ligation done by Remondino showed similar results. However, after 24 hours mRNA content of GLUT4 was decreased, while it tended to only display a slight but not significant decrease after one week. Protein level of GLUT4 tended to decrease one day after infarction, a result after 7 days was not shown (Remondino et al., 2000). This demonstrates the inconsistency of results even in two studies with identical conditions performed in the same institution.

A further study done by Sivitz demonstrated a decrease of GLUT4 mRNA content in RV to 26% of that in normal hearts in rats after 2 days of hypobaric hypoxia. Also, a fasted control group was examined because it was observed that the hypoxia group lost weight during the study. In this fasted control group GLUT4 mRNA also decreased to 64% of normal RV suggesting in part nutritional rather than hypoxic changes. The GLUT4 protein level in hypoxic animals decreased to 54% while there was no change in RV for the fasted control group. After 14 days there was no significant change of protein and mRNA in RV compared to control animals. Interestingly, they noted no significant alteration in left ventricular GLUT4 mRNA or protein as a result of hypobaric hypoxia at both time points. Thus, under these conditions right and left ventricles differed markedly on GLUT4 expression (Sivitz et al., 1992). This again underlines our results that myocardium responds to conditions of cellular stress like hypoxia or ischaemia with decreased GLUT4 expression.

Even short-term ischaemia can change GLUT4 expression. After 20 min of ligation of rat LAD followed by one to seven days of reperfusion, GLUT4 mRNA decreased by almost one half after 1 day, but almost disappeared after 7 days, indicating that even a short period of ischaemia alters the expression of GLUT4 (Tardy-Cantalupi et al., 1999). In the same study the protein content decreased significantly after one and three days of reperfusion.

However, in contrast to these results one study showed increased GLUT4 expression. GLUT4 protein in a rat heart was increased with either high exogenous glucose or with ischaemia (50 minutes ischaemia with 60 minutes reperfusion). A combination of both conditions was additive. However, mRNA was only increased in ischaemia, not with high glucose levels (Ramasamy et al., 2001).

In dogs, Brosius demonstrated no regional differences in left ventricular GLUT4 expression in normal hearts. Ischaemia was achieved by a six hour long occlusion of LAD. Average

GLUT4 mRNA expression in ischaemic hearts was approximately 50% higher than in control hearts, but the difference was not significant (P = 0,09). It was approximately twofold higher than in surgical control (sham-operated) hearts. The highest levels tended to be in the remote regions (as already mentioned with GLUT1 – see 4.2). There were no consistent differences in expression in subendocardial and subepicardial regions. The average GLUT4 polypeptide expression in ischaemic hearts was almost identical to that in normal and control hearts. There was no significant regional variation (Brosius, III et al., 1997a). This is different to our results. However, species, duration and severity of the ischaemia did not match our model.

In patients suffering from heart failure Razeghi and Depre could show a decrease of GLUT4 mRNA(Razeghi et al., 2001; Razeghi et al., 2002; Depre et al., 1998b). The GLUT1/GLUT4 ratio in normal hearts was 0,3 and in failing hearts 0,15. In idiopathic dilated cardiomyopathy GLUT1/GLUT4 was 0,02 (Depre et al., 1998b). This shows that in failing human myocardium the glucose transporters are differentially regulated compared to normal non-ischaemic conditions.

4.4 GLUT1/GLUT4 Ratio

As mentioned above some studies calculate the mRNA ratio of GLUT1/GLUT4. This shows the isoform predominantly expressed and has the further advantage that results are independent of housekeeping genes.

The ratio of GLUT1 mRNA/GLUT4 mRNA yields the predominant isoform, as each of the values is the result of an absolute measurement of copy numbers in the LightCycler capillary. In the normal heart this ratio is around 0,2 to 0,4 with higher values observed endocardially than epicardially. In concordance Depre et al. showed in a study with patients a ratio of 0,3 in apical samples (Depre et al., 1998b).

When applying this ratio to protein results one has to be aware that each GLUT value is related to a left ventricular standard sample. Therefore, this ratio shows the change of GLUT1 and GLUT4 relative to each other. It does not give an indication about the isoform predominantly expressed. As the standard is obtained from left ventricular regions the results of LV are approximately 1. Right ventricle and atria show a lower ratio, which can be interpreted as an indication that there is relatively more GLUT4 protein content and/or less GLUT1 content than in the left ventricle. In the ischaemic heart the affected regions show a lower ratio (0,64 – 0,69) than the remote LV (1,14) suggesting that the GLUT4 to GLUT1 ratio in ischaemic regions is higher than the one in remote regions. A study done by

Kraegen, who studied the protein content in non-ischaemic rat cardiac and skeletal muscle tissue revealed that the ratio varies in normal hearts from 0,1 to 0,6 (Kraegen et al., 1993). This cannot be compared to our protein ratio as mentioned above but it is in the same range of results as our mRNA ratio (0,2 – 0,4).

In ischaemic regions the mRNA ratio changed dramatically. Values were far above one (5,44 and higher) indicating an immense shift from predominant GLUT4 expression in normal regions to predominant GLUT1 expression in ischaemically injured regions. This is in contrast to the protein results. However, the study by Depre mentioned above showed a decreased ratio of GLUT1/GLUT4 mRNA values in patients with heart failure (ischaemic and non-ischaemic cardiomyopathy). The most striking ratio (0,02) was seen in patients with idiopathic dilated cardiomyopathy. This demonstrates strongly repressed GLUT1 expression in these hearts. Therefore, in different diseases of the heart glucose transporters seem to be differentially regulated. Obviously, the direction of this regulation is dependent on the type of pathologic situation. Dependent on the situation, GLUT4 or GLUT1 expression is regulated up or down. However, this does not explain the contradictory protein and mRNA data in our study. As already suggested in 4.2 a possible explanation may be that degradation of the GLUT1 polypeptides is still elevated after 7 days due to remodelling mechanisms while a compensatory increase of the mRNA expression has already begun. This would explain the connection of our study to the one of Sivitz et al. who demonstrated an increase in GLUT1 protein not earlier than 14 days after intervention.

There are several other studies showing that GLUT1 mRNA becomes predominant. Some authors compare this effect with the condition in foetal hearts (Tardy-Cantalupi et al., 1999). Others conclude vice versa that a postnatal increase in GLUT4 content is associated with an improved recovery of postischaemic myocardial function(Friehs et al., 2003). It was demonstrated that GLUT1 is predominant in foetal cardiac tissue (Santalucia et al., 1992). After birth GLUT4 content increases steadily until it becomes predominant, while in parallel GLUT1 is repressed (Santalucia et al., 1992), (Studelska et al., 1992). The predominant GLUT1 in a foetus is in line with the observations in ischaemic hearts suggesting dedifferentiation of cardiomyocytes. Before birth GLUT4 mRNA is detectable even a few days earlier than the proteins. This effect could either be due to higher sensitivity in detecting the mRNA in this study or it could also be due to pre-translational regulation.

4.5 GLUT3

GLUT3 is one of the most important glucose transporters in the adult brain (Kayano et al., 1988), (Nagamatsu et al., 1992). In human beings the presence of GLUT3 protein is also

described in the heart (Shepherd et al., 1992), (Grover-McKay et al., 1999). However, data about GLUT3 mRNA in the heart have not been published yet.

In our study the GLUT3 mRNA in the non-ischaemic heart is unexpectedly high in comparison to GLUT1 or GLUT4. The average mRNA ratio of GLUT1 : GLUT4 : GLUT3 in all regions was 2,7 : 10,2 : 1. Similar results were found in human skeletal muscle(Stuart et al., 2000) but not in myocardium. The regional distribution of GLUT3 mRNA in our study reveals the highest level of GLUT3 mRNA in the endocardial regions of the left ventricle while RV and the atria show a lower expression. Also, a regional heterogeneity of GLUT3 mRNA in the LV is shown. Such regional differences were also reported by Gropler. Only he showed lower FDG-uptake in the septal and anterior walls compared to the lateral and inferior ones(Gropler et al., 1990). In ischaemic hearts the remote regions show a higher expression level than the ischaemically injured. Although the results with and without cyclophilin do not differ much the further discussion only relates to results normalised to total mRNA (see 4.2).

As there was no antibody available to reliably detect GLUT3 protein in pig hearts, no such data could be acquired. Possible reasons for the unsatisfactory detection of GLUT3 protein can be the low affinity of the commercially available antibodies to pig GLUT3 protein in addition to a low GLUT3 protein content in the porcine heart. This suggests regulation on a translational level because mRNA content was not far below the content of GLUT1 mRNA for example.

In ischaemic heart disease less is known about GLUT3 expression. This lack of studies makes it difficult to compare with literature. Although there is no literature about ischaemic hearts, there are studies in brain tissue. There, hypoxic ischaemia increases GLUT3 mRNA and protein expression (Devaskar et al., 1999), (Urabe et al., 1996) in contrast to our findings in the heart. A further study dealt with a different kind of cellular stress (uncoupling of oxidative phosphorylation and ATP synthesis) to examine the expression of GLUT3 under this condition. It showed that disruption of oxidative phosphorylation by the mitochondial uncoupler 2,4-dinitrophenol (DNP) leads to an increased rate of glucose transport in muscle cell cultures. DNP uncouples electron transport and oxidative phosphorylation specifically in the respiratory chain and therefore electron transport does not produce ATP leading to increased oxygen consumption. This condition is associated with an elevation of the protein content of GLUT3 and GLUT1, but not GLUT4. In contrast to an increased GLUT1 mRNA level, GLUT3 mRNA levels are unaffected. The elevated GLUT3 protein content was due to an increased half-life of the protein in the cell culture (Khayat et al., 1998) demonstrating a further regulation method apart from the altering of expression levels.

However, it is not clear if the increased FDG uptake measured in our study was due to increased FDG uptake into cardiomyocytes or other cells, e.g. inflammatory cells. It could be argued that the measured results are mainly due to inflammation as GLUT3 protein is decreased in this condition (Malide et al., 1998), (Chakrabarti et al., 1994) as already mentioned in 4.2. However, there is also a study published by Mochizuki demonstrating high GLUT3 content in inflamed tissue (Mochizuki et al., 2001).

A last but important point is that in mice and rats, GLUT3 is mainly reported to be predominantly limited to nervous tissue and placenta (Gould et al., 1992), (Nagamatsu et al., 1992), (Krishnan and Haddad, 1995), (Zhou and Bondy, 1993). However, our study could also detects GLUT3 protein in rat myocardium as also described by Gavete(Gavete et al., 2002).

4.6 Hexokinase Type II

Hexokinase is the enzyme catalysing the next step after glucose has entered the cell via a glucose transporter. In this reaction glucose is phosphorylated to glucose-6-phosphate, which is the form that can be either metabolised in glycolysis or stored as glycogen. Under conditions of increased glucose uptake as in acute myocardial ischaemia or in the presence of insulin the hexokinase reaction becomes rate-limiting (Depre et al., 1998a). This suggests that this enzyme then becomes the aim of upregulatory mechanisms. And indeed it could be shown that in ischaemic regions its expression is increased in pig (McFalls et al., 2002) and rat hearts (Daneshrad et al., 2000).

An important point in our study is that the protein expression seemed to be strongly dependent on individual factors as the four hearts examined in the study revealed statistically different HKII protein expression in all the regions. This was not the case with GLUT1 or GLUT4 protein expression. Such individual factors could be feeding, insulin level, stress or other unknown factors. As slaughterhouse pigs have almost identical feeding (and therefore probably also similar insulin levels) and comparable stress there may be further factors responsible or the difference might even be congenital. At the time of the study there was no nucleotide sequence of swine hexokinase type II available, which is the predominant isoform in the heart (Tsirka et al., 2001). Therefore, our HKII results focus on the protein expression results. It was further demonstrated that there was a higher protein expression in the atria than in the left ventricle in a normal pig heart. There was no transmural gradient on HK protein content confirming a study in rats(Baruffi et al., 1983). In the ischaemic hearts the

regional distribution did not change significantly. However, there was a trend towards higher HKII protein content in the ischaemic regions, which was not significant.

So far, only very few studies investigate HKII in pig hearts. De Tata showed different hexokinase activities in LV and RV in porcine heart tissue. Also, the distribution across the left ventricular wall was non-uniform (De Tata et al., 1986). Bass published that hexokinase activity in pigs is approximately the same in atrial tissue as in ventricles, which themselves show only small differences (Bass et al., 1993). This matches in part the observations in our study, although there were no significant differences in ventricular HKII protein content.

Repetitive myocardial ischaemia in pigs, which was achieved by occluding the proximal LCX for 10 min twice per day for 4 days showed an increased hexokinase activity as well as glycogen level in comparison to remote regions. This increase is correlated with an increased FDG-uptake (McFalls et al., 2002). However, this study estimated the hexokinase activity by determining the rate of NADP production over a certain period of time. This method yields the activity of all present types of hexokinase in the tissue and not only type II that was examined in our study. The observed increase therefore could also be due to an elevated content of another isoform in ischaemia. Furthermore, ischaemia in their study was shorter and repetitive. Daneshrad showed that three weeks of normobaric hypoxia induces a rise in hexokinase activity in the rat heart (Daneshrad et al., 2000). A study in hypertrophied ferret right ventricles revealed that the activity of hexokinase was significantly increased by 26% (Do et al., 1997). But tachycardia-induced heart failure in dogs showed an unchanged activity of hexokinase (Dzeja et al., 1999).

A study published by Feldhaus showed data of hexokinase type I mRNA in different kinds of ischaemic porcine hearts. 40 min of 60% reduction of MBF lead to an increased expression in ischaemic regions compared to control hearts, whereas the comparison to remote regions yielded no difference. 40 min of reperfusion after ischaemia did not change the results much. Similar results were found in four days of chronic hibernation. However, these results are very limited due to a group size of only one pig (see 4.2).

In summary, other studies working with different sorts of hypoxia mainly showed an elevated hexokinase activity, which matches our observation of a trend of increased HKII content in the ischaemic regions, although changes of activity do not necessarily reflect changes in expression.

4.7 Conclusion

The aim of this study was to elucidate the regional differences in expression of GLUT1, 3 and 4 as well as HKII in normal porcine hearts in comparison to ischaemic hearts. Ischaemia was produced by introducing a modified stent graft in the proximal LAD of domestic pigs. After seven days PET was performed in ischaemic pigs to visualise changes in MBF and glucose metabolism. After taking samples from different defined regions, including hibernating areas, PCR and immunoblotting were performed. In normal hearts immunoblotting revealed regional differences in the examined protein content. The expression rate of GLUT1 protein was higher in the left than in right ventricle and the results for GLUT4 were the opposite. In ischaemic hearts a decreased amount of GLUT1 and GLUT4 protein in ischaemic regions could be observed while hexokinase tended to be slightly increased. In contrast to this, the mRNA expression level of GLUT1 was slightly increased in the ischaemic regions while GLUT3 and GLUT4 mRNA expression was significantly decreased. The RT-PCR of non-ischaemic hearts showed a higher GLUT4 expression level in the left than in the right ventricle while GLUT1 and GLUT3 was only expressed at a higher rate subendocardially compared to the atria.

These results in the ischaemic hearts raise the question which glucose transporters are responsible for the increased FDG uptake in the ischaemic regions while the protein content of three main transporters in parallel is decreased. However, in this study only the total transporter content was quantified. There was no discrimination between intracellular and plasmamembrane fractions elucidating translocation. It is well known that translocation of GLUT4 occurs under such conditions (Wheeler, 1988), (Sun et al., 1994), (Cartee et al., 1991) as well as GLUT1 translocation to the sarcolemma in the intact canine and rat heart during regional ischaemia (Young et al., 1997), (Young et al., 1999), (Egert et al., 1999b). Translocation is responsible for an increased glucose extraction from the blood and also for increased glucose uptake even if the blood flow is reduced (King and Opie, 1998b). The protein content in ischaemic regions compared to control hearts was diminished to 13% (GLUT1) or 21% (GLUT4), respectively and translocation may increase the sarcolemmal GLUT4 content by 60% (Russell, III et al., 1998) up to 80% (Egert et al., 1999b). However, this may in part compensate the lower total content and lead to the observed increased FDG uptake. Even if GLUT1 translocation, which increases GLUT1 in the cardiomyocyte surface by approximately 20% (Russell, III et al., 1998), is considered, it would not be enough to explain the elevation in FDG uptake. Further mechanisms such as increased transport activity of the different transporter isoforms probably play an important role, too (Shetty et al.,

1993). Changes in protein activity in myocardial infarction may be due to an altered expression of regulatory proteins (Remondino et al., 2000).

To ensure that fibrosis and inflammation do not interfere with these results further experiments will have to be done, e.g. immunohistochemistry and determination of relative content of cardiomyocytes in the samples. Furthermore, each of the examined groups consisted of only four animals causing variation in some of the results although the observed direction of the changes stayed the same in all four animals. To decrease the standard error, examination of further animals could be advantageous.

5 LITERATURE

1. Andreeva,L., Motterlini,R., Green,C.J. Cyclophilins are induced by hypoxia and heat stress in myogenic cells. Biochem.Biophys.Res.Commun. 237 (1997) 6-9

2. Arora,K.K., Fanciulli,M., Pedersen,P.L. Glucose phosphorylation in tumor cells. Cloning, sequencing, and overexpression in active form of a full-length cDNA encoding a mitochondrial bindable form of hexokinase. J.Biol.Chem. 265 (1990) 6481-6488

3. Baldwin,S.A. Mammalian passive glucose transporters: members of an ubiquitous family of active and passive transport proteins. Biochim.Biophys.Acta 1154 (1993) 17-49

4. Baldwin,S.A., Barros,L.F., Griffiths,M., Ingram,J., Robbins,E.C., Streets,A.J., Saklatvala,J. Regulation of GLUT1 in response to cellular stress. Biochem.Soc.Trans. 25 (1997) 954-958

5. Baruffi,F., De,T., V, Gori,Z. [Transmural distribution of hexokinase, glucose-6-phosphate dehydrogenase and glutamate-oxalacetate transaminase in the left ventricle of the rat]. Boll.Soc.Ital.Biol.Sper. 59 (1983) 1412-1415

6. Basaran,Y., Basaran,M.M., Babacan,K.F., Ener,B., Okay,T., Gok,H., Ozdemir,M. Serum tumor necrosis factor levels in acute myocardial infarction and unstable angina pectoris. Angiology 44 (1993) 332-337

7. Bass,A., Stejskalova,M., Ostadal,B., Samanek,M. Differences between atrial and ventricular energy-supplying enzymes in five mammalian species. Physiol Res. 42 (1993) 1-6

8. Bell,G.I., Kayano,T., Buse,J.B., Burant,C.F., Takeda,J., Lin,D., Fukumoto,H., Seino,S. Molecular biology of mammalian glucose transporters. Diabetes Care 13 (1990) 198-208

9. Bergmann,S.R. Positron Emission Tomography of the Heart. In: "Cardiac Nuclear Medicine", Gerson M.C. (Ed.), The McGran-Hill Companies, USA, 1997, 267-299

10. Bergmann,S.R., Hack,S., Tewson,T., Welch,M.J., Sobel,B.E. The dependence of accumulation of 13NH3 by myocardium on metabolic factors and its implications for quantitative assessment of perfusion. Circulation 61 (1980) 34-43

11. Bird,T.A., Davies,A., Baldwin,S.A., Saklatvala,J. Interleukin 1 stimulates hexose transport in fibroblasts by increasing the expression of glucose transporters. J.Biol.Chem. 265 (1990) 13578-13583

12. Birnbaum,M.J. Identification of a novel gene encoding an insulin-responsive glucose transporter protein. Cell 57 (1989) 305-315

13. Bourey,R.E., Koranyi,L., James,D.E., Mueckler,M., Permutt,M.A. Effects of altered glucose homeostasis on glucose transporter expression in skeletal muscle of the rat. J.Clin.Invest 86 (1990) 542-547

14. Brant,A.M., Gibbs,E.M., Gould,G.W. Examination of the glycosidation state of five members of the human facilitative glucose transporter family. Biochem.Soc.Trans. 20 (1992a) 235S

15. Brant,A.M., Gibbs,E.M., Gould,G.W., Thomas,H.M. Immunological identification of five members of the human facilitative glucose transporter family. Biochem.Soc.Trans. 20 (1992b) 236S

16. Brosius,F.C., III, Liu,Y., Nguyen,N., Sun,D., Bartlett,J., Schwaiger,M. Persistent myocardial ischemia increases GLUT1 glucose transporter expression in both ischemic and non-ischemic heart regions. J.Mol.Cell Cardiol. 29 (1997a) 1675-1685

17. Brosius,F.C., III, Nguyen,N., Egert,S., Lin,Z., Deeb,G.M., Haas,F., Schwaiger,M., Sun,D. Increased sarcolemmal glucose transporter abundance in myocardial ischemia. Am.J.Cardiol. 80 (1997b) 77A-84A

18. Camici,P., Ferrannini,E., Opie,L.H. Myocardial metabolism in ischemic heart disease: basic principles and application to imaging by positron emission tomography. Prog.Cardiovasc.Dis. 32 (1989) 217-238

19. Cartee,G.D., Douen,A.G., Ramlal,T., Klip,A., Holloszy,J.O. Stimulation of glucose transport in skeletal muscle by hypoxia. J.Appl.Physiol 70 (1991) 1593-1600

20. Chakrabarti,R., Jung,C.Y., Lee,T.P., Liu,H., Mookerjee,B.K. Changes in glucose transport and transporter isoforms during the activation of human peripheral blood lymphocytes by phytohemagglutinin. J.Immunol. 152 (1994) 2660-2668

21. Charron,M.J., Brosius,F.C., III, Alper,S.L., Lodish,H.F. A glucose transport protein expressed predominately in insulin- responsive tissues. Proc.Natl.Acad.Sci.U.S.A 86 (1989) 2535-2539

22. Charron,M.J., Katz,E.B., Olson,A.L. GLUT4 gene regulation and manipulation. J.Biol.Chem. 274 (1999) 3253-3256

23. Chomczynski,P., Sacchi,N. Single-step method of RNA isolation by acid guanidinium thiocyanate-phenol-chloroform extraction. Anal.Biochem. 162 (1987) 156-159

24. Cornelius,P., Marlowe,M., Lee,M.D., Pekala,P.H. The growth factor-like effects of tumor necrosis factor-alpha. Stimulation of glucose transport activity and induction of glucose

transporter and immediate early gene expression in 3T3-L1 preadipocytes. J.Biol.Chem. 265 (1990) 20506-20516

25. Czech,M.P., Corvera,S. Signaling mechanisms that regulate glucose transport. J.Biol.Chem. 274 (1999) 1865-1868

26. Dadd Andrew. Working efficiently with GeneQuant (R) II DNA/RNA Calculator. Science Tools from Pharmacia Biotech 1(3). 1996. Cambridge, England, Pharmacia Biotech (Biochrom) Ltd. (GENERIC)
Ref Type: Magazine Article

27. Daneshrad,Z., Garcia-Riera,M.P., Verdys,M., Rossi,A. Differential responses to chronic hypoxia and dietary restriction of aerobic capacity and enzyme levels in the rat myocardium. Mol.Cell Biochem. 210 (2000) 159-166

28. De Tata,V., Fierabracci,V., Gori,Z., Bergamini,E. Transmural distribution of glucose metabolizing enzymes across the left and the right ventricle heart walls in three different mammalian species. Comp Biochem.Physiol B 84 (1986) 549-553

29. Deeb,S.S., Malkki,M., Laakso,M. Human hexokinase II: sequence and homology to other hexokinases. Biochem.Biophys.Res.Commun. 197 (1993) 68-74

30. Depre,C., Rider,M.H., Hue,L. Mechanisms of control of heart glycolysis. Eur.J.Biochem. 258 (1998a) 277-290

31. Depre,C., Shipley,G.L., Davies,P.J., Frazier,O.H. and Taegtmeyer,H.: Glucose Transporter Isoform Expression in the Failing Human Heart. Circulation I627 (Abstract) (1998b) (Abstract)

32. Devaskar,S.U., Rajakumar,P.A., Mink,R.B., McKnight,R.A., Thamotharan,S., Hicks,S.J. Effect of development and hypoxic-ischemia upon rabbit brain glucose transporter expression. Brain Res. 823 (1999) 113-128

33. Do,E., Baudet,S., Verdys,M., Touzeau,C., Bailly,F., Lucas-Heron,B., Sagniez,M., Rossi,A., Noireaud,J. Energy metabolism in normal and hypertrophied right ventricle of the ferret heart. J.Mol.Cell Cardiol. 29 (1997) 1903-1913

34. Doyle,V., Virji,S., Crompton,M. Evidence that cyclophilin-A protects cells against oxidative stress. Biochem.J. 341 (Pt 1) (1999) 127-132

35. Dzeja,P.P., Pucar,D., Redfield,M.M., Burnett,J.C., Terzic,A. Reduced activity of enzymes coupling ATP-generating with ATP-consuming processes in the failing myocardium. Mol.Cell Biochem. 201 (1999) 33-40

36. Egert,S., Nguyen,N., Brosius,F.C., III, Schwaiger,M. Effects of wortmannin on insulin- and ischemia-induced stimulation of GLUT4 translocation and FDG uptake in perfused rat hearts. Cardiovasc.Res. 35 (1997) 283-293

37. Egert,S., Nguyen,N., Schwaiger,M. Contribution of alpha-adrenergic and beta-adrenergic stimulation to ischemia-induced glucose transporter (GLUT) 4 and GLUT1 translocation in the isolated perfused rat heart. Circ.Res. 84 (1999a) 1407-1415

38. Egert,S., Nguyen,N., Schwaiger,M. Myocardial glucose transporter GLUT1: translocation induced by insulin and ischemia. J.Mol.Cell Cardiol. 31 (1999b) 1337-1344

39. Elsasser,A., Schlepper,M., Klovekorn,W.P., Cai,W.J., Zimmermann,R., Muller,K.D., Strasser,R., Kostin,S., Gagel,C., Munkel,B., Schaper,W., Schaper,J. Hibernating myocardium: an incomplete adaptation to ischemia. Circulation 96 (1997) 2920-2931

40. Estrada,D.E., Elliott,E., Zinman,B., Poon,I., Liu,Z., Klip,A., Daneman,D. Regulation of glucose transport and expression of GLUT3 transporters in human circulating mononuclear cells: studies in cells from insulin- dependent diabetic and nondiabetic individuals. Metabolism 43 (1994) 591-598

41. Feldhaus,L.M., Liedtke,A.J. mRNA expression of glycolytic enzymes and glucose transporter proteins in ischemic myocardium with and without reperfusion. J.Mol.Cell Cardiol. 30 (1998) 2475-2485

42. Fischer,Y., Rose,H., Kammermeier,H. Highly insulin-responsive isolated rat heart muscle cells yielded by a modified isolation method. Life Sci. 49 (1991) 1679-1688

43. Fischer,Y., Thomas,J., Sevilla,L., Munoz,P., Becker,C., Holman,G., Kozka,I.J., Palacin,M., Testar,X., Kammermeier,H., Zorzano,A. Insulin-induced recruitment of glucose transporter 4 (GLUT4) and GLUT1 in isolated rat cardiac myocytes. Evidence of the existence of different intracellular GLUT4 vesicle populations. J.Biol.Chem. 272 (1997) 7085-7092

44. Fox,K.A., Abendschein,D.R., Ambos,H.D., Sobel,B.E., Bergmann,S.R. Efflux of metabolized and nonmetabolized fatty acid from canine myocardium. Implications for quantifying myocardial metabolism tomographically. Circ.Res. 57 (1985) 232-243

45. Friehs,I., Cao-Danh,H., Stamm,C., Cowan,D.B., McGowan,F.X., del Nido,P.J. Postnatal increase in insulin-sensitive glucose transporter expression is associated with improved recovery of postischemic myocardial function. J.Thorac.Cardiovasc.Surg. 126 (2003) 263-271

46. Fukumoto,H., Kayano,T., Buse,J.B., Edwards,Y., Pilch,P.F., Bell,G.I., Seino,S. Cloning and characterization of the major insulin-responsive glucose transporter expressed in human skeletal muscle and other insulin- responsive tissues. J.Biol.Chem. 264 (1989) 7776-7779

47. Gallagher Sean R., Smith John A. Electrophoretic Separation of Proteins. In: "Current Protocols in Molecular Biology", Ausubel F.M., Brent R., Kingston R.E., Moore D.D., Seidman J.G., Smith J.A., Struhl K. (Eds.), John Wiley and Sons, Current Protocols, New York, 1994, 10.2.1-10.2.9

48. Gallagher,B.M., Fowler,J.S., Gutterson,N.I., MacGregor,R.R., Wan,C.N., Wolf,A.P. Metabolic trapping as a principle of oradiopharmaceutical design: some factors resposible for the biodistribution of [18F] 2-deoxy-2-fluoro-D- glucose. J.Nucl.Med. 19 (1978) 1154-1161

49. Gavete,M.L., Agote,M., Martin,M.A., Alvarez,C., Escriva,F. Effects of chronic undernutrition on glucose uptake and glucose transporter proteins in rat heart. Endocrinology 143 (2002) 4295-4303

50. Gerrits,P.M., Olson,A.L., Pessin,J.E. Regulation of the GLUT4/muscle-fat glucose transporter mRNA in adipose tissue of insulin-deficient diabetic rats. J.Biol.Chem. 268 (1993) 640-644

51. Gould,G.W., Brant,A.M., Kahn,B.B., Shepherd,P.R., McCoid,S.C., Gibbs,E.M. Expression of the brain-type glucose transporter is restricted to brain and neuronal cells in mice. Diabetologia 35 (1992) 304-309

52. Gould,G.W., Thomas,H.M., Jess,T.J., Bell,G.I. Expression of human glucose transporters in Xenopus oocytes: kinetic characterization and substrate specificities of the erythrocyte, liver, and brain isoforms. Biochemistry 30 (1991) 5139-5145

53. Gropler,R.J., Siegel,B.A., Lee,K.J., Moerlein,S.M., Perry,D.J., Bergmann,S.R., Geltman,E.M. Nonuniformity in myocardial accumulation of fluorine-18- fluorodeoxyglucose in normal fasted humans. J.Nucl.Med. 31 (1990) 1749-1756

54. Grover-McKay,M., Walsh,S.A., Thompson,S.A. Glucose transporter 3 (GLUT3) protein is present in human myocardium. Biochim.Biophys.Acta 1416 (1999) 145-154

55. Haber,R.S., Weinstein,S.P., O'Boyle,E., Morgello,S. Tissue distribution of the human GLUT3 glucose transporter. Endocrinology 132 (1993) 2538-2543

56. Haendler,B., Hofer-Warbinek,R., Hofer,E. Complementary DNA for human T-cell cyclophilin. EMBO J. 6 (1987) 947-950

57. Hardie,D.G., Carling,D. The AMP-activated protein kinase--fuel gauge of the mammalian cell? Eur.J.Biochem. 246 (1997) 259-273

58. Harding,M.W., Handschumacher,R.E. Cyclophilin, a primary molecular target for cyclosporine. Structural and functional implications. Transplantation 46 (1988) 29S-35S

59. Heijnen,H.F., Oorschot,V., Sixma,J.J., Slot,J.W., James,D.E. Thrombin stimulates glucose transport in human platelets via the translocation of the glucose transporter GLUT-3 from alpha-granules to the cell surface. J.Cell Biol. 138 (1997) 323-330

60. Heusch,G. Hibernating myocardium. Physiol Rev. 78 (1998) 1055-1085

61. Hiraki,Y., McMorrow,I.M., Birnbaum,M.J. The regulation of glucose transporter gene expression by cyclic adenosine monophosphate in NIH3T3 fibroblasts. Mol.Endocrinol. 3 (1989) 1470-1476

62. Iitaka,M., Katayama,S. [Insulin resistance in pituitary, thyroid, and adrenal diseases]. Nippon Rinsho 58 (2000) 451-455

63. James,D.E., Strube,M., Mueckler,M. Molecular cloning and characterization of an insulin-regulatable glucose transporter. Nature 338 (1989) 83-87

64. Joost,H.G., Thorens,B. The extended GLUT-family of sugar/polyol transport facilitators: nomenclature, sequence characteristics, and potential function of its novel members (review). Mol.Membr.Biol. 18 (2001) 247-256

65. Kaestner,K.H., Christy,R.J., McLenithan,J.C., Braiterman,L.T., Cornelius,P., Pekala,P.H., Lane,M.D. Sequence, tissue distribution, and differential expression of mRNA for a putative insulin-responsive glucose transporter in mouse 3T3-L1 adipocytes. Proc.Natl.Acad.Sci.U.S.A 86 (1989) 3150-3154

66. Kahn,B.B., Charron,M.J., Lodish,H.F., Cushman,S.W., Flier,J.S. Differential regulation of two glucose transporters in adipose cells from diabetic and insulin-treated diabetic rats. J.Clin.Invest 84 (1989) 404-411

67. Kasahara,M., Hinkle,P.C. Reconstitution and purification of the D-glucose transporter from human erythrocytes. J.Biol.Chem. 252 (1977) 7384-7390

68. Katzen,H.M. The multiple forms of mammalian hexokinase and their significance to the action of insulin. Adv.Enzyme Regul. 5 (1967) 335-356

69. Katzen,H.M., Schimke,R.T. Multiple forms of hexokinase in the rat: tissue distribution, age dependency, and properties. Proc.Natl.Acad.Sci.U.S.A 54 (1965) 1218-1225

70. Kayano,T., Fukumoto,H., Eddy,R.L., Fan,Y.S., Byers,M.G., Shows,T.B., Bell,G.I. Evidence for a family of human glucose transporter-like proteins. Sequence and gene localization of a protein expressed in fetal skeletal muscle and other tissues. J.Biol.Chem. 263 (1988) 15245-15248

71. Khayat,Z.A., McCall,A.L., Klip,A. Unique mechanism of GLUT3 glucose transporter regulation by prolonged energy demand: increased protein half-life. Biochem.J. 333 (Pt 3) (1998) 713-718

72. King,L.M., Opie,L.H. Glucose and glycogen utilisation in myocardial ischemia--changes in metabolism and consequences for the myocyte. Mol.Cell Biochem. 180 (1998a) 3-26

73. King,L.M., Opie,L.H. Glucose delivery is a major determinant of glucose utilisation in the ischemic myocardium with a residual coronary flow. Cardiovasc.Res. 39 (1998b) 381-392

74. Klip,A., Tsakiridis,T., Marette,A., Ortiz,P.A. Regulation of expression of glucose transporters by glucose: a review of studies in vivo and in cell cultures. FASEB J. 8 (1994) 43-53

75. Kraegen,E.W., Sowden,J.A., Halstead,M.B., Clark,P.W., Rodnick,K.J., Chisholm,D.J., James,D.E. Glucose transporters and in vivo glucose uptake in skeletal and cardiac muscle: fasting, insulin stimulation and immunoisolation studies of GLUT1 and GLUT4. Biochem.J. 295 (Pt 1) (1993) 287-293

76. Krishnan,S.N., Haddad,G.G. Cloning of glucose transporter-3 (GLUT3) cDNA from rat brain. Life Sci. 56 (1995) 1193-1197

77. Kudo,N., Barr,A.J., Barr,R.L., Desai,S., Lopaschuk,G.D. High rates of fatty acid oxidation during reperfusion of ischemic hearts are associated with a decrease in malonyl-CoA levels due to an increase in 5'-AMP-activated protein kinase inhibition of acetyl-CoA carboxylase. J.Biol.Chem. 270 (1995) 17513-17520

78. Kyriakis,J.M., Banerjee,P., Nikolakaki,E., Dai,T., Rubie,E.A., Ahmad,M.F., Avruch,J., Woodgett,J.R. The stress-activated protein kinase subfamily of c-Jun kinases. Nature 369 (1994) 156-160

79. Laemmli,U.K. Cleavage of structural proteins during the assembly of the head of bacteriophage T4. Nature 227 (1970) 680-685

80. Langendorff O. Untersuchungen am überlebenden Säugethierherzen. Pflügers Arch.Ges.Physiol Menschen Tiere 61 (1895) 291-332

81. Lawrence,J.C., Jr., Hiken,J.F., James,D.E. Phosphorylation of the glucose transporter in rat adipocytes. Identification of the intracellular domain at the carboxyl terminus as a target for phosphorylation in intact-cells and in vitro. J.Biol.Chem. 265 (1990) 2324-2332

82. Laybutt,D.R., Thompson,A.L., Cooney,G.J., Kraegen,E.W. Selective chronic regulation of GLUT1 and GLUT4 content by insulin, glucose, and lipid in rat cardiac muscle in vivo. Am.J.Physiol 273 (1997) H1309-H1316

83. Levine,R. Insulin action: 1948-80. Diabetes Care 4 (1981) 38-44

84. Liedtke,A.J., Renstrom,B., Nellis,S.H., Hall,J.L., Stanley,W.C. Mechanical and metabolic functions in pig hearts after 4 days of chronic coronary stenosis. J.Am.Coll.Cardiol. 26 (1995) 815-825

85. Lienhard,G.E., Slot,J.W., James,D.E., Mueckler,M.M. How cells absorb glucose. Sci.Am. 266 (1992) 86-91

86. Loike,J.D., Cao,L., Brett,J., Ogawa,S., Silverstein,S.C., Stern,D. Hypoxia induces glucose transporter expression in endothelial cells. Am.J.Physiol 263 (1992) C326-C333

87. Maher,F., Clark,S., Harrison,L.C. Chronic stimulation of glucose transporter gene expression in L6 myocytes mediated via the insulin-like growth factor-1 receptor. Mol.Endocrinol. 3 (1989) 2128-2135

88. Malhotra,R., Brosius,F.C., III Glucose uptake and glycolysis reduce hypoxia-induced apoptosis in cultured neonatal rat cardiac myocytes. J.Biol.Chem. 274 (1999) 12567-12575

89. Malide,D., Davies-Hill,T.M., Levine,M., Simpson,I.A. Distinct localization of GLUT-1, -3, and -5 in human monocyte-derived macrophages: effects of cell activation. Am.J.Physiol 274 (1998) E516-E526

90. Marette,A., Richardson,J.M., Ramlal,T., Balon,T.W., Vranic,M., Pessin,J.E., Klip,A. Abundance, localization, and insulin-induced translocation of glucose transporters in red and white muscle. Am.J.Physiol 263 (1992) C443-C452

91. McCormack,J.G., Barr,R.L., Wolff,A.A., Lopaschuk,G.D. Ranolazine stimulates glucose oxidation in normoxic, ischemic, and reperfused ischemic rat hearts. Circulation 93 (1996) 135-142

92. McFalls,E.O., Murad,B., Haspel,H.C., Marx,D., Sikora,J., Ward,H.B. Myocardial glucose uptake after dobutamine stress in chronic hibernating swine myocardium. J.Nucl.Cardiol. 10 (2003) 385-394

93. McFalls,E.O., Murad,B., Liow,J.S., Gannon,M.C., Haspel,H.C., Lange,A., Marx,D., Sikora,J., Ward,H.B. Glucose uptake and glycogen levels are increased in pig heart after repetitive ischemia. Am.J.Physiol Heart Circ.Physiol 282 (2002) H205-H211

94. McNamee,M.G. Isolation and characterization of cell membranes. Biotechniques 7 (1989) 466-475

95. McNulty,P.H., Sinusas,A.J., Shi,C.Q., Dione,D., Young,L.H., Cline,G.C., Shulman,G.I. Glucose metabolism distal to a critical coronary stenosis in a canine model of low-flow myocardial ischemia. J.Clin.Invest 98 (1996) 62-69

96. Mochizuki,T., Tsukamoto,E., Kuge,Y., Kanegae,K., Zhao,S., Hikosaka,K., Hosokawa,M., Kohanawa,M., Tamaki,N. FDG uptake and glucose transporter subtype expressions in experimental tumor and inflammation models. J.Nucl.Med. 42 (2001) 1551-1555

97. Montessuit,C., Thorburn,A. Transcriptional activation of the glucose transporter GLUT1 in ventricular cardiac myocytes by hypertrophic agonists. J.Biol.Chem. 274 (1999) 9006-9012

98. Mueckler,M. Facilitative glucose transporters. Eur.J.Biochem. 219 (1994) 713-725

99. Mueckler,M., Caruso,C., Baldwin,S.A., Panico,M., Blench,I., Morris,H.R., Allard,W.J., Lienhard,G.E., Lodish,H.F. Sequence and structure of a human glucose transporter. Science 229 (1985) 941-945

100. Mueckler,M., Hresko,R.C., Sato,M. Structure, function and biosynthesis of GLUT1. Biochem.Soc.Trans. 25 (1997) 951-954

101. Myears,D.W., Sobel,B.E., Bergmann,S.R. Substrate use in ischemic and reperfused canine myocardium: quantitative considerations. Am.J.Physiol 253 (1987) H107-H114

102. Nagamatsu,S., Kornhauser,J.M., Burant,C.F., Seino,S., Mayo,K.E., Bell,G.I. Glucose transporter expression in brain. cDNA sequence of mouse GLUT3, the brain facilitative glucose transporter isoform, and identification of sites of expression by in situ hybridization. J.Biol.Chem. 267 (1992) 467-472

103. Nazareth,W., Yafei,N., Crompton,M. Inhibition of anoxia-induced injury in heart myocytes by cyclosporin A. J.Mol.Cell Cardiol. 23 (1991) 1351-1354

104. Neely J.R., Morgan H.E. Relationship between carbohydrate and lipid metabolism and the energy balance of heart muscle. Annu.Rev.Physiol. 36 (1974) 413

105. Okuno,S., Maeda,Y., Yamaguchi,Y., Takao,Y., Trocino,R.A., Takino,H., Kawasaki,E., Yokota,A., Uotani,S., Akazawa,S., . Expression of GLUT4 glucose transporter mRNA and protein in skeletal muscle and adipose tissue from rats in late pregnancy. Biochem.Biophys.Res.Commun. 191 (1993) 405-412

106. Olson,A.L., Liu,M.L., Moye-Rowley,W.S., Buse,J.B., Bell,G.I., Pessin,J.E. Hormonal/metabolic regulation of the human GLUT4/muscle-fat facilitative glucose transporter gene in transgenic mice. J.Biol.Chem. 268 (1993) 9839-9846

107. Osawa,H., Sutherland,C., Robey,R.B., Printz,R.L., Granner,D.K. Analysis of the signaling pathway involved in the regulation of hexokinase II gene transcription by insulin. J.Biol.Chem. 271 (1996) 16690-16694

108. Palma,F., Agostini,D., Mason,P., Dacha,M., Piccoli,G., Biagiarelli,B., Fiorani,M., Stocchi,V. Purification and characterization of the carboxyl-domain of human hexokinase type III expressed as fusion protein. Mol.Cell Biochem. 155 (1996) 23-29

109. Paternostro,G., Pagano,D., Gnecchi-Ruscone,T., Bonser,R.S., Camici,P.G. Insulin resistance in patients with cardiac hypertrophy. Cardiovasc.Res. 42 (1999) 246-253

110. Phelps,M.E., Schelbert,H.R., Mazziotta,J.C. Positron computed tomography for studies of myocardial and cerebral function. Ann.Intern.Med. 98 (1983) 339-359

111. Pierce. Instuctions of the BCA Protein Assay Kit. (GENERIC) Ref Type: Generic

112. Pombo,C.M., Bonventre,J.V., Avruch,J., Woodgett,J.R., Kyriakis,J.M., Force,T. The stress-activated protein kinases are major c-Jun amino-terminal kinases activated by ischemia and reperfusion. J.Biol.Chem. 269 (1994) 26546-26551

113. Postic,C., Leturque,A., Rencurel,F., Printz,R.L., Forest,C., Granner,D.K., Girard,J. The effects of hyperinsulinemia and hyperglycemia on GLUT4 and hexokinase II mRNA and protein in rat skeletal muscle and adipose tissue. Diabetes 42 (1993) 922-929

114. Quiagen. RNeasy (R) Mini Handbook. 2. 1999. Quiagen. (GENERIC) Ref Type: Pamphlet

115. Ramasamy,R., Hwang,Y.C., Whang,J., Bergmann,S.R. Protection of ischemic hearts by high glucose is mediated, in part, by GLUT-4. Am.J.Physiol Heart Circ.Physiol 281 (2001) H290-H297

116. Ratib,O., Phelps,M.E., Huang,S.C., Henze,E., Selin,C.E., Schelbert,H.R. Positron tomography with deoxyglucose for estimating local myocardial glucose metabolism. J.Nucl.Med. 23 (1982) 577-586

117. Razeghi,P., Young,M.E., Alcorn,J.L., Moravec,C.S., Frazier,O.H., Taegtmeyer,H. Metabolic gene expression in fetal and failing human heart. Circulation 104 (2001) 2923-2931

118. Razeghi,P., Young,M.E., Ying,J., Depre,C., Uray,I.P., Kolesar,J., Shipley,G.L., Moravec,C.S., Davies,P.J., Frazier,O.H., Taegtmeyer,H. Downregulation of metabolic gene expression in failing human heart before and after mechanical unloading. Cardiology 97 (2002) 203-209

119. Remondino,A., Rosenblatt-Velin,N., Montessuit,C., Tardy,I., Papageorgiou,I., Dorsaz,P.A., Jorge-Costa,M., Lerch,R. Altered expression of proteins of metabolic regulation during remodeling of the left ventricle after myocardial infarction. J.Mol.Cell Cardiol. 32 (2000) 2025-2034

120. Roche. LightCycler - DNA Master SYBR Green I. 2. 1999. Mannheim, Germany, Roche. (GENERIC)
Ref Type: Pamphlet

121. Roche. LightCycler - DNA Master Hybridization Probes. 3. 2000. Mannheim, Germany, Roche. (GENERIC)
Ref Type: Pamphlet

122. Roche. LightCycler - FastStart DNA Master Hybridization Probes. 4. 2001. Mannheim, Germany, Roche. (GENERIC)
Ref Type: Pamphlet

123. Roche Molecular Biochemicals. LightCycler Manual. 3.5. 2000. Mannheim, Germany, Roche. (GENERIC)
Ref Type: Pamphlet

124. Rosamond,T.L., Abendschein,D.R., Sobel,B.E., Bergmann,S.R., Fox,K.A. Metabolic fate of radiolabeled palmitate in ischemic canine myocardium: implications for positron emission tomography. J.Nucl.Med. 28 (1987) 1322-1329

125. Rosenblatt-Velin,N., Montessuit,C., Papageorgiou,I., Terrand,J., Lerch,R. Postinfarction heart failure in rats is associated with upregulation of GLUT-1 and downregulation of genes of fatty acid metabolism. Cardiovasc.Res. 52 (2001) 407-416

126. Russell,R.R., III, Yin,R., Caplan,M.J., Hu,X., Ren,J., Shulman,G.I., Sinusas,A.J., Young,L.H. Additive effects of hyperinsulinemia and ischemia on myocardial GLUT1 and GLUT4 translocation in vivo. Circulation 98 (1998) 2180-2186

127. Ryan,H.E., Lo,J., Johnson,R.S. HIF-1 alpha is required for solid tumor formation and embryonic vascularization. EMBO J. 17 (1998) 3005-3015

128. Ryder,J.W., Kawano,Y., Chibalin,A.V., Rincon,J., Tsao,T.S., Stenbit,A.E., Combatsiaris,T., Yang,J., Holman,G.D., Charron,M.J., Zierath,J.R. In vitro analysis of the glucose-transport system in GLUT4-null skeletal muscle. Biochem.J. 342 (Pt 2) (1999) 321-328

129. Sambrook J., Fritsch E.F., Maniartis T. Quantification of DNA and RNA. In: "Molecular Cloning - A Laboratory Manual", AnonymousCold Spring Harbor Laboratory Press, Cold Spring Harbor, New York, 1989,

130. Santalucia,T., Camps,M., Castello,A., Munoz,P., Nuel,A., Testar,X., Palacin,M., Zorzano,A. Developmental regulation of GLUT-1 (erythroid/Hep G2) and GLUT-4 (muscle/fat) glucose transporter expression in rat heart, skeletal muscle, and brown adipose tissue. Endocrinology 130 (1992) 837-846

131. Schwaiger,M., Hicks,R. Regional heterogeneity of cardiac substrate metabolism? J.Nucl.Med. 31 (1990) 1757-1760

132. Schwarz,E.R., Schoendube,F.A., Kostin,S., Schmiedtke,N., Schulz,G., Buell,U., Messmer,B.J., Morrison,J., Hanrath,P., vom,D.J. Prolonged myocardial hibernation exacerbates cardiomyocyte degeneration and impairs recovery of function after revascularization. J.Am.Coll.Cardiol. 31 (1998) 1018-1026

133. Sharma,S., Razeghi,P., Shakir,A., Keneson,B.J., Clubb,F., Taegtmeyer,H. Regional heterogeneity in gene expression profiles: a transcript analysis in human and rat heart. Cardiology 100 (2003) 73-79

134. Shepherd,P.R., Gould,G.W., Colville,C.A., McCoid,S.C., Gibbs,E.M., Kahn,B.B. Distribution of GLUT3 glucose transporter protein in human tissues. Biochem.Biophys.Res.Commun. 188 (1992) 149-154

135. Sherry,B., Yarlett,N., Strupp,A., Cerami,A. Identification of cyclophilin as a proinflammatory secretory product of lipopolysaccharide-activated macrophages. Proc.Natl.Acad.Sci.U.S.A 89 (1992) 3511-3515

136. Shetty,M., Loeb,J.N., Vikstrom,K., Ismail-Beigi,F. Rapid activation of GLUT-1 glucose transporter following inhibition of oxidative phosphorylation in clone 9 cells. J.Biol.Chem. 268 (1993) 17225-17232

137. Sivitz,W.I., Lund,D.D., Yorek,B., Grover-McKay,M., Schmid,P.G. Pretranslational regulation of two cardiac glucose transporters in rats exposed to hypobaric hypoxia. Am.J.Physiol 263 (1992) E562-E569

138. Slot,J.W., Geuze,H.J., Gigengack,S., James,D.E., Lienhard,G.E. Translocation of the glucose transporter GLUT4 in cardiac myocytes of the rat. Proc.Natl.Acad.Sci.U.S.A 88 (1991) 7815-7819

139. Smith,T.A. Mammalian hexokinases and their abnormal expression in cancer. Br.J.Biomed.Sci. 57 (2000) 170-178

140. Smith,T.R., Elmendorf,J.S., David,T.S., Turinsky,J. Growth hormone-induced insulin resistance: role of the insulin receptor, IRS-1, GLUT-1, and GLUT-4. Am.J.Physiol 272 (1997) E1071-E1079

141. Sochor,M., Baquer,N.Z., Hothersall,J.S., McLean,P. Effect of experimental diabetes on the activity of hexokinase isoenzymes in tissues of the rat. Biochem.Int. 22 (1990) 467-474

142. Stanley,W.C., Hall,J.L., Hacker,T.A., Hernandez,L.A., Whitesell,L.F. Decreased myocardial glucose uptake during ischemia in diabetic swine. Metabolism 46 (1997a) 168-172

143. Stanley,W.C., Hall,J.L., Smith,K.R., Cartee,G.D., Hacker,T.A., Wisneski,J.A. Myocardial glucose transporters and glycolytic metabolism during ischemia in hyperglycemic diabetic swine. Metabolism 43 (1994) 61-69

144. Stanley,W.C., Lopaschuk,G.D., Hall,J.L., McCormack,J.G. Regulation of myocardial carbohydrate metabolism under normal and ischaemic conditions. Potential for pharmacological interventions. Cardiovasc.Res. 33 (1997b) 243-257

145. Stephens,J.M., Carter,B.Z., Pekala,P.H., Malter,J.S. Tumor necrosis factor alpha-induced glucose transporter (GLUT-1) mRNA stabilization in 3T3-L1 preadipocytes. Regulation by the adenosine- uridine binding factor. J.Biol.Chem. 267 (1992) 8336-8341

146. Stoffel,M., Froguel,P., Takeda,J., Zouali,H., Vionnet,N., Nishi,S., Weber,I.T., Harrison,R.W., Pilkis,S.J., Lesage,S., . Human glucokinase gene: isolation, characterization, and identification of two missense mutations linked to early-onset non-insulin-dependent (type 2) diabetes mellitus. Proc.Natl.Acad.Sci.U.S.A 89 (1992) 7698-7702

147. Stryer L Proteine können durch Gelelektrophorese getrennt und anschließend sichtbar gemacht werden. In: "Biochemie", Stryer L (Ed.), Spektrum Akademischer Verlag, Heidelberg, Berlin, Oxford, 1995, 48-50

148. Stuart,C.A., Wen,G., Gustafson,W.C., Thompson,E.A. Comparison of GLUT1, GLUT3, and GLUT4 mRNA and the subcellular distribution of their proteins in normal human muscle. Metabolism 49 (2000) 1604-1609

149. Studelska,D.R., Campbell,C., Pang,S., Rodnick,K.J., James,D.E. Developmental expression of insulin-regulatable glucose transporter GLUT-4. Am.J.Physiol 263 (1992) E102-E106

150. Sun,D., Nguyen,N., DeGrado,T.R., Schwaiger,M., Brosius,F.C., III Ischemia induces translocation of the insulin-responsive glucose transporter GLUT4 to the plasma membrane of cardiac myocytes. Circulation 89 (1994) 793-798

151. Taha C. and Klip,A.: Role of p38 and MAPK in the stress-mediated induction of GLUT1 and GLUT3 glucose transporters. Diabetes 45 (1996) 184A (Abstract)(Abstract)

152. Takeuchi,K., McGowan,F.X., Jr., Glynn,P., Moran,A.M., Rader,C.M., Cao-Danh,H., del Nido,P.J. Glucose transporter upregulation improves ischemic tolerance in hypertrophied failing heart. Circulation 98 (1998) II234-II239

153. Tamaki,N., Yonekura,Y., Konishi,J. Myocardial FDG PET studies with the fasting, oral glucose-loading or insulin clamp methods. J.Nucl.Med. 33 (1992) 1263, 1266-1263, 1268

154. Tardy-Cantalupi,I., Montessuit,C., Papageorgiou,I., Remondino-Muller,A., Assimacopoulos-Jeannet,F., Morel,D.R., Lerch,R. Effect of transient ischemia on the expression of glucose transporters GLUT-1 and GLUT-4 in rat myocardium. J.Mol.Cell Cardiol. 31 (1999) 1143-1155

155. Tegeder,I., Schumacher,A., John,S., Geiger,H., Geisslinger,G., Bang,H., Brune,K. Elevated serum cyclophilin levels in patients with severe sepsis. J.Clin.Immunol. 17 (1997) 380-386

156. Thai,M.V., Guruswamy,S., Cao,K.T., Pessin,J.E., Olson,A.L. Myocyte enhancer factor 2 (MEF2)-binding site is required for GLUT4 gene expression in transgenic mice. Regulation of MEF2 DNA binding activity in insulin-deficient diabetes. J.Biol.Chem. 273 (1998) 14285-14292

157. Thorens,B., Cheng,Z.Q., Brown,D., Lodish,H.F. Liver glucose transporter: a basolateral protein in hepatocytes and intestine and kidney cells. Am.J.Physiol 259 (1990a) C279-C285

158. Thorens,B., Lodish,H.F., Brown,D. Differential localization of two glucose transporter isoforms in rat kidney. Am.J.Physiol 259 (1990b) C286-C294

159. Tordjman,K.M., Leingang,K.A., James,D.E., Mueckler,M.M. Differential regulation of two distinct glucose transporter species expressed in 3T3-L1 adipocytes: effect of chronic insulin and tolbutamide treatment. Proc.Natl.Acad.Sci.U.S.A 86 (1989) 7761-7765

160. Tordjman,K.M., Leingang,K.A., Mueckler,M. Differential regulation of the HepG2 and adipocyte/muscle glucose transporters in 3T3L1 adipocytes. Effect of chronic glucose deprivation. Biochem.J. 271 (1990) 201-207

161. Tsai,H.J., Wilson,J.E. Functional organization of mammalian hexokinases: both N- and C-terminal halves of the rat type II isozyme possess catalytic sites. Arch.Biochem.Biophys. 329 (1996) 17-23

162. Tsai,H.J., Wilson,J.E. Functional organization of mammalian hexokinases: characterization of the rat type III isozyme and its chimeric forms, constructed with the N- and C-terminal halves of the type I and type II isozymes. Arch.Biochem.Biophys. 338 (1997) 183-192

163. Tsirka,A.E., Gruetzmacher,E.M., Kelley,D.E., Ritov,V.H., Devaskar,S.U., Lane,R.H. Myocardial gene expression of glucose transporter 1 and glucose transporter 4 in response to uteroplacental insufficiency in the rat. J.Endocrinol. 169 (2001) 373-380

164. Urabe,T., Hattori,N., Nagamatsu,S., Sawa,H., Mizuno,Y. Expression of glucose transporters in rat brain following transient focal ischemic injury. J.Neurochem. 67 (1996) 265-271

165. van der Lee,K.A., Vork,M.M., De Vries,J.E., Willemsen,P.H., Glatz,J.F., Reneman,R.S., Van der Vusse,G.J., Van Bilsen,M. Long-chain fatty acid-induced changes in gene expression in neonatal cardiac myocytes. J.Lipid Res. 41 (2000) 41-47

166. Volkow,N.D., Mullani,N.A., Bendriem,B. Positron emission tomography instrumentation: an overview. Am.J.Physiol Imaging 3 (1988) 142-153

167. Walker,P.S., Donovan,J.A., Van Ness,B.G., Fellows,R.E., Pessin,J.E. Glucose-dependent regulation of glucose transport activity, protein, and mRNA in primary cultures of rat brain glial cells. J.Biol.Chem. 263 (1988) 15594-15601

168. Walker,P.S., Ramlal,T., Donovan,J.A., Doering,T.P., Sandra,A., Klip,A., Pessin,J.E. Insulin and glucose-dependent regulation of the glucose transport system in the rat L6 skeletal muscle cell line. J.Biol.Chem. 264 (1989) 6587-6595

169. Wertheimer,E., Sasson,S., Cerasi,E., Ben Neriah,Y. The ubiquitous glucose transporter GLUT-1 belongs to the glucose- regulated protein family of stress-inducible proteins. Proc.Natl.Acad.Sci.U.S.A 88 (1991) 2525-2529

170. Wheeler,T.J. Translocation of glucose transporters in response to anoxia in heart. J.Biol.Chem. 263 (1988) 19447-19454

171. Wheeler,T.J., Fell,R.D., Hauck,M.A. Translocation of two glucose transporters in heart: effects of rotenone, uncouplers, workload, palmitate, insulin and anoxia. Biochim.Biophys.Acta 1196 (1994) 191-200

172. Younes,M., Brown,R.W., Stephenson,M., Gondo,M., Cagle,P.T. Overexpression of Glut1 and Glut3 in stage I nonsmall cell lung carcinoma is associated with poor survival. Cancer 80 (1997a) 1046-1051

173. Younes,M., Lechago,L.V., Somoano,J.R., Mosharaf,M., Lechago,J. Immunohistochemical detection of Glut3 in human tumors and normal tissues. Anticancer Res. 17 (1997b) 2747-2750

174. Young,L.H., Renfu,Y., Russell,R., Hu,X., Caplan,M., Ren,J., Shulman,G.I., Sinusas,A.J. Low-flow ischemia leads to translocation of canine heart GLUT-4 and GLUT-1 glucose transporters to the sarcolemma in vivo. Circulation 95 (1997) 415-422

175. Young,L.H., Russell,R.R., III, Yin,R., Caplan,M.J., Ren,J., Bergeron,R., Shulman,G.I., Sinusas,A.J. Regulation of myocardial glucose uptake and transport during ischemia and energetic stress. Am.J.Cardiol. 83 (1999) 25H-30H

176. Young,M.E., Razeghi,P., Cedars,A.M., Guthrie,P.H., Taegtmeyer,H. Intrinsic diurnal variations in cardiac metabolism and contractile function. Circ.Res. 89 (2001) 1199-1208

177. Zhong,H., Simons,J.W. Direct comparison of GAPDH, beta-actin, cyclophilin, and 28S rRNA as internal standards for quantifying RNA levels under hypoxia. Biochem.Biophys.Res.Commun. 259 (1999) 523-526

178. Zhou,J., Bondy,C.A. Placental glucose transporter gene expression and metabolism in the rat. J.Clin.Invest 91 (1993) 845-852

6 LIST OF ABBREVIATIONS

A	Adenosine
A, A_{260}	Absorbance, Absorbance at wavelength 260 nm
AA	Amino acid
ADP	Adenosine diphosphate
AMPK	Adenosine monophosphate-activated protein kinase
AMV	Avian myeloblastosis virus
APS	Ammonium persulfate
ATP	Adenosine triphosphate
BCA	Bicinchoninic acid
bp	Base pairs
C	Cytidine
cAMP	Cyclic adenosine monophosphate
CBC	Complete blood count
cDNA	Copy-DNA
CH	Crude homogenate
CoA	Coenzyme A
conc.	Concentration
CYCL	Cyclophilin
dA	Desoxyadenosine
dC	Desoxycytidine
DEPC	Diethyl pyrocarbonate
dG	Desoxyguanosine
DNA	Deoxyribonucleic acid
DNP	2,4-Dinitrophenol
dsDNA	double stranded DNA
dT	Desoxythymidine
E	Extinction
e.g.	for example
ECG	Electrocardiogramm
EDTA	Ethylenediamine-N,N,N',N'-tetraacetic acid
EDV	Enddiastolic Volume
EGTA	Ethylene glycol-bis(2-aminoethyl)-tetraacetic acid
ENT	Ear Nose Throat
ER	Endoplasmatic reticulum
ESV	Endsystolic Volume
eV, keV, Mev	Electon volt (kilo-, mega-)
FDG	F(18)-Deoxyglucose
FRET	Fluorescence Resonance Energy Transfer
G	Guanosine
g	Gramm; Earth's gravitation
GAPDH	Glycerine aldehyde phosphate dehydrogenase
GLUT	Glucose transporter
h	Hour
Hepes	Hydroxyethylpiperazine ethanesulfonic acid

HK	Hexokinase
HKII	Hexokinase Type II
Hybprobe	Hybridization Probe
Hz, kHz	Hertz (s^{-1}), Kilohertz
kb	Kilobase
kD	Kilodalton
LAD	Left anterior descending artery
LCX	Left circumflex artery
LV	Left Ventricle
m, mm, µm, nm	Meter, Millimeter, Micrometer, Nanometer
MAP	Mitogen-activated protein
MBF	Myocardial blood flow
MEK	MAP kinase kinase
mg	Milligramm
min	Minute
MRGU	Myocardial rate of glucose utilisation
mRNA	Messenger RNA
NIDDM	Non-insulin-dependent diabetes mellitus
ns	not significant
OD	Optical density
PAGE	Polyacrylamide gelelektrophoresis
PCR	Polymerase chain reaction
PI3K	Phosphatidylinositol 3-kinase
PKC	Protein kinase C
PM	Plasma membrane fraction (170000g fraction)
PTCA	Percutaneous transluminal coronary angioplasty
RNA	Ribonucleic acid
RNase	Ribonuclease
rpm	rounds per minute
rRNA	Ribosomal RNA
RT	Reverse transcription
RV	Right Ventricle
s	Second
SD	Standard deviation
SDS	Sodiumdodecylsulfate
SEM	Standard error of the mean
ssDNA	single stranded DNA
T	Thymidine
TBE	Tris, Boric acid and EDTA
TCA	Trichloroacetic acid
TCA	Tricarboxylic acid
Temed	N,N,N´,N´-Tetramethylethylenediamine
Tris	Tris(hydroxymethyl)aminomethane
Triton X-100	Polyoxyethylene(10) isooctylphenyl ether
tRNA	Transfer RNA
Tween 20	Polyoxyethylensorbitanmonolaurate
U	Unit

7 ACKNOWLEDGEMENTS

I would like to thank **Prof. Dr. Markus Schwaiger** for giving me the opportunity to work on this topic in his well equipped laboratories and having many helpful ideas for realizing and processing the work.

Further I would like to thank **Dr. Silvia Egert** who taught me all the necessary techniques for working on the protein-part of the work. She also supervised and guided the whole work with many detailed and helpful ideas. Although she had the difficult task of looking after for her lovely little daughter and supervising my scientific work I never felt having a lack of support by her.

Dr. Elisabeth Gleiter introduced me to and supervised my work with RNA and DNA. She helped me to establish the LightCycler method with pig tissue. She always had solutions for my “beginners’ problems” with this sensitive technique. Although she has a family she always managed to be there when I needed her support.

Special thanks I have to **Dr. Marcus Simoés** who introduced me into the principle and interpretation of PET. He established our PET protocol and performed the PET data analysis. He also added very helpful ideas and hints to my work due to his general and very analytic view of problems.

Prof. Dr. Manfred Gratzl and **Dr. Martina Haasemann** enabled me to receive financial support via the Graduiertenkolleg 333 of the Deutsche Forschungsgemeinschaft. The Graduiertenkolleg also made it possible to see and learn different laboratory techniques in order to broaden the spectrum.

Sybille Reder helped me processing a huge amount of samples for RNA preparation and LightCycler realtime PCR.

Prof. Neumeier, Head of the Department of Clinical Chemistry and also **PD Dr. Nadja Harbeck** of the Department of Gynecology and Obstetrics enabled me to use the LightCycler devices in their departments.

Dr. Olfert Landt from TIB Molbiol supported me when designing primers and hybridisation probes for the LightCycler PCR.

Mr. Henning of the Department of Medical Statistics and Epidemiology helped me with the statistical data analysis.

I also want to thank all my **colleagues** in the lab not only for their hints and discussions but also for the friendly personal atmosphere.

My wife **Christine** gave me many scientific hints. By her I had the possibility to see general scientific aspects in widened biological context. She always encouraged me to go on, especially in times when the amount of problems seemed to be larger than the solutions.

And last but not least I would like to thank **my parents**, who always encouraged me to make my way. Without them I never could have done my studies and this work.